ABSTRACT

Title of Dissertation: LANDSAT-BASED OPERATIONAL WHEAT
                                AREA ESTIMATION MODEL FOR PUNJAB,
                                PAKISTAN

                                Ahmad Khan, Doctor of Philosophy 2019

Dissertation Directed by: Professor Matthew C. Hansen,
                                Department of Geographical Sciences

Wheat in Punjab province of Pakistan is grown during the Rabi (winter) season within a heterogeneous smallholder agricultural system subject to a range of pressures including water scarcity, climate change and variability, and management practices. Punjab is the breadbasket of Pakistan, representing over 70% of national wheat production. Timely estimation of cultivated wheat area can serve to inform decision-making in managing harvests with regard to markets and food security. The current wheat area and yield reporting system, operated by the Punjab Crop Reporting Service (CRS) delivers crop forecasts several months after harvest. The delayed production data cannot contribute to in-season decision support systems. There is a need for an alternative cost-effective, efficient and timely approach on producing wheat area estimates, in ensuring food security for the millions of people in Pakistan. Landsat data, medium spatial and temporal resolutions, offer a data source for characterizing wheat in smallholder agriculture landscapes. This dissertation presents

methods for operational mapping of wheat cultivate area using within growing season Landsat time-series data. In addition to maps of wheat cover in Punjab, probability-based samples of in-situ reference data were allocated using the map as a stratifier. A two-stage probability based cluster field sample was used to estimate area and assess map accuracies. The before-harvest wheat area estimates from field-based sampling and Landsat map were found to be comparable to official post-harvest data produced by the CRS Punjab. This research concluded that Landsat medium resolution data has sufficient spatial and temporal coverage for successful wall-to-wall mapping of wheat in Punjab's smallholder agricultural system.

Freely available coarse and medium spatial resolution satellite data such as MODIS and Landsat perform well in characterizing industrial cropping systems; commercial high spatial resolution satellite data are often advocated as an alternative for characterizing fine-scale land tenure agricultural systems such as that found in Punjab. Commercial 5 m spatial resolution RapidEye data from the peak of the winter wheat growing season were used as sub-pixel training data in mapping wheat with the growing season free 30 m Landsat time series data from the 2014-15 growing season. The use of RapidEye to calibrate mapping algorithms did not produce significantly higher overall accuracies (± standard error) compared to traditional whole pixel training of Landsat-based 30 m data. Continuous wheat mapping yielded an overall accuracy of 88% (SE $= \pm 4\%$) in comparison to 87% (SE $= \pm 4\%$) for categorical wheat mapping, leading to the finding that sub-pixel training data are not required for winter wheat mapping in Punjab. Given sufficient expertise in supervised classification model calibration, freely available Landsat data are sufficient for crop

mapping in the fine-scale land tenure system of Punjab. For winter wheat mapping in Punjab and other similar landscapes, training data for supervised classification may be collected directly from Landsat images with probability based stratified random sampling as reference data without the need for high-resolution reference imagery. The research concluded by exploring the use of automated models in wheat area mapping and area estimation using growing season Landsat time-series data. The automated classification tree model resulted in wheat / not wheat maps with comparable accuracies compared to results achieved with traditional manual training. In estimating area, automated wheat maps from previous growing seasons can serve as a stratifier in the allocation of current season in-situ reference data, and current growing season maps can serve as an auxiliary variable in model-assisted area estimation procedures. The research demonstrated operational implementation of robust automated mapping in generating timely, accurate, and precise wheat area estimates. Such information is a critical input to policy decisions, and can help to ensure appropriate post-harvest grain management to address situations arising from surpluses or shortages in crop production.

LANDSAT-BASED OPERATIONAL WHEAT AREA ESTIMATION MODEL
FOR PUNJAB PAKISTAN

by

Ahmad Khan

Advisory Committee:
  Professor Matthew C. Hansen, Chair
  Professor Klaus Hubacek, member
  Associate Research Professor Peter Potapov, member
  Dr. Thomas Loveland, member
  Professor Joseph Sullivan, Dean's representative

Foreword

This dissertation consists of five chapters. Chapters 2-4 are jointly authored chapters. Ahmad Khan lead the research for the jointly authored work, while the co-authors who are mentioned in the corresponding chapters, have contributed at various steps of the research.

Acknowledgement

This dissertation's five chapters represent five years of hard work at Global Land Assessment and Discovery Lab of my advisor, Prof. Matthew Hansen. A thanks has limitation to express my indebtedness to Prof. Matthew Hansen for his support, encouragement, and friendship throughout the course of my stay at UMD. He not only provided me with a job at UMD to meet my ends, but also supported me during my emotional distresses, whenever I faced it. His friendship is an asset that will go life long. Thank you for not making me a prey to the depressing moments that I had from time to time, either due to my research or due to my family commitments, and for enabling me to complete this work to achieve the milestone of Ph.D.

I am thankful to Prof. Klaus Hubacek for enabling me to take up Ph.D. at the UMD and to become a member of the scientific comity. His encouragement is vital in achieving this milestone as he guided me since arrival at UMD on August 13, 2012 and helped me during the early efforts to settle down at UMD and find my ways to GLAD.

During the past six years, a number of people at UMD helped me, taught me and supported me. First comes my GLAD team, the family I am associated to. I owe a thank you to every one, Peter Potapov, Bernard Adusei, Jan Dempewolf, Jon Nordling, Amy Pickens, Samuel Jantz, Janet Nackoney, Patrick Lola Amani and others. I would like to remember Alexander Krylov, a wonderful human being whom we lost to depression and mental distress. I owe him a thank you for his help, particularly on RapidEye data processing for the chapter 3 part of this dissertation. I am grateful to Allison Gost and Maureen Kelly for prompt responses and help with

I dedicate this work to my great support and ideal in life, my father Sarfraz Khan (late) and my inspirational son Yaseen Ahmad Khan (late), who passed away on January 12 and February 2nd, 2012 respectively.

Table of contents

List of Tables

List of Figures

Chapter 1: Introduction

1.1. Introduction

1.1.1. Crop forecasting methods in Pakistan and policy needs

Pakistan, like other developing countries, carries forward inherited systems from the colonial era. Agriculture is one example, with crop reporting methods inherited from British India (Akhtar 2012). The 'List Frame' as it is called, is a survey framework implemented to derive crop area and production forecasts at province level, which are used to serve national level reporting. As early as 1919, the Agriculture Board in India had recommended crop cutting experiments for yield estimation (Singh and Goyal 2000), which according to Hubback (1946) were implemented in 1923 – 25 for rice yield estimation in Orissa for the first time through random samples of plots from randomly selected fields and villages. The "crop cuts" experiment of Hubback (1946) was yield estimation of wheat and gram in Bihar primarily to guide courts' proceedings in rent lawsuits and to benefit public in stabilizing prices (Hubback 1946, Mahalanobis 1945). Fermont and Benson (2011) have mentioned that in the 1940s statisticians in India developed crop yields estimation method "crop cuts" based on sampling of small subplots within cultivated fields. Food and Agriculture Organization of the United Nations (FAO) recommended the "area list frame" method and many countries adopted it for crop yield estimation. Pakistan implements a similar method "list frame" for crop forecasting in the country.

Pakistan is 8th in the world by production of wheat and Punjab province with its expanded irrigated and rain-fed cultivated plains has earned the title of "breadbasket'

The chapter 2 presented here has been published as "Khan, A; Hansen, MC; Potapov, P.; Stehman, SV. Chattha, AA. (2016). Landsat-based wheat mapping in the heterogeneous cropping system of Punjab. Inte*rnational Journal of Remote Sensing,* 37(6), 1391 – 1410*".*

for the country. The Punjab province is meeting 70% of the staple food demand of the 207 million people in Pakistan. With enormous population pressure on food resources, timely operational decisions are required, which need inputs of timely and accurate crop statistics. The country has semi-arid climate, where a climatic variability can result in significant impact on production of wheat, while placing the country as the 8th most affected among countries from climate change impacts. Climate change poses enormous risks for crops in general and wheat in particular. This climate vulnerability further signifies the need for a robust forecasting model for wheat, as the major staple food for more than 207 million people.

Hanuschak (2010) mentioned that a crop forecast made as early in a growing season is correspondingly of higher economic value. Akhtar (2012) mentioned that pre-harvest wheat area and production estimates decide post-harvest transportation, storage, export and import of a crop according to assessed surplus or shortage in a country. Conventional crop forecasts, particularly in developing countries such as Pakistan, derived from conventional ground based survey efforts are inconsistent in methods, capacity and application across regions and nations. With conventional survey methods reports are made typically months after harvest, even for the most important crops such as wheat. Delayed availability of crop statistics are not beneficial to policy and operational decision making (Doraiswamy et al. 2003). Successful response to and management of crisis situations emerging from shortage or surplus production, such as the wheat shortage in 2007 – 09 and post 2010 floods surplus production in Pakistan, can be mitigated provided that reliable and timely pre-harvest crop statistics are available. Verma et al. (2011) defines the conventional method as

resource intensive approach, which like its many conventional variants results in estimates months after the harvest has taken place in a given year. Akhtar (2012) pointed out that delay in results from an expensive ground based effort like 'list frame' is neither economical nor does it contribute to the food security of the 207 million people of Pakistan.

There have been alternate methods to conventional in-situ methods, including modeling with edaphic and climatic parameters, and applying remote sensing or a combination of both (Atzberger 2013, Gallego 2004). Synoptic monitoring and modeling efforts offer the promise of consistent, automated approaches that are less costly than traditional methods. Scientists have conducted several studies to formulate models for wheat forecasting in Pakistan. Most of these studies were conducted in the 1970s and 1980s when Pakistan faced shortages of wheat production and policy makers were concerned with food security, especially for staple foods. The most commonly used inputs in these models were rainfall, fertilizer, temperature, tractors and labor. For example, Azhar et al (1972, 1974) used rainfall during the November to January period, Qureshi (1974) used three variables to capture rainfall: rainfall from July to September, rainfall from October to December and 'maximum effective' rainfall from January to March. Chaudhary and Kemal (1974) found that deviation of rainfall from normal levels during the period from July to January was the most appropriate rainfall variable for wheat production in irrigated areas of Pakistan. This study, along with another study by Griffiths et al. (1999), concluded that the choice between actual rainfall and the deviations from normal rainfall was a matter for empirical investigation and the results were not robust. The empirical literature finds strong correlation of wheat production

with fertilizer use. In the absence of any direct measure of fertilizer use for the wheat crop at the aggregate level, the literature adopts alternative procedures such as the purchase of fertilizer during the sowing season for wheat or a fertilizer consumption based on the share of the wheat crop in total cropped area (see Azhar et al (1972, 1974); Mukhtar and Mukhtar (1988); Saleem (1989)).

Remote sensing has evolved over time from low spatial resolution to high spatial resolution detail, and from low to high temporal resolutions. These advances provide opportunities to quickly and reliably derive agricultural statistics over large areas, thereby advancing decision support of governments. Application of remote sensing data in agriculture is particularly important to countries whose economies are reliant on agriculture, such as Pakistan. Policy and operational response in agricultural countries are subject to the availability of timely accurate crop statistics. The conventional methods, such as the 'list frame' in practice in Pakistan, provide inputs months after harvest, and do little beyond meeting an official reporting requirement. There have been applications of remote sensing in crop forecasting in Pakistan. Dempewolf et al. (2014) analyzed MODIS time series and related NDVI to historical wheat yields to forecast wheat production. The method resulted in forecasting yield before harvest using previous years historical yield data and NDVI relationship in a regression tree.

Pakistan's Upper Space and Atmospheric Research Commission (SUPARCO) with assistance from Food and Agriculture Organization of the United Nations (FAO) has been employing 10 m Spot data to produce crop acreage estimates. This application

of remote sensing results in forecasts for cereal crops such as wheat, rice and corn at national level. This is a comprehensive effort with field based validation from area list frame. A combination of high-resolution data with area list frame makes the effort an expensive endeavor, which under national or provincial budgets or a budget without external assistance may not be an affordable option.

The University of Maryland during 2010 – 2014 provided technical assistance to FAO in capacity building of the staff of Punjab and Sindh Crop Reporting Service Departments and SUPARCO in application of remote sensing and using Global Land and Agricultural Monitoring System (GLAM) to estimate crop area and yield. The project could not result in a sustainable effort and to translate into a fully national scale operational GLAM system for the country due to phasing out of the project.

1.1.2. History of satellite data in mapping crop types

Remote sensing applications in agriculture begun in the 1950's with aerial photography (Gerald 1979, Macdonald 1984, Allen 1990, Nellis et al. 2009) and gained momentum with availability of remote sensing data from launch of satellites carrying earth observation sensors. The range of applications of remote sensing data, initially restricted to military and strategic use, expanded to sensing earth surface and resources with development of new sensors and space born platforms (Gerald 1979). According to (Craig and Atkinson 2013) earth observations with sensors onboard satellites took over the aerial photography, the initial form of remote sensing. According to MacDonald and Landgrebe (1967), USDA and NASA had assessed importance of remote sensing in 1960's at the early stages of remote sensing development, when

NAS-NRC committee on "Aerial Survey Methods in Agriculture" was formed (Macdonald 1984). The evolution of satellite imagery from print imagery to digital format has significantly advanced remote sensing applications, analysis and availability. MacDonald and Landgrebe (1967) reviewed early efforts of remote sensing applications with potential applications in the future for various disciplines including crop area estimation and yield forecasting. In 1971, under the corn blight watch experiment (CBWE) in 1971, NASA and USDA with other partners successfully applied remotely sensed data in monitoring corn blight in the corn producing seven states. This is considered the first successful application of remote sensing in agriculture (Macdonald 1984) Gallego et al. (2009) reflects on the evolution of methods over the past couple of decades in use of remotely sensed data for crop area and production estimation. According to them, remote sensing techniques from early days were considered to offer cost effective solutions (Gerald 1979)to data gathering, and timely provision of data inputs for decision making process The Naval Research Office and the National Academy of Sciences' Committee on Geography jointly worked towards improvement in application of remote sensing to earth and biological resources. Their joint work resulted in "remote sensing of environment' as a scientific field that progressed over time (Macdonald 1984). In 1972, wheat crop failure in Russia had enormous impact on markets across the globe. This event provided impetus to a wider range application of remote sensing in agriculture, and consequently hatching the LACIE project.

The LACIE (Large Area Crop Inventory Experiment) and AgRISTARS (Agriculture and Resources Inventory Surveys Through Aerospace Remote Sensing)

programs, which began in 1974 and 1980, respectively, had the goal of improving crop monitoring via the use of remotely sensed data sets (Boatwright and Whitefield 1986). A more recent operational successor to these programs is the Crop Condition Data Retrieval and Evaluation (CADRE) system used by the USDA Foreign Agricultural Service (FAS) (Reynolds 2001), which focuses on the delivery of agro-meteorological data and incorporates earth observations in assessing crop development. The USDA National Agricultural and Statistics Service (NASS) operationally incorporates satellite data and derives products in reporting on crop type acreage through the production of earth observation-based, state-level Cropland Data Layer products (Hanuschak and Mueller 2002). The porting of such approaches, particularly to places where high latency in reporting is hampered by antiquated methods, represents a low cost opportunity to improving crop monitoring in countries such as Pakistan. Rembold and Maselli (2006) and (Chang et al. 2007) used low resolution imagery in crop area estimation. Their procedure was tested in Tuscany, Italy using high-resolution Landsat TM and ETM+ imagery and CORINE land cover to create an accurate, masked mapping base. The low resolution updating imagery was AVHRR. The U.S Department of Agriculture (USDA), the National Aeronautics and Space Administration (NASA), the South Dakota State University (SDSU) and the University of Maryland (UMD) jointly developed the Global Agriculture Monitoring Project (GLAM) using coarse resolution MODIS (Moderate Resolution Imaging Spectroradiometer) on board the Earth Observing System (EOS) Terra satellite. The GLAM system aimed at meeting Decision Support System operational capability needs of the USDA Foreign Agricultural Service (FAS), and has been providing near real

time and reliable earth observation data to monitor crop conditions and forecast vital agricultural statistics. The information help monitoring crops condition and production at global scale, thus benefiting crop management policies and crop marketing dynamics (Becker-Reshef et al. 2010). The information also help in assessing drought conditions, and expected crop demands and market volatility.

Providing historical background to importance of remote sensing application in agricultural statistics, MacDonald and Landgrebe (1967) summarized its future value for national and international policies, economic development, and food security of underdeveloped nations. Remote sensing is becoming popular in agriculture monitoring applications (Carfagna and Gallego 2005). Fermont and Benson (2011) mentioned spectral reflectance as a unique quality of green plants, and as features captured by sensors onboard satellites. The data captured in satellite images can be analyzed for addressing various properties of plants/crops, including crop condition and crop type (Fermont and Benson 2011). According to Mosiman (2003) multi-spectral satellite images respond to reflectance in different parts of the electromagnetic spectrum from vegetation, which helps in characterizing different crop types and different crop conditions. Reflectance properties vary within and between species and therefore slight variation in reflectance is detected by sensors onboard a satellite. Markham and Barker (1985) suggested that these variations in reflectance enable scientists to differentiate between different crop types covers or between different health conditions of a crop. According to Carfagna and Gallego (2005) spectral response of a crop among pixels of the same crop with different climatic and edaphic conditions have higher variations than variability between different crops. GonzÁLez-

Alonso and Cuevas (1993) , DeFries et al. (1995), Vuolo et al. (2013), and Dempewolf et al. (2014) attributed successfully identifying different crops covers due to phenological characteristics captured by high temporal resolution of satellite time-series data.

In 1970's and 80's USDA-NASS implemented the Large Area Crop Inventory Experiment (LACIE) and Agriculture and Resources Inventory Surveys through Aerospace Remote Sensing (AgRISTARS), to determine if crop acreage estimates could be derived using multispectral imagery and ground truth data (MacDonald et al. 1975, MacDonald and Hall 1980, Bailey and Boryan 2010, Kleweno and Miller 1981). This popularity relies on consistent and free low and medium resolution data acquisition and advances in software development particularly open source modules, enhanced capability in image interpretation and analysis. Accordingly. MacDonald and Hall (1980) presented comprehensive details of the early crop area and production estimation effort, LACIE project, a joint venture of several U.S.A. governmental organizations. According to Erickson (1984) and Ustin (2004) LACIE helped develop methods for applying remote sensing in crop forecasting, while AgRISTARS programme of USDA, NASA and NOAA built upon the LACIE methods and extended these to other crops. Atzberger (2013) suggested that satellite remote sensing provides unbiased information over large areas, which can be used as evidence for decision making. The sharp rise in food prices in 2008 due to various causes including market dynamics, bad climatic conditions and climate change impacts increased the realization for and awareness of the importance of constant agricultural monitoring (Gallego et al. 2010). The Landsat mission with medium spatial resolution aimed at providing timely

estimates of crop acreage with significantly smaller sampling errors than the coarse resolution based acreage estimates that were in practice (Allen 1990). The release of the Landsat archive for free access (Woodcock et al. 2008) enhanced the capabilities for consistent monitoring of land cover land use changes including agricultural crops areal and production estimation.

According to Carfagna and Gallego (2005), the application of remote sensing in agriculture includes two overarching uses of remote sensing: 1) at the level of survey design and stratification and 2) in the estimation of area using remote sensing data as an auxiliary information source. The crop area estimate directly from remote sensing imagery, was not satisfactorily done as an effort of the Monitoring of Agriculture with Remote Sensing (MARS) project in 90's, primarily due to complexity in the landscape of Europe Gallegio (1999). The lower efficiency here could not be translated to operational use of the available remote sensing data.

1.1.3. Open Landsat archive and new capabilities for mapping

Revision of the military classification regulations regarding remote sensing in 1964 opened remote sensing for civilian use (Macdonald 1984). Before this, it was a classified data for military use with minimal availability to unclassified research community. The Landsat series of sensors, including Landsat Multispectral Scanner (MSS Landsat 1 – 4), Landsat Thematic Mapper (Landsat 4 – 5 TM), Landsat Enhanced Thematic Mapper Plus (Landsat 7 ETM+) and Operational Land Imager (Landsat 8 OLI) in combination with Thermal Infrared Sensor (TIRS), has been producing consistent multi-spectral temporal medium resolution data for over 40 years. Given

improved time-series collections in recent years, Landsat data offer the opportunity to operationally monitor crop condition, areal extent by type, growth stage and yield. The launch of the first Landsat satellite in 1972 represented a groundbreaking development in the application of remote sensing data in agricultural applications. A primary motivation for the use of Landsat was to improve agricultural monitoring.

Wulder et al. (2012) highlight the opportunities that exist with free-of-cost availability of Landsat archive since 2008 (Woodcock et al. 2008), which overcome the limitations from use of coarse resolution imagery such as AVHRR in land cover classification and crop area estimation. This also enabled scientists in wall-to-wall mapping of required land cover classes, and improving reliability and accuracy of area estimation as demonstrated from regional scale (Potapov et al. 2012, Song et al. 2017, King et al. 2017, Khan et al. 2018, Dempewolf et al. 2014, Khan et al. 2016) and global scale change detection products (Hansen et al. 2013, Hansen and Loveland 2012).

1.1.4. Remote sensing application in crop area estimation

According to Huddleston (1978), crop production forecasts/estimates are the product of area to be harvested and expected yield per unit area (GonzÁLez-Alonso and Cuevas 1993, Baruth 2008, Dempewolf et al. 2013). In the context of production estimation, MacDonald and Hall (1980) provide a rationale on the need for crop foresting. They describe reliability, timeliness, and effectiveness as key attributes of quality agricultural information. Since 1970's, satellite remote sensing has been applied in agricultural statistics in auxiliary role within operational services in crop acreage estimation and assessment (Gallego et al. 2010, Allen 1990, Boryan et al. 2011,

Rembold and Maselli 2006). According to Allen (1990) using remote sensing data as an auxiliary variable maintained statistical rigor in the context of existing methods. GonzÁLez-Alonso and Cuevas (1993) used remote sensing data with ground based surveys and compared regression estimator vs adjusted regression estimator. They found that using adjusted proportions obtained from confusion matrix in a regression estimator produces area estimates with lower Co-efficient of Variation (CV) than using the values directly in a standard regression estimator. They therefore have argued that adjusted regression methods seem appropriate in area estimation of a crop when combining ground surveys with remote sensing data. Vogelmann et al. (2001) and Song et al. (2017) indicated to the progress being made in classifying multi-spectral Landsat medium resolution data that has advantages of synoptic and repeat coverage with the unique advantage of providing timely and spatially contiguous information on crop growth at regional to global scales. Harris, et al. (1989) suggested that TM data produced statistically more accurate crop area estimates with less analysis time as compared to SPOT data.

The ground surveys and classified crop layers, are treated independent of each other, but are complementing processes. These two sources of data when integrated in accuracy frameworks result in error adjustments. This approach has successfully been applied in forest and agricultural area mapping and area estimation (Hansen et al. 2008, Hansen and Loveland 2012, Tyukavina et al. 2015, Broich et al. 2011). In-situ area estimate from ground samples surveyed are used as dependent variable with classification map as ancillary variable in regression estimator (Gallego 2004, Boryan et al. 2011, GonzÁLez-Alonso and Cuevas 1993). Gallego et al. (2008) described the

need for the use of remote sensing data as auxiliary information to augment ground based survey results. Gallego et al. (2010) mention that in the 1980s and 1990s accurate field based in-situ sample data was combined in different ways with less accurate remote sensing data covering the region of interest. However, integration of image processing with agricultural statistics, with few exceptions, is fraught with challenges. Unal et al. (2006) describes a pilot study to use remote sensing imagery in conjunction with a ground survey to estimate wheat acreage in the provinces of Konya and Adana in Turkey. The approach taken for acreage estimation was to determine the proportional distribution of the crops in the sampled segments (500 x 500 m), over the agricultural areas and apply this proportion to the total agricultural land area from the classification. The classification used Landsat TM and ETM+ data in conjunction with data from the ground survey. Image materials for the ground survey were prepared using high-resolution imagery (SPOT 5 in Konya and IKONOS for Adana). Wheat acreage alone was estimated in Adana, but a wheat-barley combination was estimated in Konya, since it is difficult to separate wheat and barley through satellite imagery classification. In both provinces wheat (Adana) and wheat-barley (Konya) acreage was below official figures for both the classified and extrapolated (from segment proportions) estimates. Maas (1998) observed strong positive correlation between yield and reflectance values over mid-season, the period of the growth of cotton bolls, while late in the growing season and prior to defoliation observed significant negative correlation between yield and reflectance.

There have been efforts on integrating remote sensing with time series climate data, experimental physical parameters, and ground based surveys to deliver accurate

and reliable wheat production/yield estimates. Hanuschak et al. (1980) estimated soybean and corn area for Iowa state incorporating Landsat data into ground surveys. He found substantial improvement in estimated area using Landsat data as auxiliary variable in a regression estimator in comparison to using ground data only. Dempewolf et al. (2014) successfully implied MODIS and Landsat data integration with historical yield data to estimate wheat production for Pakistan. However, using Remote Sensing as a source of pre-harvest area estimates hasn't been attempted. Saeed et al. (2017) integrated weather data and MODIS NDVI time series to forecast winter wheat yield in Punjab, Pakistan.

Boatwright and Whitefield (1986) and MacDonald and Hall (1980) provide an insight into the evolution of remote sensing use in agricultural crop forecasting. According to Craig (2010), these programs were successful at generating unbiased statistical estimates of crop area at the state and county level and reducing the statistical variance of acreage indications from farmer reported surveys. NASS' remote sensing applications evolved over the years and in 1997 the present CDL (GIS-based Cropland Data Layer) program was developed, which is used in various ways in addition to deriving supplementary crop area estimates (Mueller and Seffrin 2006). Boryan et al. (2011) described the USDA-NASS CDL program for its processing methods, classification and validation techniques, accuracy assessment, and the crop acreage methods, which range in accuracy from 85% to 95% for the major crops.

According to Stehman (2013) errors are likely when using mapped information in deriving crop area, and therefore sample based validation of the mapping process be

conducted rather than pixel counting from map. According to Carfagna and Gallego (2005), in large area mapping classification accuracy is poorer in comparison to small pilot areas. In heterogeneous agricultural systems with small fields and multiple cropping patterns, satellite images with mixed pixels produce non-sampling errors, as against the thumb rule of pure pixels availability for acreage estimation (Gallego et al. 2010). Agricultural landscape in Punjab is representative of heterogeneity, and therefore non-sampling errors are non-avoidable. In our research, we observed most of the commission errors were associated with multiple cropping particularly wheat under fruit orchards, and most of the commission errors were associated with dryland / rain-fed farming. Carfagna and Gallego (2005) have pointed out that very few organizations apply remote sensing in producing their agricultural statistics. Application of remote sensing imagery at medium resolution such as Landsat (Carfagna and Gallego 2005) in agricultural statistics has enormous advantages of timeliness, cost-effectiveness, wide swath and geographic coverage over large areas. In our research, we successfully applied Landsat 30 m multi-spectral multi-temporal data to Punjab province to derive in-season wheat area.

1.1.5. Limitations of methods when porting to developing countries

The Crop Reporting Service (CRS) in Punjab, Pakistan is responsible for implementation of the "area list frame" survey to estimate crops' area and production. The CRS Punjab had more than 1500 field staff, allocated budget of Pak. Rs. 690.056 million (~ US $ 6.0 million) in 2017-18 and extensive field logistical support. However, the CRS releases its final wheat forecast in July or August each year, a few months after harvest has taken place. The conventional crop statistics method in practice in

Punjab, Pakistan does not correspond to requirement of timely inputs, which is considered the most important consideration in agricultural monitoring due to short growing season and risks of highly variable conditions (Atzberger 2013, Food and Agriculture Organization 2011) for operational decisions on grain management, transportation of produce, export and import. This compromises food security of the dependent population on one hand, and often result in expensive measures to meet demand in a case of shortfall or mismanagement of surplus in a case of higher productivity on the other. Although these conventional crop forecasting efforts are elaborate data collection efforts as collect a variety of information on various aspects of agriculture (Food and Agriculture Organization 2015), yet not practically suitable to developing countries conditions on the basis that these are labor intensive and require significant financial and human resources (Verma et al. 2011, Doraiswamy et al. 2003). In spite of the efforts involved, the methods often result in unsatisfactory and untimely information with no use for post-harvest grain management. Agricultural development in developing countries is compromised from delay in information availability for operational measures and policy decisions, which is a major obstacle to the economic development there (MacDonald and Landgrebe 1967)

According to Gallego and Delince (2010), if a responding farmer community is educated and has access to communication means such as telephone and email, then area list sampling will be cost-effective. In Pakistan, in general farmer community is illiterate or has very low education levels, and have limited access to and understand of modern technologically advanced. These limitations make ground based surveys time consuming, expensive, and in some cases practically not a viable option. Rembold

and Maselli (2006) describes the development and testing of a methodology for using multi-temporal, low spatial resolution images to update crop area changes on a regional scale. The primary issue with using low-resolution imagery in this way is the large number of mixed land-use pixels. The methodology presented in this paper was based on the assumption that the variations within mixed pixels are reflected in changes in the shape of the multi-temporal NDVI pixel profiles. Specifically, the methodological approach described was based on the sequential use of spectral angle mapping (SAM) and a linear regression estimator. Cihlar (2000) provided a detailed analysis of the limiting factors of coarse and fine scale remote sensing data where *a priori* knowledge of land cover classes over large area is required along with sufficient spatial and temporal resolution for effective crop type identification. Fermont and Benson (2011) elaborated various issues in crop forecasting of smallholder agriculture, including challenges of a lack of cadastral information on land use, intercropping, non-uniform plots with variable sizes, multiple harvesting periods, multiple cropping patterns, and management practices. Use of coarse resolution imagery in agricultural statistics is still challenged by accuracy and precision in crop type identification due to various complexities including crop landscape heterogeneity, mixed phenological stages, field size especially in small holder agricultural systems, and management practices (Song et al. 2017).

Boryan et al. (2011) has explained the historical background and efficacy of CDL, operational crop area estimation model that has been applied in United States since 2008. However, according to Song et al. (2017) and Boryan et al. (2011), CDL and or similar models such as the Crop Inventory (CI) of Canada are not suitable for

application in developing countries like Pakistan given that 1) these methods require expensive and time consuming geospatially referenced training inputs, and 2) are more suitable for large farm situations such as that of United States and Canada.

The estimates from the AGRIT survey were used as benchmarks for performance evaluation of the resulting wheat area estimates. It is, however, of limited value for crop area prediction in the early stages of the season. Rembold and Maselli (2006) mention the following limitations of the process: 1) distinct NDVI profiles must exist for the classes to be updated, which makes the procedure applicable only to broad vegetation categories with characteristic phenological behavior; 2) accurate maps describing the reference distribution of the main crops must be available; and 3) good quality low-resolution images must be available to provide correct multi-temporal NDVI updating information. Our research presented here addresses this issue in wheat area estimation in the complex landscape of small farms and intensive agriculture of Punjab in Pakistan. Specifically, an operational mapping model for wheat is developed to facilitate *in situ* data collection and pre-harvest area estimation.

1.1.6. Current needs and the research response

According to Everaers (2009) repeated surveys are burden on farmers and decreasing response rates have been the reasons to explore other data sources and information gathering techniques such as remote sensing and GIS tools to produce agricultural statistics. Our research presented here, while exploring the application of Landsat in-growing season time series data addresses the issues described in section 1.5, and present an automated model that can provide timely and accurate inputs for

operational decision making, and meeting the challenge of addressing food security issues in a timely manner.

In the presented research, undertaken at the Global Land Analysis and Discovery Laboratory (GLAD) at the University of Maryland, we have experimented with remote sensing data to produce reliable, timely and accurate wheat area estimates for Punjab, Pakistan. In our research, following up on global wall-to-wall Landsat mapping (Hansen et al. 2013), we produced wall-to-wall Landsat based wheat maps for Punjab. Using sample based data from the wall-to-wall Landsat wheat maps as auxiliary variable with probability based field samples, we found a decrease in standard error, thus deriving more accurate information than using ground data or map alone. Our methods, which employ Landsat multi-temporal spectral data and classification and regression trees, result in the development of an operational classification model that generates wheat maps for direct use in area estimation methods. The model, if adopted by the crop area forecasting agencies in Pakistan and elsewhere, will result in saving resources through timely inputs for policy and operational decisions making on post-harvest crop situation.

The research is presented in three papers. The first paper (Chapter 2) establishes the wheat mapping method and the use of the map in allocating field data collection in deriving area estimates. A stratified two stage random sample of 20 km x 20 km blocks is performed, with 10 randomly selected pixels examined from within each block. A regression estimator method is employed, with the auxiliary variable derived from a wall to wall classification of multi-temporal multi-spectral Landsat within wheat

growing season (2013-14) time-series data. The second paper (Chapter 3) presents a comparative use of Landsat multi-temporal spectral data and high-resolution RapidEye data in mapping wheat cover. Given the small field sizes of Punjab, the possible advantage of mapping with very high spatial resolution data as an input to mapping with Landsat is evaluated. Resulting maps are used as auxiliary variables with field data collected from 21 two stage random samples within a population of 10km x 10km blocks, with 10 pixels randomly sampled from each block. Wheat areas were estimated from Landsat regression map using a continuous map, a thresholded map at 50% and a thresholded map at <25% and >75% representing pure non-wheat and pure wheat pixels respectively. We recorded a decrease in standard error of the sample based wheat area estimate by using each of the maps generated with the above inputs in a difference estimator. Results illustrate that Landsat data can be mapped using traditional categorical wheat / not wheat labels, obviating the need for commercial data inputs for calibration.

The third paper (Chapter 4) presents an operational model for wheat area estimation. The model depends on training data derived from previous years Landsat mapping. In this, we combined two wheat maps from previous years to derive wheat and non-wheat agreement as a training layer, which is visually interpreted against the Landsat multi-temporal spectral metrics for adjustments and corrections. The training data were related to the metrics in a classification tree model to derive wheat area cover for the study area. Ground based samples comprising of 45 sample blocks of 5km x 5km with 10 pixels randomly selected from each block were employed to derive an independent wheat area estimate. The map based area estimates were used as auxiliary

variable estimating area of cultivated wheat. Results show that an operational, turn-key algorithm can be used for mapping wheat using Landsat data, with subsequent field data collection guided by the Landsat map.

We confidently present our wheat area estimation method for use by the CRS Punjab and other such organizations in Pakistan and in the neighboring countries. Adopting this model can save millions of rupees in budget allocation, hundreds of man-days employed on data collection, and provision of area estimates at least a couple of weeks before the wheat harvest in comparison to months after harvest. Specifically, the use of automated wheat mapping from Landsat inputs enables the efficient allocation of field data collection and the generation of in season wheat area estimates with low uncertainties. The implementation of such a method would represent an advance on current *in situ* methods that have high latency, reducing their utility to inform decision-making.

Chapter 2: Landsat-based wheat mapping in the heterogeneous cropping system of Punjab, Pakistan

1.2. Introduction

The More than 180 million population of Pakistan is directly or indirectly dependent on the agriculture sector (World Bank 2014) with wheat as an important staple food (FAO 2013). About 43.7% of the labor force in Pakistan is employed in the agriculture sector (Ministry of Finance 2014) and Pakistan is the eighth largest wheat producer globally (FAO 2013). Wheat is the most important agricultural crop for 80% of farmers and constitutes nearly 40% of the country's total cultivated land (FAO 2013). However, the annual national wheat production of approximately 21 million tonnes (MT) does not cover the total demand of 24.0 MT (FAO 2013, SUPARCO 2012). To meet gaps in demand and supply, Pakistan imports wheat on variable scales each year.

Wheat is grown during the winter season or Rabi, which begins in October to December and ends in April to May. Recurring droughts and changing weather patterns strongly influence crop yields in Pakistan with climate change a suspected factor in recent production variations (ADB 2009, Zhu 2014, Abbasian and Pound 2013). The country's extensive irrigated cropland system, one of the largest contiguous networks in the world (Bastiaanssen and Ali 2003), depends on sustained water flows in the Indus river basin (Roohi 2006). However, water flows in the Indus River have not been consistent in recent decades (Lydia et al. 2000). Flood and drought cycles have been more frequent and are affecting crop production (ADB 2009, Zhu 2014).

Accurate estimation of cultivated wheat area and associated production is important for

the country to address changes occurring from climate change impacts and water dynamics.

Traditional monitoring of croplands is implemented by the provincial Crop Reporting Services (CRS) Departments. The system is labor intensive and suffers from delays in producing results suitable for timely decision making (Akhtar 2012). The data collected by CRS Departments are derived from surveys compiled at the start, midpoint and post-harvest periods of the growing season. Survey results are extrapolated to district and provincial levels. According to the crop calendar of the Bureau of Statistics, the first estimate is made on 1 February, the second on 1 April, and the final on 1 August. In practice, estimates and results of the final harvest are available months after crop harvest (GoPakistan 2011). Given that harvest typically occurs in April, the delayed crop reporting system does not provide actionable information in response to below normal crop development and production. Delayed reporting renders CRS data unusable for planning and management purposes (Verma et al. 2011) and as inputs to critical decision support system concerning the import and export of wheat (Akhtar 2012). Due to the absence of timely and accurate data, decisions regarding wheat shortage or surplus are often arbitrary or ad hoc in response to emerging situations.

The CRS crop yield estimates are derived from a sample of randomly selected villages stratified by population size. This stratification does not represent the agricultural zones equally and is also limited by accessibility to remote areas (FAO 2012). There is therefore a clear need for a system that can provide both timely and

accurate crop area estimates and yields forecasts before harvesting. Such data products can be used for timely decision making in addressing food security within the country, maintaining adequate food stocks, setting national support prices, planning transportation and processing facilities, and other logistics (Akhtar 2012, Dempewolf et al. 2013, Bauer 1975).

Early assessment of crop condition, area estimation and yield forecasting can avert potential disasters that might result from production shortfalls due to a disease, drought, pest infestation, and other factors (Erickson 1984, Doraiswamy et al. 2003, Minamiguchi 2005). As such, Earth observation data can enable strategic planning to bridge the gap between demand and supply (Doraiswamy et al. 2003).

The early Large Area Crop Inventory Experiment (LACIE) and Agriculture and Resources Inventory Surveys Through Aerospace Remote Sensing (AgRISTARS) programs of the United States, which began in 1974 and 1980, represent initial concerted efforts to improve crop monitoring via the use of remotely sensed data sets (Boatwright and Whitefield 1986). These initiatives employed Landsat imagery and climate data from the World Meteorological Organization to model crop yields (Erickson 1984). Operational systems resulted from these initial experiments, including the Crop Condition Data Retrieval and Evaluation system used by the USDA Foreign Agricultural Service (Reynolds, 2001) and the Cropland Data Layer of the USDA's National Agricultural Statistics Service. Similar crop monitoring systems integrating satellite data have been added and include the Monitoring of Agriculture by Remote Sensing system of the European Union, China's CropWatch, and others

(Becker-Reshef et al. 2010). Satellite data being modeled are mostly multi-year time series data or modeled with meteorological and/or physical data to estimate crop areas for wheat, rice and other crops (Becker-Reshef et al. 2010, Becker-Reshef et al. 2010, Dempewolf et al. 2014, Bairagi and Hassan 2002).

Despite much research in the area of cropland mapping using Earth observation data sets, a number of factors have limited operational map production. First, differentiating crop types requires fine temporal-scale imagery to enable the identification of the subtle differences between various crop phenologies. Second, cropped fields are discrete entities in landscapes and require appropriate spatial resolution in order to be unambiguously resolved. For Earth observation satellites, the typical engineering trade-off is temporal versus spatial resolution. Higher spatial resolution data sets do not have high return rates in terms of repeated imaging over a given locale. Sensors with coarser spatial resolution such as $250\,\mathrm{m} \times 250\,\mathrm{m}$ Moderate Resolution Imaging Spectrometer (MODIS) have wider swaths ($2330\,\mathrm{km} \times 10\,\mathrm{km}$) that allow for higher rates of repeated imaging, but are limited in terms of generating accurate area estimates in small farm sizes. However, since the launch of Landsat 8 in 2013, we now have two Landsat sensors, the Enhanced Thematic Mapper Plus (ETM+) on-board the Landsat 7 spacecraft and the Operational Land Imager (OLI) on Landsat 8, systematically acquiring global land observations. Landsat data have been freely available since 2008 (Woodcock et al. 2008), and researchers are able to evaluate the improved nominal 8-day repeat coverage of 30m Landsat observations in characterizing agricultural lands (Arvidson et al. 2001).

In this paper, we exhaustively mine the Landsat archive for the 2013–2014 winter wheat growing season of the Punjab, Pakistan. Our work builds on the forest monitoring work of Potapov et al. (2012) and Hansen et al. (2013) Hansen et al. (2013) who employed per pixel processing of the entire Landsat archive to quantify forest disturbance at national and global scales. Crop type is a much more challenging thematic target compared to forests, relying more on temporal variation to enable discrimination (Wardlow and Egbert 2008). By combining data from the ETM+ and OLI sensors, we posit that image frequency is sufficient to enable crop type discrimination. Here, we process all Rabi growing season Landsat images, generating time-series metrics that capture within season phenological variation. The presented study advances the previous data intensive analyses of forests by focusing on a key commodity crop of Pakistan, winter wheat.

Punjab province is the primary wheat growing region, accounting for about 76% (FAO 2013) of the total area under wheat in Pakistan. Punjab has a small-scale land tenure system with an average field size of 2.1 ha (GoPakistan 2010). About 10% of fields in Punjab province are less than 1 ha in size. Wheat is often planted as part of mixed cropping systems that may include sugarcane, clover, vegetables, and fruit orchards. Remote sensing techniques are sometimes found unsuitable in countries with small farm sizes and heterogeneous cropping systems (Basso et al. 2013). Thus, a number of challenges exist to the successful characterization of Pakistan wheat extent from satellite data.

This paper reports the first production of a provincial wheat cultivated area map using Landsat data based on images within the Rabi growing season. The Results are validated using field data and comparisons with official statistics. Finally, the area estimates were combined with a national yield estimate (SUPARCO 2014) to derive wheat production for the 2013–2014 Rabi wheat growing season.

1.3. Materials

1.3.1. Study area

Pakistan consists of five provinces and one region, of which Punjab province is the second largest in terms of land area with 205,344 km2 (figure 2.1). Punjab, the most populace province with about 56% of the total population of the country has 12.4 million hectares (Mha) of cultivated area (SUPARCO 2012). Punjab is divided into three major agro-ecological zones: the Potohar plateau in the north with rain-fed agriculture, accounting for 10% of the total agricultural area of the province (Qasim 2012); the arid desert in the southern Punjab and arid semi-desert in mid-province with little agricultural production; and the main crop growing region of Indus basin irrigated croplands (SUPARCO 2012).
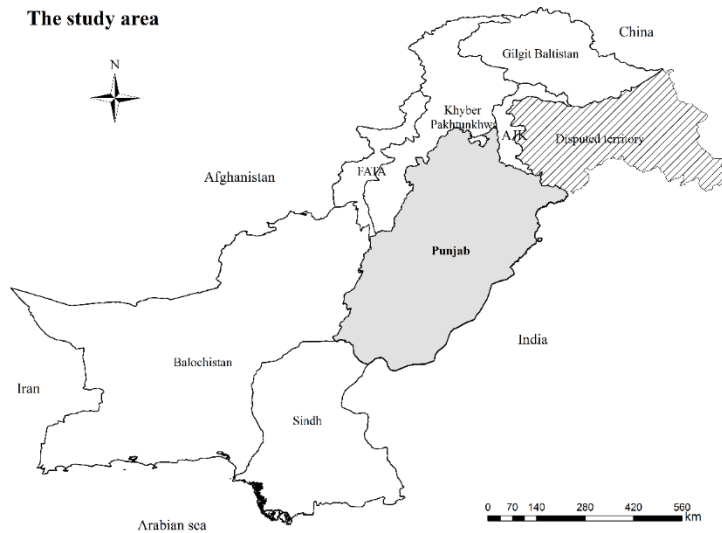
Figure 2.1: The study location, Punjab province of Pakistan (FATA: Federally Administered Tribal Areas; AJK: Azad Jammu and Kashmir).

1.3.2. Data sets

▪ **Remote sensing data sets**

All Landsat imagery from the onset of the Rabi growing season in December 2013 through the peak of the growing season at the end of February 2014 were used to create a multi-temporal feature space for mapping wheat in Punjab. A total of 281 level 1 terrain corrected images from 21 Path and Rows (Table 2.1) were used including 145 Landsat 8 OLI and 136 Landsat 7 ETM+ scenes. We employed four spectral bands from Landsat 7 ETM+: bands 3 red (RED 0.626–0.693 µm), 4 near-infrared (NIR 0.776–0.904 µm), 5 Short-wave Infrared (SWIR: 1.567–1.784 µm), and 7 (SWIR: 2.097–2.349 µm); and corresponding bands from Landsat 8 OLI: bands 4 (RED: 0.630–0.680 µm), 5 (NIR: 0.845–0.885 µm), 6 (SWIR: 1.560–1.660 µm), and 7 (SWIR: 2.100–2.300 µm). Shorter wavelength visible blue and green ETM+ bands 1 and 2 and

OLI bands 2 and 3 were not used due to their greater sensitivity to atmospheric effects (Ouaidrari and Vermote 1999).   ETM+ band 6 (THERMAL: 10.40–12.50 µm) and Landsat 8 OLI Thermal Infrared Sensor band 10 (THERMAL: 10.60–11.19 µm) were used for multispectral time-series metrics production (see below), but were not included in variables for mapping. Normalized difference vegetation index (NDVI) (Tucker 1979) and normalized difference water index (NDWI) (Gao 1996) values were calculated for all observations as inputs to time-series metrics.

Table 2. 1: Landsat tiles world reference system (WRS) path and rows covering Punjab, Pakistan.

Serial No	Path	Row	Number of images	
			L7	L8
1	148	038	6	7
2	148	039	6	6
3	149	037	7	8
4	149	038	6	7
5	149	039	5	8
6	149	040	8	8
7	150	036	6	6
8	150	037	8	8
9	150	038	8	8
10	150	039	8	7
11	150	040	8	8
12	150	041	8	9
13	151	036	6	8
14	151	037	8	8
15	151	038	8	8
16	151	039	8	8
17	151	040	9	8
18	151	041	9	8
19	152	039	2	4
20	152	040	2	3
Total			136	145
Total images (L7 + L8)			281	

Three procedures were performed to radiometrically normalize Landsat observations: (1) top-of-atmosphere reflectance calculation, (2) MODIS-based bias adjustment, and (3) MODIS-based anisotropy adjustment. Each Landsat image was initially converted to top-of-atmosphere reflectance (Chander et al. 2009). The data

were then normalized to spectral reflectance for each Landsat image using MODIS top-of-canopy reflectance data composite as a normalization target (Potapov et al. 2012). To create the cloud-free growing season MODIS reference data, all 16-day MODIS composites from 2000 through 2011 were ranked by NDVI value and then average reflectance values for red, NIR, and SWIR bands were calculated from composites corresponding to 50th–90th percentile ranks. The next step of Landsat image normalization was to apply a Landsat to MODIS bias adjustment, which largely accounted for atmospheric scattering. The final step was a cross-track adjustment to account for effects of surface anisotropy. To perform the cross-track adjustment, Landsat to MODIS bias-adjusted spectral reflectance is modeled as a function of sensor view angle per band; the derived relationship is then applied to all pixels within the image. These methods are referenced in Hansen et al. (2008), Potapov et al. (2012) and Loveland and Dwyer (2012). The implemented radiometric normalization algorithm reduced between and within image reflectance differences caused by variation in atmospheric conditions, dates and surface anisotropy. Using the method from Potapov et al. (2012), quality assessment codes were assigned to each pixel to reflect its probability to be a cloud-free land or water observation. All viable observations within the defined study period were aggregated and used to derive a set of spectral-statistical derivations called metrics. Metrics represent a generic feature space that facilitates large area mapping and have been used extensively with Advanced Very High-resolution Radiometer (AVHRR) and MODIS data (Hansen and DeFries 2004, Chang et al. 2007) and more recently with Landsat data (Potapov et al. 2012). Landsat-based metrics are calculated between a start and end date without direct relation to the day of

the year, in this case, the Rabi growing season of December, January and February, inclusive. Metrics are statistical derivations of all good quality assessed pixels and have been shown to capture salient phenological information for mapping land cover (DeFries et al. 1995, Reed et al. 1994). Landsat-based metrics enable mapping the same crop type within a broad geographic context and over large regions (Pittman et al. 2010, Chang et al. 2007). Using metrics instead of single-date images allowed us to create a complete, wall-to-wall dataset without observation gaps, which is well suitable for regional classification. To create a set of spectral metrics (Table 2.2), we implemented a per-pixel ranking of spectral reflectance values from all cloud-free observations within the growing season. Selected ranked (minimum, maximum, median, selected percentiles) values and averages between selected ranks were recorded as output metric data layers. In addition to single-band ranking, we ranked cloud-free observations by corresponding NDVI, NDWI value, and brightness temperature. This allowed us to collect spectral information corresponding to major phenological stages (e.g. peak of growing season, warmest time of year, etc.). In addition to metrics, time-sequential monthly composites for December, January, and February were created based on a median value taken from all cloud/shadow-free observations within each calendar month. These composite images were used in facilitating image interpretation and assignment of training data.

Table 2. 2: List of metrics used as predictor variables in class wheat cover in Punjab

Metric description	Number of metrics
Interquartile means of ranked bands 3, 4, 5, and 7 and binned and ranked on NDVI, THERM, and NDWI (0–10%, 0–25%, 10–25%, 10–50%, 25–50%, 50–75%, 50–90%, 75–90%, 75–100%, and 90–100%)	320
Interquartile means of ranked bands 3, 4, 5, and 7 (0–100%, 10–90%, 25–75%)	24
Interquartile means of ranked NDWI and NDVI (0–100%, 10–90%, 25–75%, 0–10%, 0–25%, 10–25%, 10–50%, 25–50%, 50–75%, 50–90%, 75–90%, 75–100%, 90–100%)	52
Percentiles of ranked bands 3, 4, 5, and 7 and binned and ranked on NDVI, THERM, and NDWI (0%, 10%, 25%, 50%, 75%, 90%, and 100%)	224
Percentiles of ranked NDWI and NDVI (0%, 10%, 25%, 50%, 75%, 90%, and 100%)	28
Bands 3, 4, 5, and 7, and NDVI and NDWI Mean of three first, median of three first, mean of three last, median of three last, first, and last	72
Bands 3, 4, 5, and 7 and NDVI and NDWI time-series regression slope	12
Bands 3, 4, 5, and 7 and NDVI and NDWI standard deviation	12
Elevation, slope, and aspect	5

Topographic data were also used as independent variables, including elevation, slope, and aspect. These layers were computed from 90 m spatial resolution void–filled seamless digital elevation model derived from the National Aeronautics and Space Administration (NASA) Shuttle Radar Topography Mission (downloaded from CGIAR-CSI: http://srtm.csi.cgiar.org).

▪ **Classification algorithm**

We related the Landsat-derived metrics to training data via a bagged classification tree algorithm (Breiman 1996, Hansen et al. 1996, Potapov et al. 2012, Bwangoy et al. 2013). A classification tree software developed by our research group following the algorithm described by Ripley (1996) was used. Classification trees employ an entropy measure, referred to as deviance, to split multidimensional space of dependent variables into successively more homogeneous hyper volumes, called nodes. The best univariate

split was sought from all independent variables, and the process was repeated until a perfect tree was fit or preset conditions for termination of tree growth were met. We terminated each classification tree when additional splits decreased model deviance by less than 0.001 of the deviance of the total training set population (Bwangoy et al. 2010, Bwangoy et al. 2013). To further avoid overfitting, we used a set of seven bagged tree models each derived from a 20% random sample of training pixels. Each tree reporting a per-pixel probability of wheat cover class membership; the per-pixel median of the seven model outputs was taken as the result (Potapov et al. 2012). Wheat was categorized if this median value was equal to or greater than 50%.

- **Training data**

Training data consisted of manually labeled wheat and not-wheat pixels. To prepare the data for classification and build the classification tree model for discriminating wheat and not-wheat land cover, we used visual image interpretation (Hansen et al. 2008, Potapov et al. 2012) of Landsat time series. Composites from December, January, and February, representing the early, mid and late growing season were visualized in SWIR, NIR, and RED false color combination. The selection of training data was made in light of wheat phenology in Pakistan, following the crop calendar (SUPARCO 2012) and the previous work of Dempewolf (2014) and Becker-Reshef et al. (2010). Water bodies were masked out during data preparation and compositing using the water mask from the Global Forest Cover Change product (Hansen and Loveland 2012). Based on spectral response and landscape context, pixels were trained as wheat and not-wheat classes. As the not-wheat land cover included a number of vegetation types and land forms, not-wheat samples dominated in training population

to account for class heterogeneity. The training data were augmented following each iteration of the bagged tree classification, with output products manually checked using Landsat composites, Google Earth™ high-resolution imagery, and a priori knowledge of the area.

- **Wheat map Validation**

To validate the classification results, we adopted a combination of field visit and photo-interpretation as the response design (Stehman and Czaplewski 1998). A population of 20 km × 20 km blocks covering all of Punjab was created and each block assigned to one of three strata based on wheat area as indicated using an antecedent wheat layer derived using MODIS data (Dempewolf et al. 2013); three MODIS-indicated wheat strata were employed: low (0–22%), medium (22–47%), and high (>47%) wheat cover. For practical consideration related to travel costs, we constrained the sample to 12 sample blocks of 20 km × 20 km each. We allocated four blocks to each of the three wheat strata. The blocks within strata were selected randomly. In each selected sample block, we randomly selected 50 sample points (pixels) with a target to validate 10 points per block (figure 2.2). We followed a protocol of visiting the first 10 randomly generated sample pixels in each of the randomly selected 20 km × 20 km spatial blocks. However, if a sampled pixel could not be accessed within a sample block due to field conditions, social resistance or other security reasons, the next sample pixel in the randomly ordered list was substituted. A total of 35 sample pixels were substituted due to various reasons with most of the omitted sample pixels located where accessibility was limited due to an impassable river (block 7) or by desert terrain (block

6). One sample block was largely within a limited access government installation and was not included in the analysis.
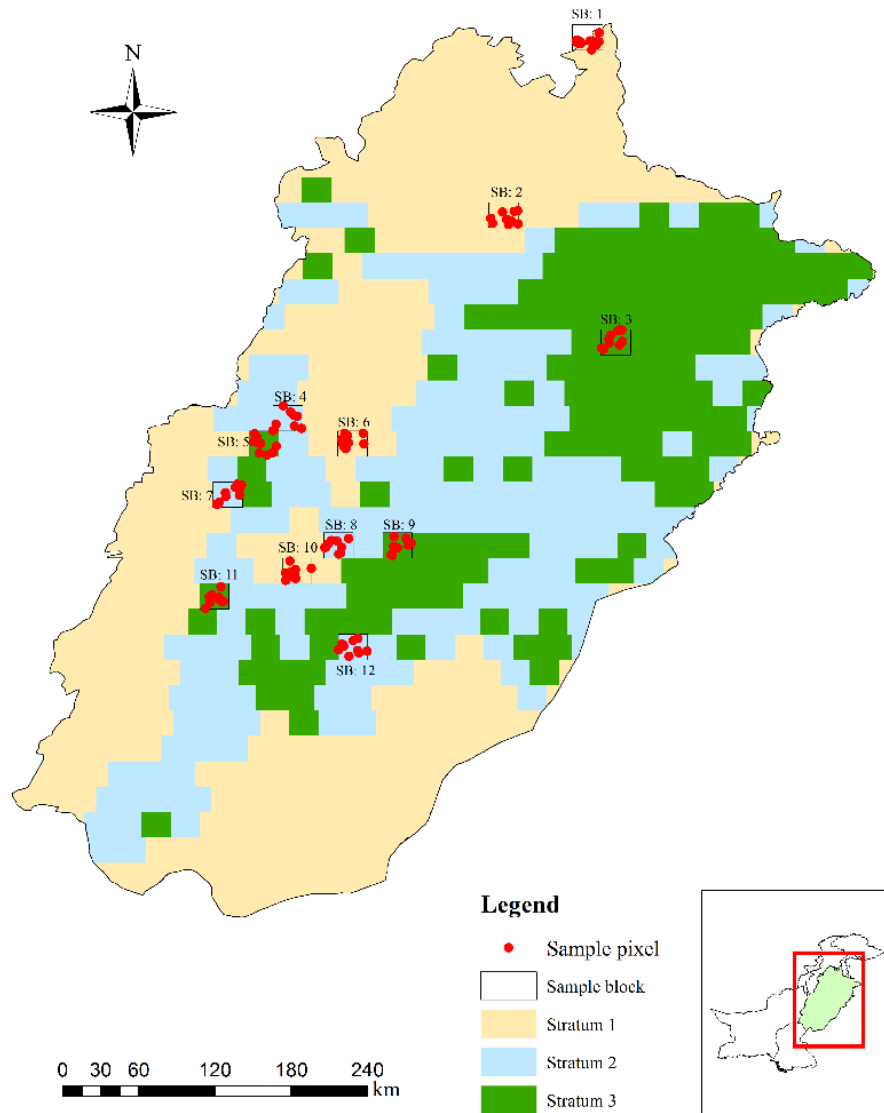
Figure 2.2. Stratified random sample blocks and sampled pixels generated for field data collection on wheat and not-wheat areas from Punjab, Pakistan, for Rabi season 2013 -2014

For each sampled pixel, we quantified the per cent wheat area using field interpretation with additional information from Google Eart incorporated if non-cropland cover such as trees and built-up area was found within the sample pixel. The percentage of wheat in each of the sampled pixels was recorded using 10% increments (i.e. 0%, 10%, 20%, 30%, etc.). Map accuracy and sample-based wheat area were estimated using a stratified two-stage cluster sampling formula Statistical Analysis Software (SAS), Version 9.3, Cary, SAS Institute Inc., North Carolina, USA – details provided in section 2.2.5).

In addition to sample-based validation, we performed an inter-comparison with the second wheat crop forecast released in August 2014 by the Punjab CRS using their crop reporting system (CRS 2014). Provincial and district level wheat area data from the CRS were compared to our Landsat-derived map of wheat cover.

- **Estimation Formulas**

The estimates summarizing the accuracy of the wheat map and the estimates of area of wheat derived from the field-based reference sample data were produced using the SURVEYMEANS procedure of the SAS. For the sampling design implemented, a pixel is indexed by the subscript u, the primary sampling unit is a cluster (indicated by the subscript i), and each cluster is assigned to a stratum h. The notation used to produce the estimates include the following:

K_h = number of blocks in stratum h

k_h = number of blocks sampled in stratum h

$N_{h,i}$ = number of pixels in block i of stratum h

$n_{h,i} = n$ = number of sample pixels within each block ($n = 10$ in this design)

$p_{h,i,u}$ = field-based proportion of wheat for pixel u in block i of stratum h

i   *Estimating area of wheat:*

For sample block i of stratum h, the estimated number of pixels of wheat is $\hat{Y}_{h,i} = N_{h,i}\bar{p}_{h,i}$

where $\bar{p}_{h,i}$ is the sample mean of the $n = 10$ reference sample pixel proportions $p_{h,i,u}$ within

block i of stratum h. The estimated total number of pixels of wheat for stratum h is then

estimated by

$$\hat{Y}_h = \frac{K_h}{k_h} \sum_{i=1}^{k_h} \hat{Y}_{h,i} \tag{1}$$

The estimated total number of pixels of wheat in the entire study region is the sum of

the $\hat{Y}_{h,i}$ values over the three strata. Because each pixel represents 0.0009 km² of area, the

estimated total number of pixels of wheat is multiplied by 0.0009 km² to convert to area of

wheat (in km²). To estimate the standard error of the estimated area of wheat, we begin with

the estimated variance for each stratum,

$$\hat{V}(\hat{Y}_h) = \frac{K_h^2}{k_h}\left(1 - \frac{k_h}{K_h}\right)s_h^2 \tag{2}$$

where s_h^2 is the sample variance of the k_h values of $\hat{Y}_{h,i}$ in stratum h. The variance estimator

does not include the second-stage sampling contribution to variance as this contribution is

typically much smaller relative to the first-stage contribution of variance (Lohr 2010). The

standard error for the estimated area of wheat is the square root of the estimated variance from

(2) multiplied by 0.0009 km².

ii   *Estimating accuracy:*

The basic estimator for accuracy measures used is a ratio estimator for two-stage cluster

sampling within a stratified design (see online documentation provided by SAS version 9.3),

$$\hat{R} = \frac{\sum_{h=1}^{H} \sum_{i=1}^{k_h} \sum_{u=1}^{n} w_{h,i,u} y_{h,i,u}}{\sum_{h=1}^{H} \sum_{i=1}^{k_h} \sum_{u=1}^{n} w_{h,i,u} x_{h,i,u}} \qquad (3)$$

where u is the index of the sampled pixels ($u = 1,\ldots, n$), i is the cluster index in stratum h ($i =$

1, 2, $\ldots, k_h$), h is the stratum index ($h = 1, 2, \ldots, H$), $x_{h,i,u}$ and $y_{h,i,u}$ are defined to yield the

parameter of interest (see below), and $w_{h,i,u} = (K_h N_{h,i})/(k_h n)$ is the estimation weight (i.e. inverse

of the inclusion probability) for sample pixel u in cluster i of stratum h. The variance estimator

for $\hat{R}$ is based on a Taylor series approximation (Sarndal et al. 1992):

$$\hat{V}(\hat{R}) = \sum_{h=1}^{H} \hat{V}_h(\hat{R}) = \sum_{h=1}^{H} \frac{k_h(1-\frac{k_h}{K_h})}{(k_h-1)} \sum_{i=1}^{k_h} (g_{h,i\cdot} - \bar{g}_{h\cdot\cdot})^2 \qquad (4)$$

where

$$g_{h,i\cdot} = \frac{\sum_{u=1}^{n} w_{h,i,u}(y_{h,i,u} - x_{h,i,u}\hat{R})}{\sum_{h=1}^{H} \sum_{i=1}^{k_h} \sum_{u=1}^{n} w_{h,i,u} x_{h,i,u}} \qquad (5)$$

and

$$\bar{g}_{h\cdot\cdot} = (\sum_{i=1}^{k_h} g_{h,i\cdot})/k_h . \qquad (6)$$

The error matrix summarizing the accuracy of the wheat map is constructed using the approach

of sub-pixel fractional error matrices (Latifovic and Olthof 2004). Define $m_{h,i,u}$ as the mapped

proportion of wheat (0 if no wheat, 1 if wheat) and define $r_{h,i,u}$ as the reference proportion of

wheat for pixel u in cluster i of stratum h. The error matrix is constructed such that the map

classification is displayed as the rows and the reference classification as the columns. For

example, the cell entry for the intersection of the first row and first column represents area of

agreement for wheat. The information required to estimate the proportion of area in row r and

column c of the error matrix is denoted by $Y_{rc,h,i,u}$. To compute the sub-pixel fractional values

for each pixel, we need to recognize two cases.

Case 1: $m_{h,i,u} < r_{h,i,u}$ (i.e. the map proportion of wheat is less than the reference proportion of wheat for pixel u in cluster i of stratum h). The sub-pixel fractional values are then as follows:

$$Y_{11,h,i,u} = m_{h,i,u} \tag{7}$$

$$Y_{12,h,i,u} = 0 \tag{8}$$

$$Y_{21,h,i,u} = r_{h,i,u} - m_{h,i,u} \tag{9}$$

$$Y_{22,h,i,u} = 1 - Y_{11,h,i,u} - Y_{12,h,i,u} - Y_{21,h,i,u} \tag{10}$$

Case 2: $m_{h,i,u} \geq r_{h,i,u}$ (i.e. the map proportion of wheat is greater than or equal to the reference proportion of wheat for pixel u in cluster i of stratum h). The sub-pixel fractional values are then as follows:

$$Y_{11,h,i,u} = r_{h,i,u} \tag{11}$$

$$Y_{12,h,i,u} = m_{h,i,u} - r_{h,i,u} \tag{12}$$

$$Y_{21,h,i,u} = 0 \tag{13}$$

$$Y_{22,h,i,u} = 1 - Y_{11,h,i,u} - Y_{12,h,i,u} - Y_{21,h,i,u} \tag{14}$$

To estimate user's accuracy of wheat based on the estimator $\hat{R}$ (equation 3), define

$$y_{h,i,u} = Y_{11,h,i,u} \tag{15}$$

and

$$x_{h,i,u} = Y_{11,h,i,u} + Y_{12,h,i,u}. \tag{16}$$

To estimate producer's accuracy of wheat based on equation (3), define

$$y_{h,i,u} = Y_{11,h,i,u} \tag{17}$$

and

$$x_{h,i,u} = Y_{11,h,i,u} + Y_{21,h,i,u}. \tag{18}$$

Lastly, to estimate overall accuracy, define

$$y_{h,i,u} = Y_{11,h,i,u} + Y_{22,h,i,u} \tag{19}$$

and

$$x_{h,i,u} = 1. \tag{20}$$

1.4. Results

1.4.1. Estimated wheat area and production for Punjab

The resulting Landsat-based wheat map depicts 6.13 Mha of wheat area in Punjab

during the 2013–2014 Rabi crop season (see figure 2. 3). This is 9.44% lower than

the 6.77 Mha wheat area in Punjab as estimated in the second report of the Punjab

CRS (2014).
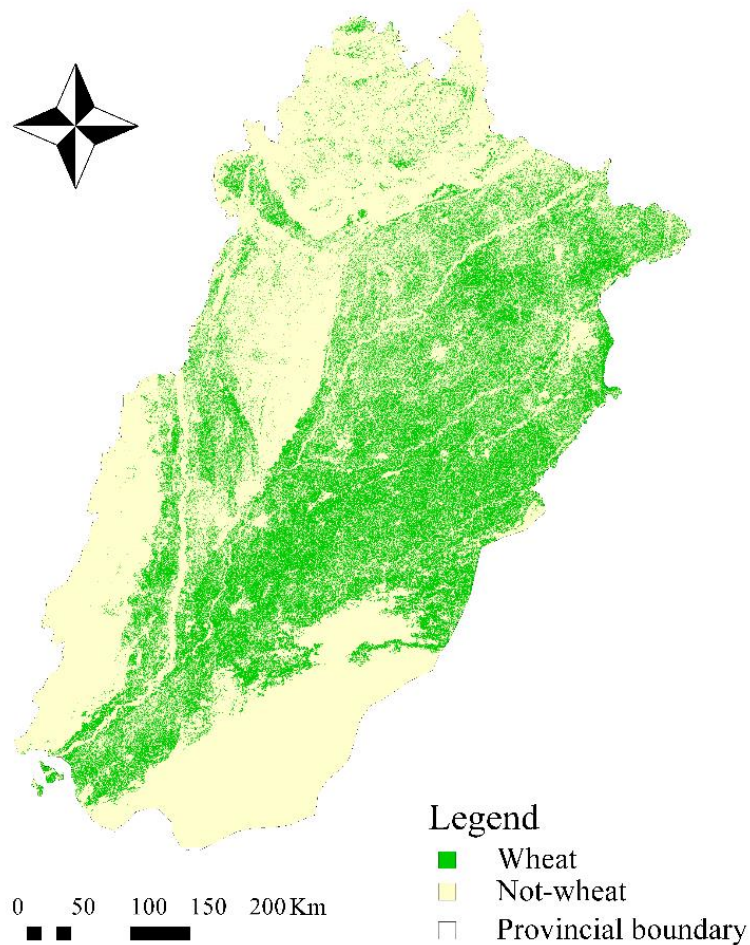
Figure 2.3. Rabi season 2013-2014 wheat classification map for Punjab, Pakistan.

We calculated per-district crop area from our wheat map for the 36 districts of Punjab and compared these estimates to those of the second official estimate released by the Government of Punjab (CRS 2014). The linear regression reveals a strong association (Coefficient of determination R2 = 0.71) between the two estimates (figure 2.4). While our overall Landsat-based result for Punjab is lower than the official estimate, the estimate for 13 districts is higher, ranging from +3 to +54% higher in Lahore and Sahiwal, respectively. For the remaining 23 districts, our estimate is lower, from -1 to -77% for Faisalabad and Attock, respectively.

We also calculated a wheat yield forecast, using the minimum average production of 3000 kg ha–1 for the 2013–2014 wheat growing season (SUPARCO, 2014). The CRS Punjab estimated 19.11 MT of wheat in their second report, while our classification estimated 18.34 MT, or 4.0% lower than that of the CRS forecast. The linear regression (figure 2.5) reveals a strong association between the yield estimate per district and the CRS yield estimate ($R^2 = 0.85$).
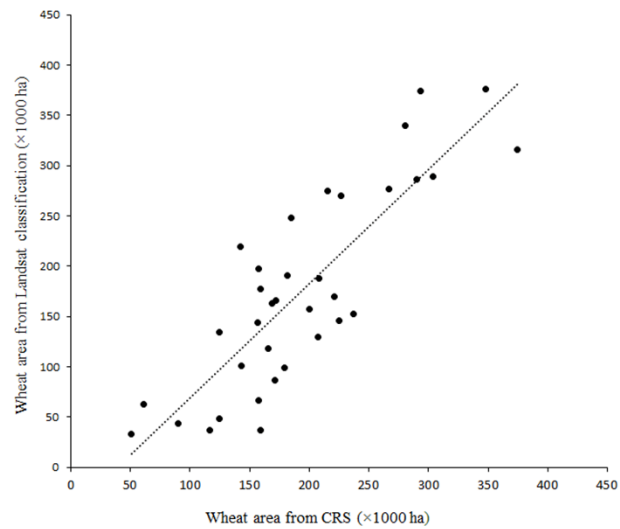
Figure 2.4. Relationship of per-district wheat area derived from CRS Punjab and Landsat -derived wheat classification map.
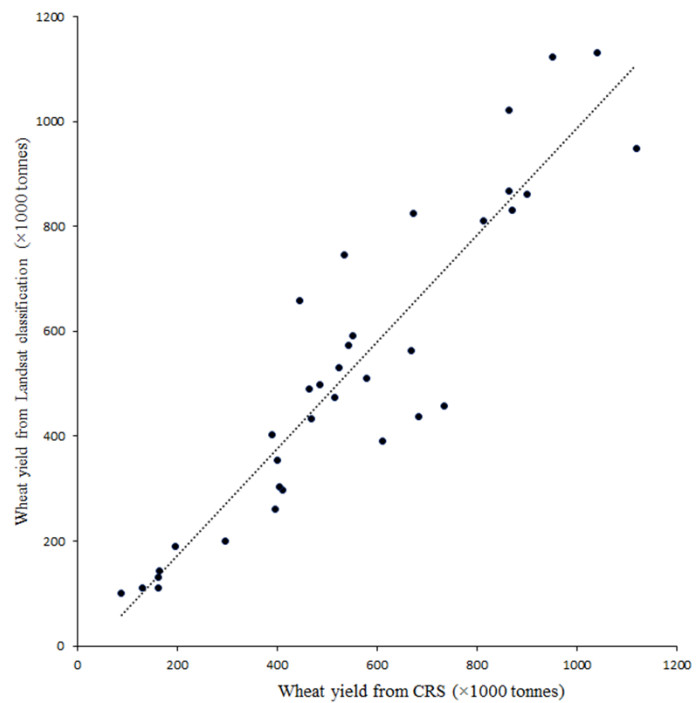
Figure 2.5. Relationship of per-district wheat yield estimates derived from CRS Punjab and Landsat-derived wheat classification map.

1.4.2. Validation of Landsat wheat mapping for Punjab with field data

To validate our Landsat-derived wheat map, we overlaid our field-based sample points on the classification results to assess product accuracy (Table 2.3). Our estimated overall accuracy was 76% (standard error (SE) = 7.0%). User's accuracy was 62% (SE = 8%) for wheat and 84% (SE = 7%) for not-wheat, whereas producer's accuracy was 70% (SE = 7%) for wheat and 78% (SE = 8%) for not-wheat. Based on the sample of field-based interpretation of wheat we estimated that 33.75% or 6.96 Mha was under wheat in Punjab.

Table 2. 3: Accuracy of wheat map with field (reference) per cent area of wheat determined to nearest 10%

		Field observation		Row total (%) (standard error)	User's accuracy(%) (standard error)
		Wheat (% area)	Not-wheat (% area)		
Classification	Wheat (% area)	23.7	14.5	38.2 (6.5)	62 (8)
	Not-wheat (% area)	10.1	51.8	61.8 (6.5)	84 (7)
	Column total (%) (standard error)	33.8 (5.2)	66.3 (5.2)		
	Producer's accuracy (%) (standard error)	70 (7)	78 (8)		

Cell entries represent per cent area; overall accuracy is 76% with a standard error of 7%.

Disagreement in the classification results for wheat and not-wheat area mainly occurred from commission errors of clover fields identified as wheat. The classification could not separate clover from wheat due to its similar spectral response during the growing season; further complicating matters, wheat is often grown mixed with clover to produce quality fodder for livestock. Omission errors of wheat occurred mostly in small farms or mixed cropping zones, particularly fruit orchards with wheat as an understorey crop. Another source of omission error of wheat was attributable to mixed crops usually with mustard being present along with wheat. The

spectral response from wheat in these mixed crop situations was often dominated by other not-wheat crops, resulting in wheat omission errors.

In fruit orchards, particularly large mango orchards, where the ground is either fallow or cultivated with clover or wheat, the classification patterns were different. The mature stands of mango orchards were classified as not-wheat, but immature and young stands or mature stands with larger tree-to-tree distance had either clover or wheat and were largely mapped as wheat. The omission of understorey wheat in the classified map is believed to be the main reason for wheat underestimation by our Landsat-based product. Though not considered a major contributor to the accuracy of the classification, variation of sowing time by a month between the southern and northern parts of the province might also be a factor.

1.4.3. Sample based estimate comparison with classification map and CRS estimate

We estimated Rabi season 2013–2014 wheat area for Punjab using the field-sampled data from within the 11 sample blocks. The sample-based area estimate yielded 6.96 Mha of wheat, higher than the CRS estimate of 6.77 Mha and higher than the 6.13 Mha estimated from the Landsat-based wheat map. However, due to the small sample size of blocks, both the Landsat map and CRS wheat estimates were within the 95% confidence interval of the field-based estimate (figure 2.6).
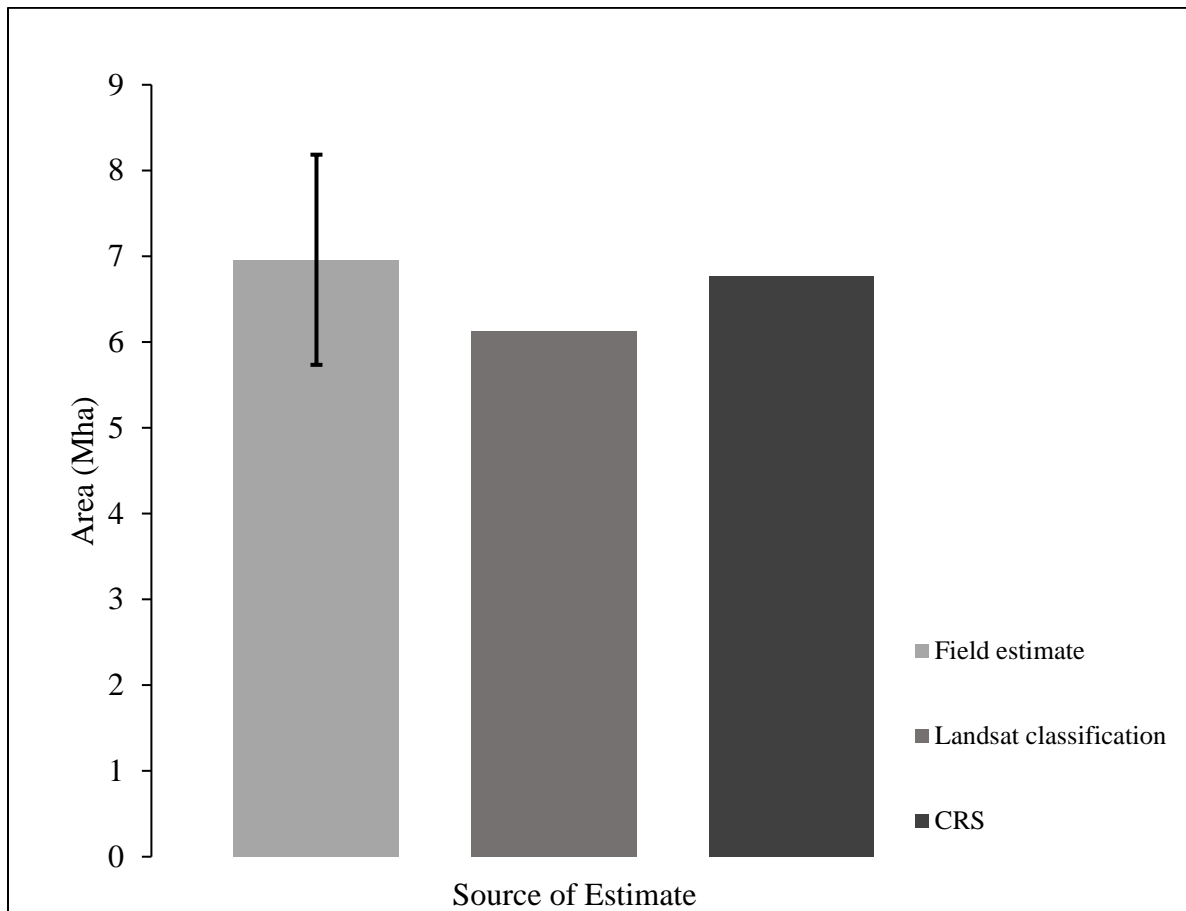
Figure 2.6: Wheat area estimates for Punjab (2013-2014).

Note: standard errors are shown for field sample and map-based area estimate only: CRS does not report estimate error.

1.5. Discussion

We classified Punjab land cover into wheat and not-wheat areas for the Rabi cropping

season of 2013–2014 using seven bagged classification trees (figure 2.3). On

average, each of the tree models contained 50 nodes (maximum 59, minimum 42).

The 90th percentile of NDVI metric (18%) and the interquartile mean of the 75th–

100th percentile of NDWI (17%) contributed most in reducing model deviance.

Other significant metrics included the interquartile mean of the 50th and 90th

percentiles of NIR reflectance (10%), the interquartile mean of the 50th–90th

percentile NDWI (9%), the interquartile mean of the 75th–90th percentile NDWI

(8%) and the seasonal mean of NDWI (8%).   A third tier of metrics included the

seasonal mean of NIR (5%), slope (4%), and the interquartile mean of the 50th–90th

percentile of NIR binned on NDVI (3%). From the total of 750 metrics evaluated, the

first 29 metrics explained 90% of the root deviance decrease. The results from the

tree models illustrate the importance of NIR-based ratios in identifying wheat

phenology.

Our results demonstrate the utility of Landsat time-series data in quantifying

wheat extent in a landscape characterized by small field sizes and high crop diversity.

Winter Rabi crop cover is dominated by wheat, facilitating its characterization. We

found other cover types, particularly clover, to be associated with errors of

commission. Omission errors were largely related to landscape complexity,

specifically mixed cropping. For example, wheat crops within mango orchards were

largely omitted. Overall, our map-based and sample-based results are within 10% of

the official statistics for crop area and yield. This strengthens the view that Landsat

time-series characterization of wheat cover could be a first source for within-growing

season wheat assessment and estimation. The approach could easily complement the

conventional "Village List Frame" method used by the CRS of Punjab by providing

an interim assessment in lieu of the more field-intensive and delayed CRS reporting.

Timely information on wheat production can support key decisions regarding wheat

management, transportation, and storage. The results from the Landsat classification

can be reliably used for making decisions on disposal of stock in case of surplus

production or importing in case of lower production, ultimately reducing risks of wheat shortage and ensuring food security.

The field-based sampling validated the Landsat time-series wall-to-wall classification of wheat and not-wheat map. A more intensive application of stratified field-based estimation, guided by Landsat, is a promising research topic. Also, incorporating very high spatial resolution imagery, such as RapidEye 5m pixel-1 data, would be another promising area of investigation. Landsat-based maps could serve as a crop indicator to guide allocation of field samples and/or very high spatial resolution imagery acquisitions to further reduce the uncertainty of cultivated wheat area estimation in regions like Punjab.

Very high spatial resolution imagery could explain the impacts of field size and mixed cropping methods on errors in the Landsat-based product. Subsequent efforts could be calibrated to account for such errors in the operational use of freely available Landsat data. The Landsat-like spectral bandwidths of the Sentinel 2 satellites (Drusch et al. 2012) promise a further enrichment of freely available, systematically acquired, medium spatial resolution, time-series multispectral data. In particular, the 10m red and NIR bands and 20m SWIR bands of Sentinel 2 may increase wheat mapping accuracy. Our results highlight the utility of the NIR band for Rabi season wheat mapping, particularly in combination with red and SWIR bands; the NDVI and NDWI indices were the most valuable in characterizing wheat cover.

1.6. Conclusion

Exhaustive use of available Landsat data for the 2013–2014 Rabi (winter) growing season in the Punjab province of Pakistan resulted in a wheat map that corresponds closely to official statistics and field validation data. The presented method has advantages over the currently used "Village List Frame" method, particularly in the possibility of delivering actionable cultivated area data at or near the end of the growing season. Because the method uses freely available data and can be applied before wheat crop harvest, it potentially has high value for decision support systems concerning wheat production and trade. Specifically, wheat crop management, storage and transportation arrangements, decisions on exports and imports of wheat grain and food security can be facilitated using the results from the demonstrated method if implemented at or near the end of the Rabi season.

Finally, the use of all available Landsat data to create a feature space appropriate for large area crop type mapping was demonstrated, building upon previous forest extent and change mapping efforts. For countries without robust geospatial survey data or those seeking more timely data on crop extent, national-scale mapping using Landsat data is a viable option. Testing Landsat data in other agricultural landscapes and characterizing different crop types should be a focus of future research.

Chapter 3:Evaluating Landsat and RapidEye data for Winter Wheat Mapping and Area Estimation in Punjab, Pakistan

1.7. Introduction

Coarse and medium resolution remote sensing data have advantages over high-resolution data due to their spatial coverage, temporal resolution, and availability at near real time (Junior et al. 2014). For large-scale fields (>50 ha) in intensively managed commercial landscapes, Landsat has proven to be sufficient for accurate mapping of crop type (King et al. 2017, Song et al. 2017). However, the use of medium spatial resolution remote sensing data for crop characterization in finer-scale land tenure systems, such as found in Punjab in Pakistan, is challenged by a supposed preponderance of mixed pixels (Carfagna and Gallego 2005) that results in higher uncertainty of area estimates and lower map accuracy (Dempewolf et al. 2014, Khan et al. 2016). Spatial resolution (pixel size for digital data) determines the area of the smallest separate field that can be identified (Mulla 2013), which is significant for land tenure systems such as those found in Punjab, where the average field size is 5.6 ha (GoPakistan 2010). One way to improve the performance of medium spatial resolution data is to integrate it with high spatial resolution commercial imagery. High-resolution data provide more spatially detailed observations of complicated land tenure systems, thereby potentially improving map accuracies. Areal extent of temporally frequent growing season imagery for high spatial resolution data is still limited, despite recent progress (Zheng et al. 2016). More importantly, the cost of commercial data limits their general use. In this study, we tested the integration of available growing season RapidEye images (5 m) and Landsat 30 m data for Punjab

province in Pakistan for winter wheat mapping. Accurate within-season area estimation of cultivated wheat (Khan et al. 2016) is crucial to pre-harvest decision making on transportation, storage, and trade (WB and FAO 2011). The Crop Reporting Service (CRS) of the Agriculture Department of Punjab has the mandate to produce official wheat area and production data in support of policy decisions. CRS uses a labor intensive "area list frame" sampling approach to generate crop statistics months after wheat harvest (Verma et al. 2011, Heremans et al. 2011), reducing the utility of the data for quick policy and market responses (WB and FAO 2011, Atzberger 2013). An alternative approach to overcome the challenges of timely reporting (Akhtar 2012, Yao et al. 2013, GoPakistan 2010) and accurate estimation (Dempewolf et al. 2014, Khan et al. 2016) of wheat cultivated area is needed. Khan et al. ((2016) employed 30 m Landsat data to characterize wheat in Punjab using a classification tree algorithm, which yielded an overall accuracy of 76%. With the focus to improve map accuracy in the context of Punjab's small field, multiple cropping agriculture system, we evaluated the use of high spatial resolution commercial data as a training data source for Landsat-scale mapping. The objectives were to: (1) Evaluate which type of training data (continuous versus categorical) and which type of wheat map (per cent wheat versus binary wheat / no wheat) produced the best accuracy; and (2) evaluate the benefit of the maps when the maps are used for the purpose of reducing standard errors of wheat area estimates derived from the field sample. The first objective focuses on the common problem of how to produce the most accurate map, whereas the second objective focuses on a practical use of a map which is to provide auxiliary information for increasing precision of area estimates.

Following good practice guidance (Olofsson et al. 2014), we implemented a probability sampling design to obtain *in situ* reference data to assess the accuracy of the wheat maps. Antecedent crop type maps were used to stratify the study area into high, medium and low strata for use in selecting the sample (Khan et al. 2016, Song et al. 2017, King et al. 2017). We also used these field sample data to estimate wheat area for the 2014–2015 growing season. In our area estimation method, the maps are used as auxiliary information incorporated in what is called a "difference estimator". We posited that the more accurate map product would yield a greater reduction in standard error of the wheat area estimate derived from the field sample. This part of our study was designed to assess if sub-pixel per cent wheat cover, enabled by high-resolution training data from RapidEye, would serve as better auxiliary information for purposes of reducing the standard error of the area estimate of wheat compared to auxiliary information in the form of a categorical wheat/no wheat map.

1.8. Materials and Methods

1.8.1. Study Area

Punjab is the most populated province of Pakistan with 56% of the total population and is the second largest in terms of land area with 205,344 km^2 (figure 3.1). The province, with 12.4 million hectares (Mha) of cultivated area, is considered the bread basket for Pakistan (SUPARCO 2012). During Rabi season (December–April) of 2014–2015, official reported area of winter wheat equalled 6.98 million hectares (CRS 2015). The province is divided into three major agro-ecological zones: (1) the Potohar plateau in the north with rain-fed agriculture, accounting for 10% of the total agricultural area of the province (Qasim 2012); (2) the arid desert and semi-

desert in the south and central region of the province with little agricultural production; and (3) the main irrigated crop growing region of Indus basin (SUPARCO 2012). Punjab province produces wheat and other staple food (Ministry of Finance 2014, Khan et al. 2016, Dempewolf et al. 2014) to ensure food security of over 200 million people (Jabeen et al. 2015, GoPakistan 2017) and contributes significantly to region's economic development (Branca et al. 2011). The livelihoods of approximately 66% of the rural communities in Pakistan are associated with agriculture (Dempewolf et al. 2013).
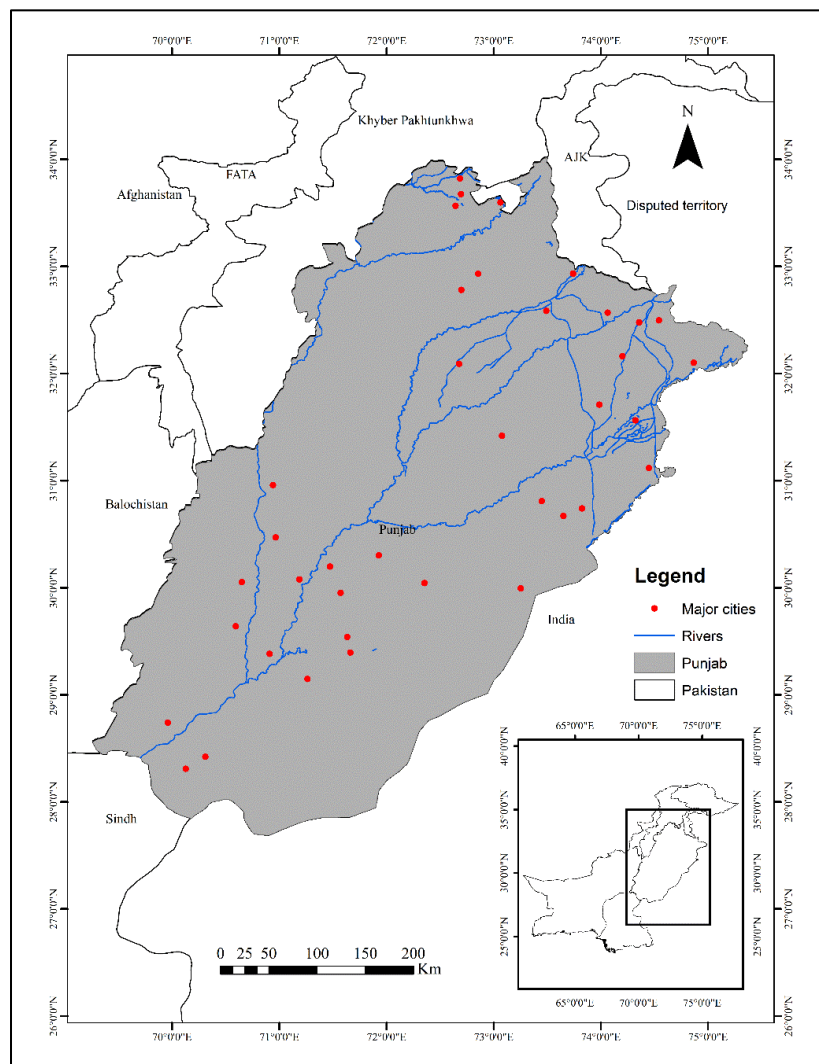
Figure 3.1. Map of the study area, Punjab Province (Pakistan).

1.8.2. Data and Methods

▪ **Remotely Sensed Data**

In this research, time-series of Landsat 30-m per pixel data and single-date 5-m per pixel RapidEye imagery were used. Given that Landsat data are freely available, all Landsat images within the Rabi winter wheat growing season of 2014–2015 were downloaded and used to generate 750 multi-temporal spectral metrics. Nine RapidEye images from the peak of the growing season were purchased from the data provider. RapidEye images cover 20% of the province area.

i   Landsat Data

The Landsat imagery for the Rabi growing season starting in December 2014 and ending in March 2015 were used to create a set of multi-temporal spectral metrics for mapping wheat in Punjab. A total of 307 level 1 terrain corrected (L1T) images from 20 WRS2 path/rows (figure 3.2) were used including 160 Landsat 8 OLI and 147 Landsat 7 ETM+ scenes.
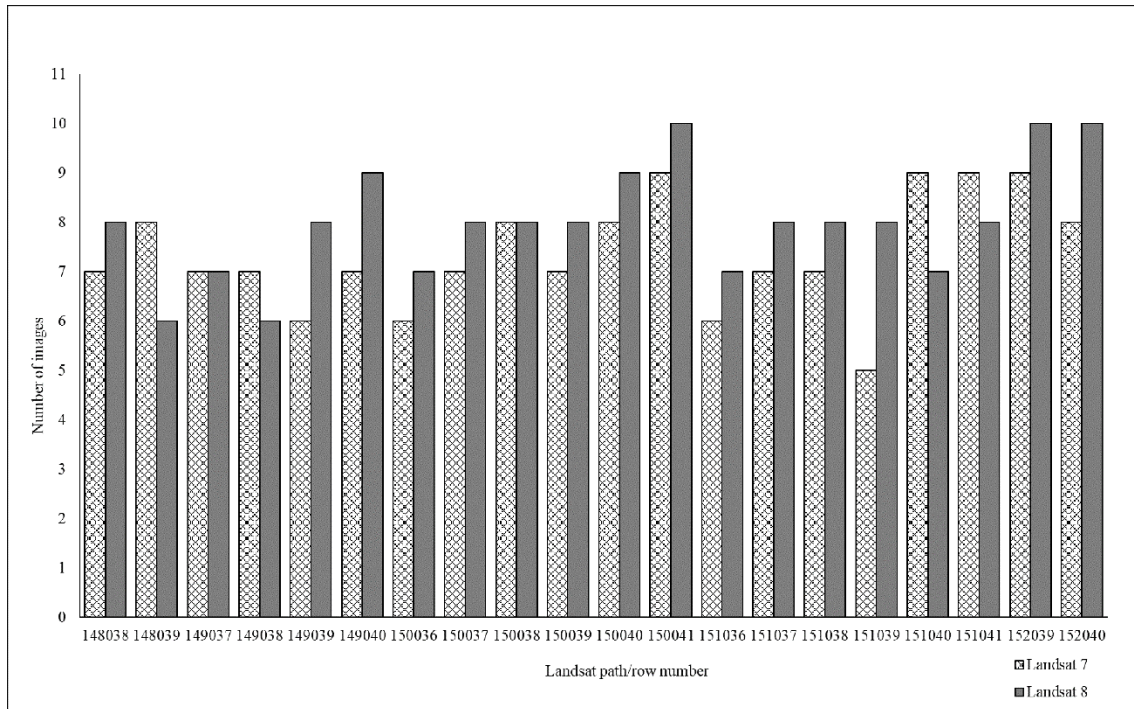
Figure 3.2. Landsat data volumes used in this study.

Four spectral bands, including red (0.626–0.693 µm), near infrared (NIR; 0.776–0.904 µm), and short wave infrared (SWIR1; 1.567–1.784 µm and SWIR2; 2.097–2.349 µm) were used as input data from the Landsat 7 ETM+ images. For the Landsat 8 OLI images, the corresponding bands were used: red (0.630–0.680 µm), NIR (0.845–0.885 µm), SWIR1 (1.560–1.660 µm), and SWIR2 (2.100–2.300 µm). The shorter wavelength visible blue and green spectral bands were not employed due to their greater sensitivity to atmospheric effects (Ouaidrari and Vermote 1999). Thermal infrared bands (ETM+ 10.40–12.50 µm and TIRS 10.60–11.19 µm) were used for multi-temporal spectral metrics production (see below), but were not included as variables for mapping. Normalized Difference Vegetation Index (NDVI) (Tucker 1979) and Normalized Difference Water Index (NDWI) (Gao 1996) values were calculated for all observations as inputs to generate metrics (Khan et al. 2016), which were created using all cloud-free Landsat observations within the wheat

growing season. These multi-temporal spectral metrics were designed to capture spatial and reflectance variations within the wheat growing season and facilitate large area mapping (Potapov et al. 2012).

Multi-spectral data for each Landsat image were initially converted to top-of-atmosphere reflectance (Chander et al. 2009). Reflectance data were then normalized using Moderate Resolution Imaging Spectroradiometer (MODIS) top-of-canopy reflectance data composite as a normalization target (Potapov et al. 2012). To create the cloud-free growing season MODIS reference data, all 16-day MODIS composites from 2000 through 2011 were ranked by NDVI value. Using 16-day composites corresponding to NDVI ranks between 50th and 90th percentile, we calculated mean surface reflectance for each spectral band. For individual Landsat image the per-pixel difference between top-of-atmosphere spectral reflectance and MODIS surface reflectance composite was used to (i) apply reflectance bias adjustment, which largely accounted for atmospheric scattering; and (ii) apply a cross-track adjustment to account for effects of surface anisotropy. To perform the cross-track adjustment, the reflectance bias was modeled as a function of sensor view angle per band; the derived relationship was then to apply bias adjustment to all pixels of the Landsat image. The radiometric normalization algorithm reduced between and within image reflectance differences caused by variation in atmospheric conditions, dates and surface reflectance anisotrophy (Hansen et al. 2008). Using the method from (Potapov et al. 2012), quality assessment codes were assigned to each pixel to reflect its probability to be a cloud-free land or water observation.

All viable observations within the defined study period were aggregated and used to derive a set of spectral-statistical derivations called multi-temporal spectral metrics. Metrics represent a generic feature space that facilitate large area mapping and have been used extensively with Advanced Very High-resolution Radiometer (AVHRR) and MODIS data (Hansen and DeFries 2004, Chang et al. 2007) and more recently with Landsat data (Khan et al. 2016, Potapov et al. 2012). Landsat-based metrics are calculated between a start and end date without direct relation to the day of the year, in this case the Rabi growing season of December, January and February (Figure 3.3). Multi-temporal spectral metrics are statistical derivations of all good quality assessed pixels and have been shown to capture salient phenological information for mapping land cover (DeFries et al. 1995, Reed et al. 1994). Landsat-based metrics enable mapping the same crop type within a broad geographic context and over large regions (Pittman et al. 2010, Chang et al. 2007). Using metrics instead of single-date images allowed us to create a complete, wall-to-wall dataset without observation gaps, which is well suited for regional classification. To create a set of multi-temporal spectral metrics, we ranked all cloud-free Landsat observations per pixel corresponding to (i) band reflectance value; (ii) NDVI value; (iii) NDWI value; and (iv) brightness temperature value. For each spectral band and ranking method, minimal, 10th, 25th, 50th, 75th, and 90th percentile, and maximal values were recorded as a set of metrics. In addition, we calculated and recorded mean reflectance for all values between minimum and 10th percentile, minimal and 25th, 10th and 25th, 25th and 50th, 50th and 75th, 25th and 75th, 10th and 50th, 75th and maximal, 90th percentile and maximal, 10th and 90th percentile, and minimal and maximal

values for each band and ranking. Multi-temporal spectral metrics allowed us to

collect spectral information corresponding to major phenological stages (e.g., peak of

growing season, warmest time of year, etc.). In addition to metrics, time-sequential

monthly composites for December to March were created based on a median value

taken from all cloud/shadow-free observations within each calendar month to

facilitate image interpretation and assignment of training data.
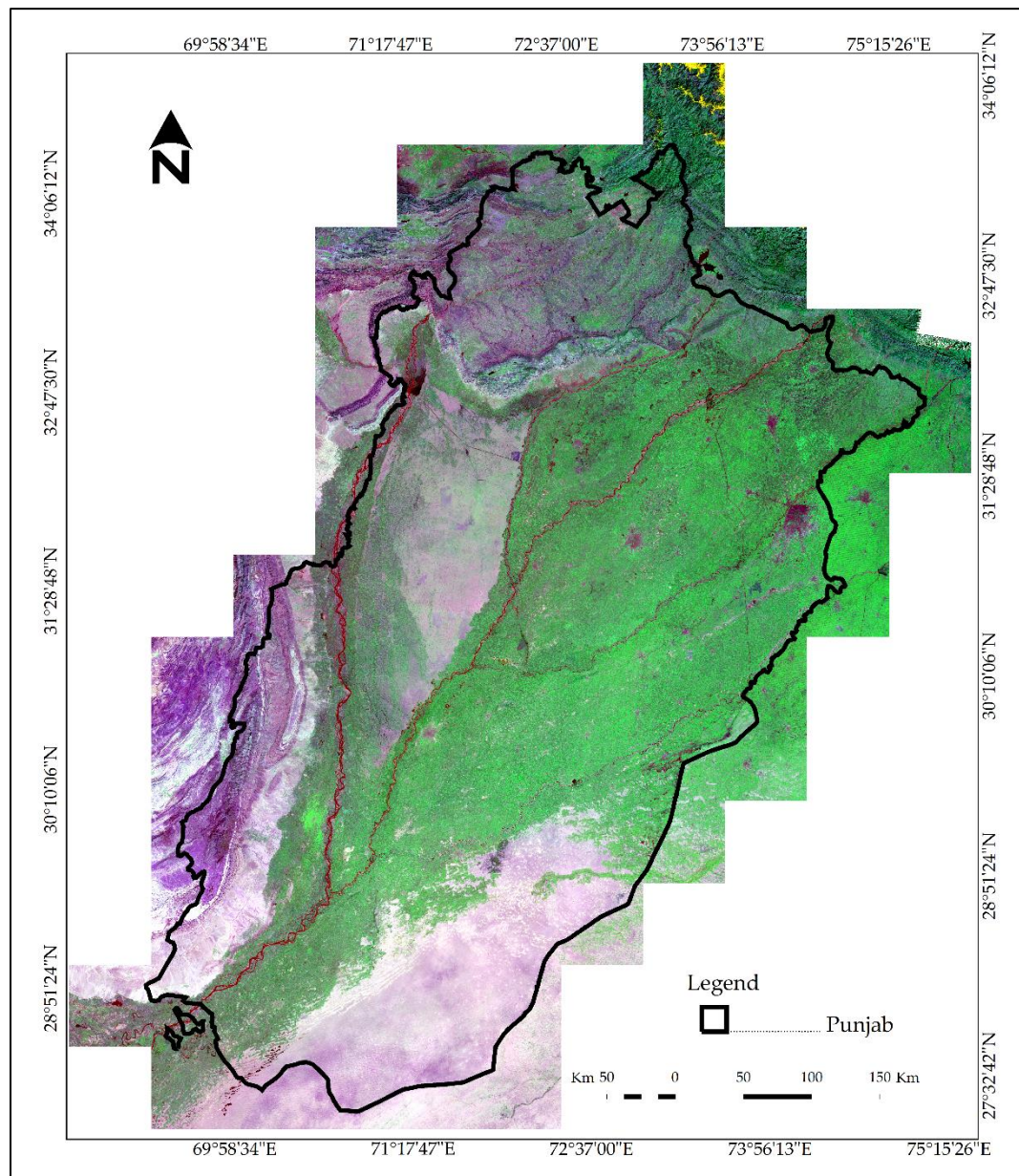
Figure 3.3. Median growing season Landsat metrics for SWIR (1.6 µm), NIR, and RED in r-g-b.

ii   ***RapidEye Data***

RapidEye, a constellation of five satellites, delivers high spatial resolution

data (Stoll et al. 2012) that enable fine scale mapping (Arnette et al. 2015). RapidEye

5 m spatial resolution 1B images acquired between January and March 2015 were

procured. From available RapidEye data collections during the Rabi season of 2015, nine

images within the peak and end of the growing season were used in this study (Table

3.1). Images collected during the peak of growing season were most useful for crop

type interpretation (figure 3.4). Late growing season images provided enough

information for crop identification even though wheat crops were ripe in the southern

part of the province. Images outside of the mid-January to late March interval were

not useful in separating wheat from other land cover (Atzberger and Rembold 2013).

Table 3. 1: RapidEye data used in development of winter wheat training data.

Sr. #	RapidEye Image Acquisition Date	Image ID	Season
1.	16 January 2015	23434141_326753	Early growth stage
2.	31 January 2015	23433903_326754	Before peak season
3.	09 February 2015	23433753_326753	Peak growing season
4.	20 February 2015	23434179_326753	Peak growing season
5.	18 March 2015	23434146_326755	Late growing season
6.	18 March 2015	23434725_326754	Late growing season
7.	20 March 2015	23434185_326753	Late growing season
8.	25 March 2015	23433892_326753	Before harvest
9.	25 March 2015	23433908_326754	Before harvest

The RapidEye data were resampled to a 5 m raster grid nested to Landsat 30

m pixels. All spectral bands (blue, 0.44–0.51 μm; green, 0.52−0.59 μm; red,

0.63−0.69 μm; red edge, 0.69−0.73 μm; and NIR, 0.76−0.85 μm) were used as inputs

to classification. Three spectral bands (red, red edge and NIR) were used for visual

interpretation of wheat crops. The red edge band sensitivity to chlorophyll content

(Crnojevic et al. 2014) was a useful input in facilitating wheat cover identification

(Schuster et al. 2012). The RapidEye data were used to derive per pixel per cent

wheat area and per pixel categorical wheat/no wheat training data for the respective

regression and classification tree analyses.
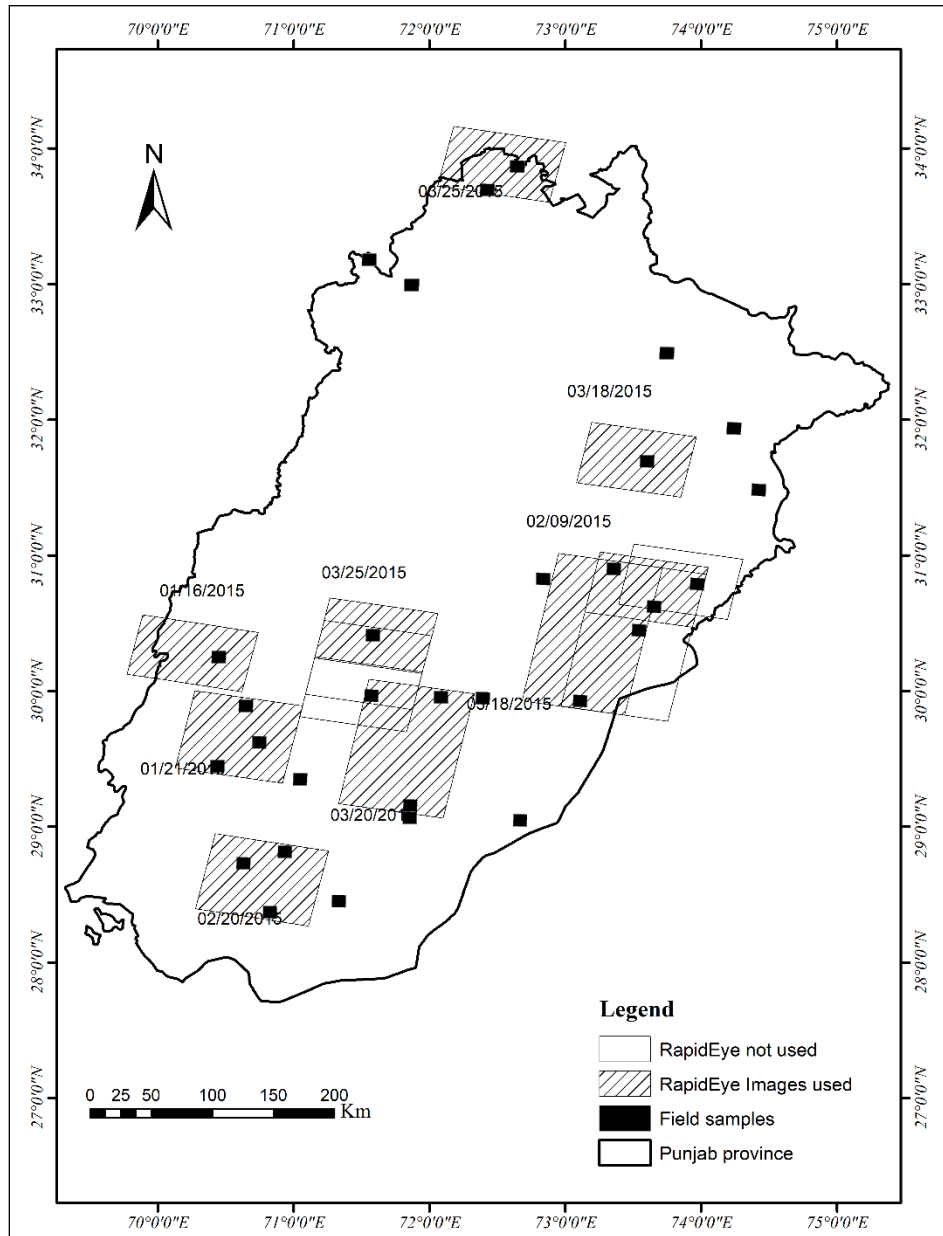
Figure 3.4. Locations of RapidEye growing season images.

iii *Topographic Data*

Topographic data were also used as independent variables, including elevation, slope and aspect. These layers were computed from 30 m spatial resolution void–filled seamless Digital Elevation Model (DEM) derived from the National Aeronautics and Space Administration (NASA) Shuttle Radar Topography Mission (SRTM) (downloaded from CGIAR-CSI: http://srtm.csi.cgiar.org).

- **Wheat Mapping: Regression and Classification Trees**

We related the 5 m RapidEye multispectral data to visually derived categorical training data via a bagged decision tree algorithm to obtain wheat/no wheat maps at the 5 m spatial resolution within each image footprint (figure 3.5). The individual 5 m RapidEye classifications were aggregated and resampled to 30 m spatial resolution by calculating the per cent of 5 m wheat pixels within each 30 m output cell. The 30 m Landsat multi-temporal spectral metrics were related to 30 m RapidEye-derived categorical and per cent wheat-training data via respective bagged classification and regression tree models (Breiman 1996, Hansen et al. 1996, Potapov et al. 2012, Bwangoy et al. 2013, Khan et al. 2016). The classification and regression tree software implemented by our research group follows the algorithm described by (Ripley 1996). Classification trees employ an entropy measure, referred to as deviance, to split a multi-dimensional space of dependent variables into successively more homogeneous subsets (Hansen et al. 2011). In regression trees, a sum of squares criterion is used to split the independent variables into successively less varying subsets of a continuous variable (Hansen et al. 2011). The best univariate split that yields the maximum reduction in entropy or variability is selected to build the classification or regression tree model, respectively (Hansen et al. 2011). We

terminated each classification or regression tree when additional splits decreased

model deviance or variability by less than 0.001 of the deviance of the total training

set population (Bwangoy et al. 2010, Bwangoy et al. 2013, Breiman et al. 1984,

Hansen et al. 2002). To further avoid over fitting, we used a set of seven bagged tree

models, each derived from a 20% random sample of training pixels. Each

classification tree yielded a per pixel probability of wheat cover class membership,

and each regression tree yielded a per pixel per cent wheat cover estimate (figure 3.5).

For both the classification and regression tree models, the per-pixel median of the

seven model outputs was selected as the final result (Potapov et al. 2012). To derive

the categorical wheat classification (from the regression tree output), the pixel was

labelled as wheat if the median value from the seven regression tree outputs was

equal to or greater than 50%.
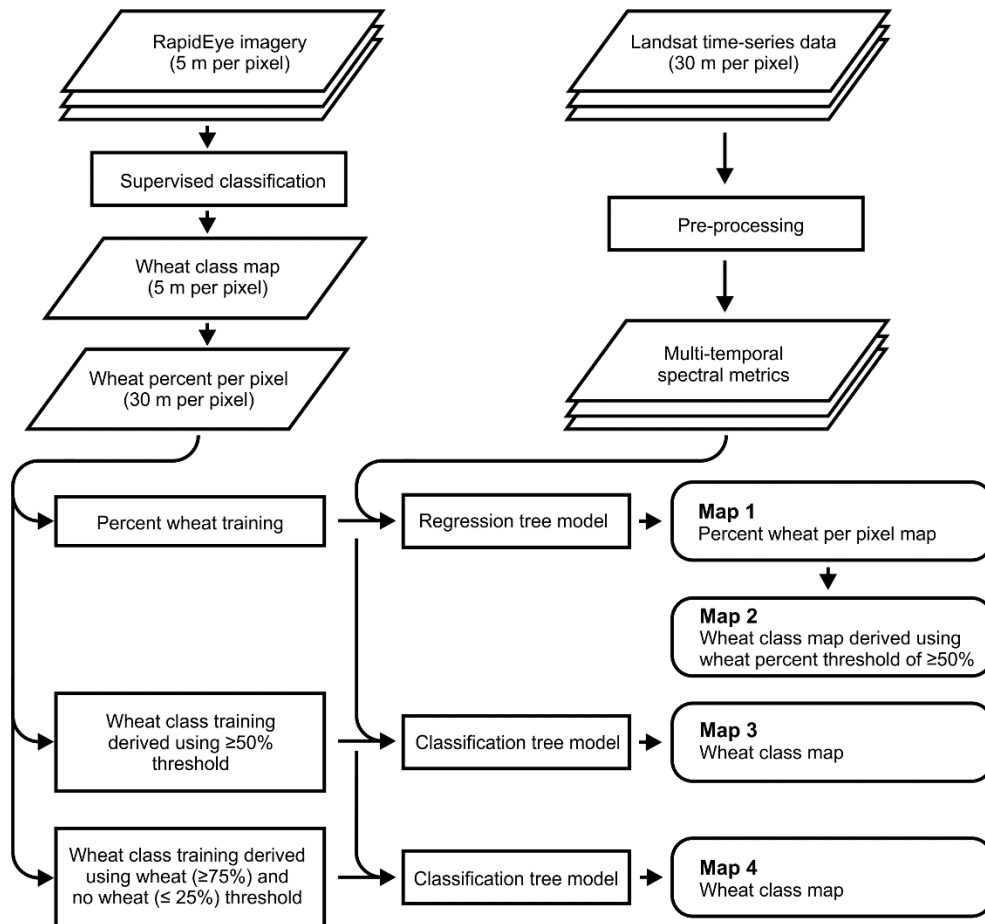
Figure3.5. Flow chart of the research.

▪ **RapidEye-Derived Training Data**

The nine RapidEye images procured for Punjab Pakistan from January, February and March were visualized as false color composites of NIR, red edge and red spectral bands. The training data for the RapidEye images consisted of manually labelled wheat and non-wheat pixels with visual image-interpretation of each image based on spectral properties and landscape context (Hansen et al. 2008, Potapov et al. 2012). The selection of training data was made in light of wheat phenology in Pakistan, following the crop calendar (SUPARCO 2012) and previous work (Becker-Reshef et al. 2010, Khan et al. 2016, Dempewolf et al. 2014). To account for the heterogeneity within the not-wheat class, the training sample size of the not-wheat

class dominated the sample size of the wheat class. The training data were augmented

following successive classification iterations with output products manually checked

using RapidEye images, Landsat composites, Google Earth™ high-resolution

imagery and a priori knowledge of the area. The results were aggregated to 30 m per

pixel per cent wheat values. The 30 m continuous training data set consisted of 46

million pixels covering approximately 20% of the total area of Punjab province

(figure 3.6).
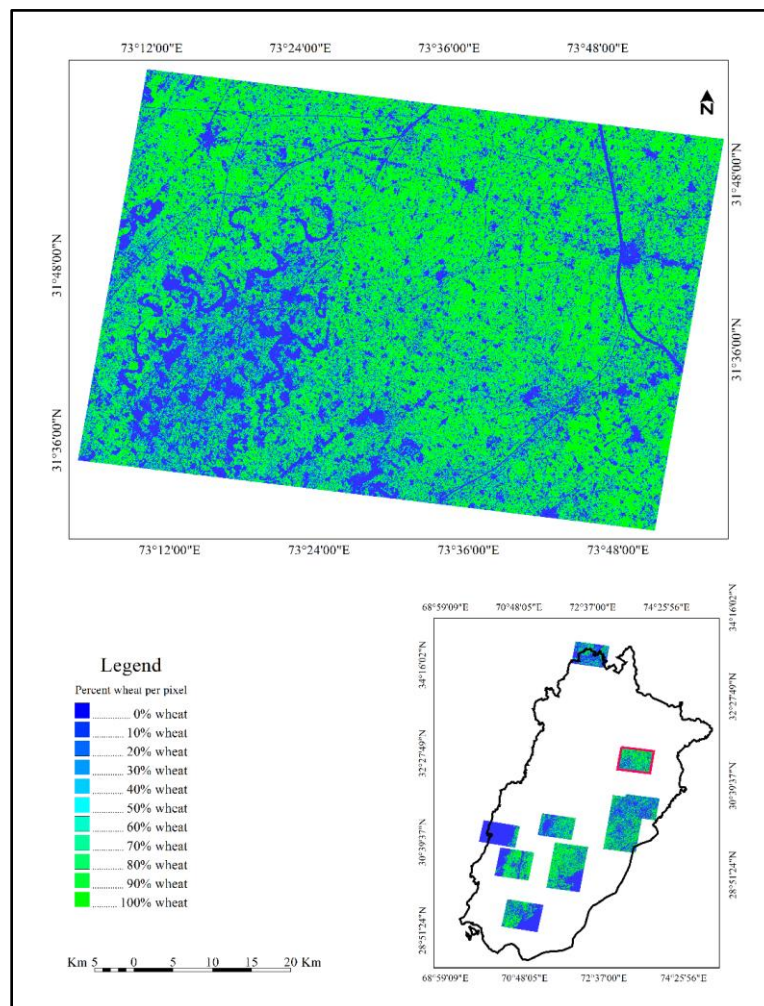
Figure 3.6. RapidEye-derived per cent wheat training data.

▪ **Landsat-Derived Map Products**

The 30 m continuous and categorical training data derived from the RapidEye imagery were used to create four wheat maps for Punjab (figure 3.6). Map 1, the 30 m per cent wheat per pixel map produced by relating the RapidEye derived 30 m continuous training data to 30 m Landsat multi-temporal spectral metrics. Map 2 was a 30 m binary wheat/no wheat classification derived from the per cent wheat map (Map 1) with a per pixel threshold labelled as wheat if the per cent wheat value exceeded 50%. From categorical training data, we produced two wheat/no wheat classifications. Map 3 was a 30 m binary classification derived using training data based on a 50% wheat/no wheat threshold defined for all RapidEye-derived training pixels at 30 m scale. Map 4, was a second binary classification map produced using only 30 m per cent wheat RapidEye-derived training pixels that were either ≥75% (wheat) or ≤25% (no wheat) (figure 3.7). That is, for Map 4 we eliminated those pixels from the training data that were ambiguous in regard to whether wheat or not wheat. Map 4 represents a map derived from "pure pixel" training data. The wheat area for Punjab for each map was calculated simply by summing the area proportion of each pixel mapped as wheat in the case of the per cent wheat map or summing the area of all pixels mapped as wheat in the case of the categorical wheat/no wheat maps.
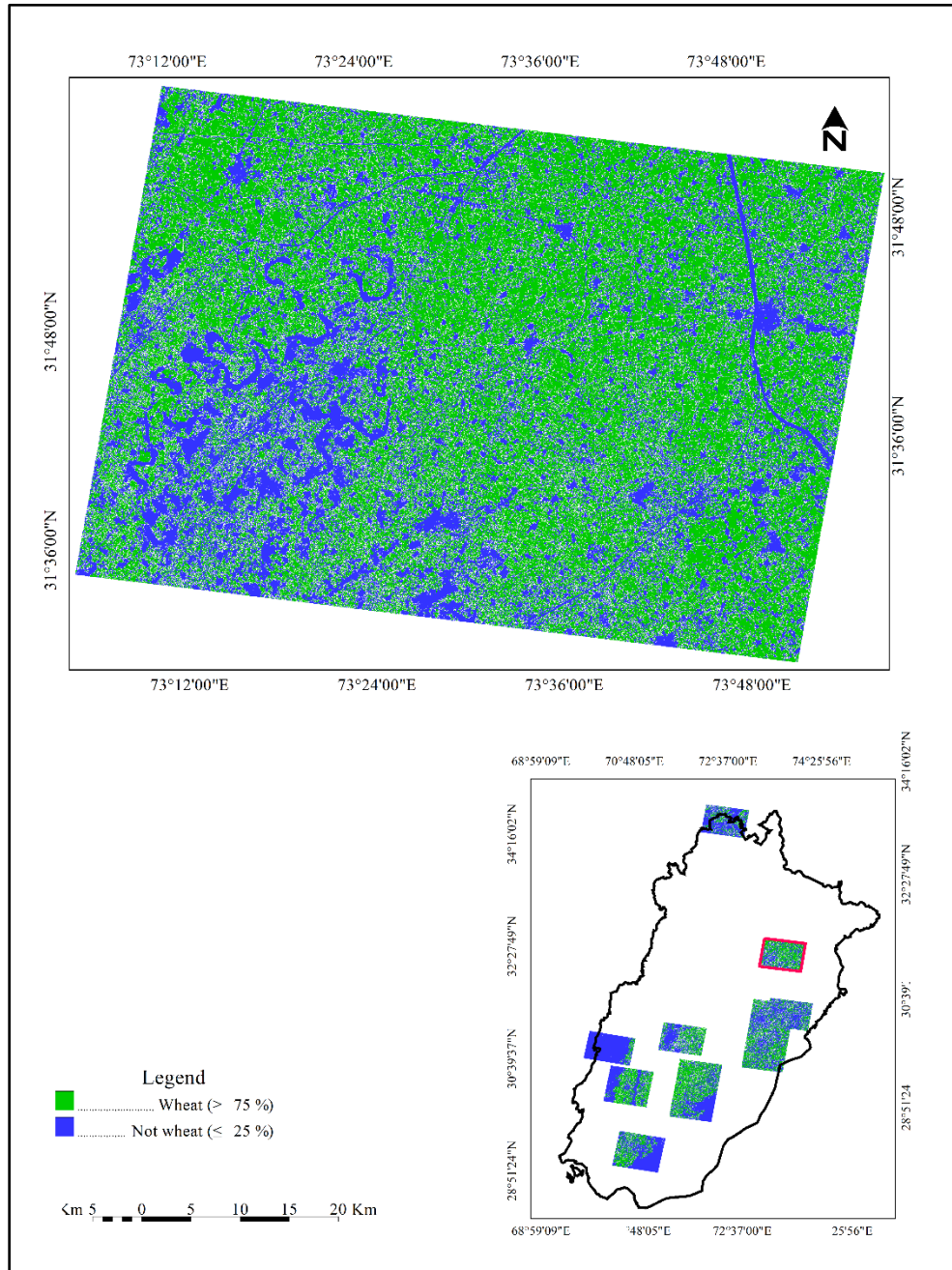
Figure 3.7. Per cent wheat training data of Figure 3.6 thresholded at ≤25% and ≥75% to derive categorical wheat/no wheat training data set.

▪ **In-situ Data for Area Estimation and Map Validation**

To estimate map accuracy and wheat area from the reference classification, an independent *in situ* data set was collected using a stratified two-stage cluster sample. An initial population of 2261 blocks, (each block 10 km × 10 km) covering all of Punjab was created. Blocks with less than 25% of their area inside the provincial boundary of the Punjab were excluded resulting in 105 blocks being removed. Each block was assigned to one of three strata based on wheat area as determined from a previous Landsat-derived wheat classification for the Punjab produced by (Khan et al. 2016). These three strata were employed: low wheat (blocks with 0–22% wheat), medium wheat (22–47%) and high wheat cover (>47%) . These strata boundaries were selected so that the low wheat stratum represented half of the population (i.e., the low wheat boundary was the median wheat per cent cover of the population of blocks), the high wheat stratum included the blocks with the greatest wheat cover so that the total area of wheat in the high stratum represented 50% of all wheat area of the map used to create the stratification, and the medium wheat stratum had all remaining blocks not assigned to the low or high wheat strata. The purpose of the stratification was to form strata that were internally relatively homogeneous but with blocks in different strata having different wheat per cent cover and to capture the diversity in wheat crop across the province. From the population of 2156 blocks, 1035 were assigned to the low stratum, 680 to the medium stratum, and 441 to the high stratum.

Considering logistical constraints in field data collection and recognizing spatial and phenological variation in wheat crop across Punjab, seven sample 10 km × 10 km blocks from each stratum were randomly selected. The rationale for allocating

equal effort to the three strata was to quantify the full range of different wheat densities, particularly given the small total sample size due to the high cost of field data collection. If proportional allocation had been used, the low wheat stratum would have received the largest sample size. We did not believe the effort spent in the low stratum would have been beneficial. Within each selected sample block, we used simple random sampling to select ten 30 m pixels for field visit (figure 3.8). The sample pixels that fell outside of the provincial boundary (5 sample pixels total) were not visited resulting in a total of 205 sample pixels visited of the 210 sample pixels selected from the 21 sample blocks.

For each sampled pixel, we quantified the proportion of wheat area in the field. For non-cropland land cover, we incorporated information from Google Earth™ in interpreting cover such as trees and built-up area. The percentage of wheat in each of the sampled pixels, as observed in the field, was recorded. Error matrices for the four maps were calculated using wheat per cent for the sampled pixels from the field (i.e., the reference data) compared to the continuous and binary wheat characterizations (i.e., the wheat maps). Because the reference value was the proportion of wheat area within each sample pixel, the error matrix cell entries were quantified differently from the more typical case in which the reference data represent a hard classification (i.e., proportion of wheat is 0 or 1). The formulas for estimating accuracy of the different maps and for estimating area of wheat based on the field interpretations are those presented as appendix in (Potapov et al. 2014).

Olofsson et al. (Olofsson et al. 2014) noted the value of using the reference sample data as the basis for estimating area. We examined two approaches for

estimating wheat area from the field sample data. In the first approach, we estimated area using only the sample interpretations (i.e., we did not use information from the four wheat maps in the estimator of area). This approach is sometimes called a "direct estimator" because the estimate is directly from only the field sample data. However, it is generally possible to reduce the standard error of the area estimate relative to the direct estimator by incorporating information from the wheat maps. In this study, we used a "difference estimator" (Sarndal et al. 1992) for this purpose. The difference estimator is applied to the stratified two-state cluster sampling design and (Appendix in (Potapov et al. 2014)) provides the specific formulas for the difference estimator and its estimated standard error. The starting point for the difference estimator is the total area mapped as wheat from one of the four maps produced. Because the wheat map has classification error, the total area based on the map is expected to be biased. We can remove that bias using the reference sample data, specifically the difference between the proportion of area of wheat (for each sampled pixel) from the map and the proportion of area according to the reference data. A sample estimate of the bias adjustment of mapped wheat area is then obtained. Because the complete coverage wheat map is used in the difference estimator of wheat area, we expect the map information to translate into smaller uncertainty of the wheat area estimate. The standard error of the difference estimator or wheat area provides quantitative evidence for the reduction in uncertainty achieved. We produced four area estimates using the difference estimator, one for each of the four wheat maps (the reference sample data are the same for all four estimates). The four area estimates produced using the difference estimator will depend on the wheat map incorporated in the

difference estimator. The standard errors of the estimates indicate how much benefit

was gained by using each map in the difference estimator of area, and we can also

assess the value of the maps by comparing the standard error of the difference

estimates to the standard error of the direct estimate. Smaller standard errors are

preferable.
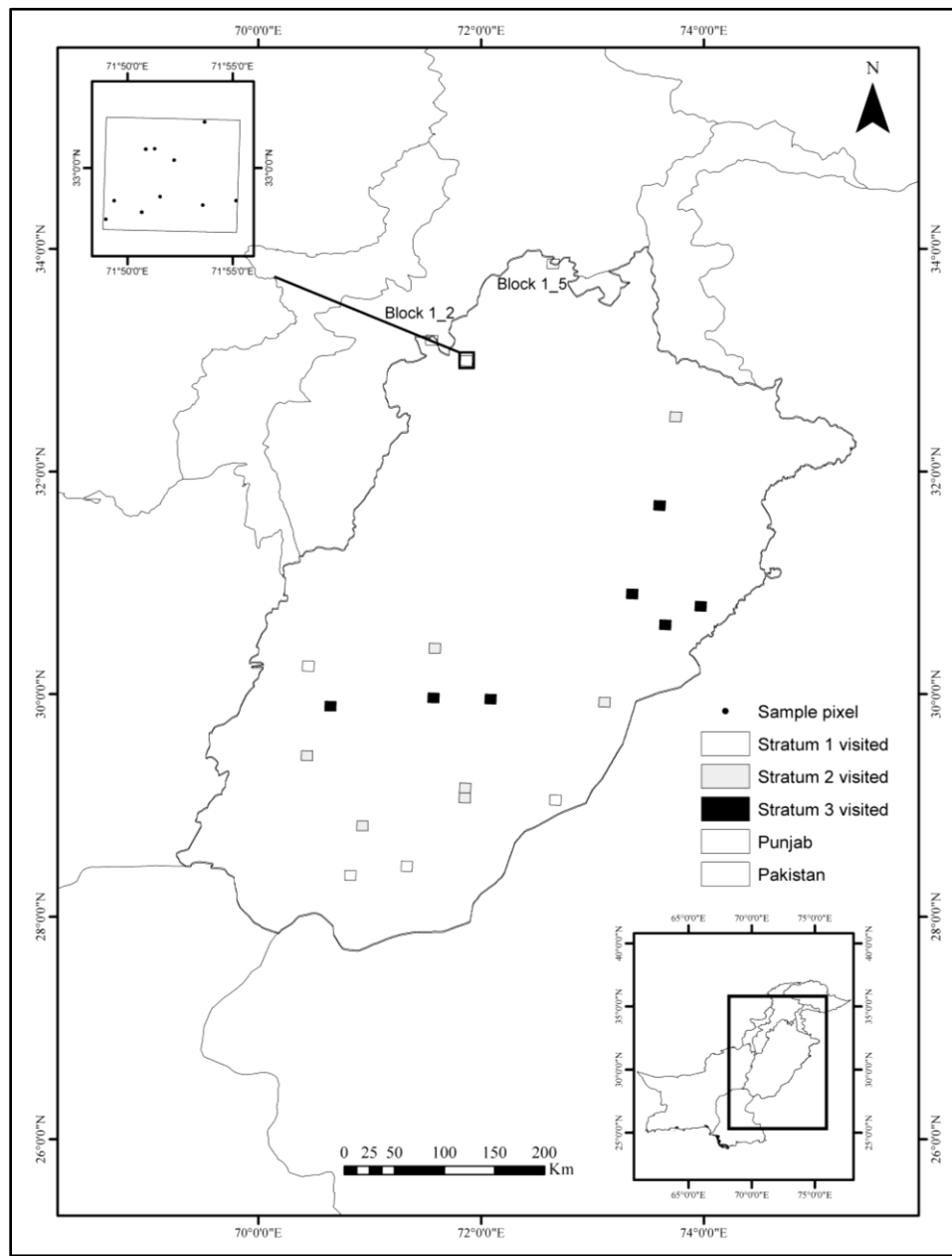
Figure 3.8. Stratified random sample blocks and sample pixels from Punjab.

In addition to the sample-based validation of the wheat maps based on the *in situ* reference data, we performed an inter-comparison of wheat area estimates with the wheat crop forecasts of Punjab Crop Reporting Service (CRS) using their crop reporting system (CRS 2015) and wheat area estimates from Space and Upper Atmosphere Research Commission (SUPARCO 2015). Provincial and district level wheat area data from the CRS were compared to our wheat maps for district-level area comparison. These estimates were used as auxiliary information available for validation of our mapped wheat area estimates for the province.

1.9. Results

1.9.1. Intercomparison of Wheat Area Estimates

The direct sample estimate of the total area of wheat in the Punjab based on the field sample data was 7.17 Mha for the 2014–2015 Rabi growing season. By comparison, the total area of cultivated wheat in Punjab estimated from the four difference estimators (i.e., a difference estimator was produced using each of the four wheat maps as the auxiliary data) varied from 7.25 Mha to 7.76 Mha (figure 3.9), indicating that the general effect of the difference estimator was to increase the estimated area relative to the direct estimator that incorporated no map information. Although we have a small sample size, both the Landsat maps and CRS wheat estimates were within the 95% confidence interval of the field-based estimate (figure 3.9). Of all map-based area estimates, Landsat trained with first and last quartile RapidEye classification data was closest to the CRS estimate (Table 3.2).

The difference estimator increased the total wheat area relative to the direct estimator, and with one exception, the difference estimator reduced the standard error

relative to the direct estimator. Incorporating the wheat map information via the difference estimator reduced the standard error of the area estimate to approximately 80% of the standard error of 1.08 Mha obtained for the direct estimate that does not incorporate the wheat map information. Consequently, a substantial reduction in standard error can be achieved by incorporating information from the wheat map into the sample-based estimate of wheat area.
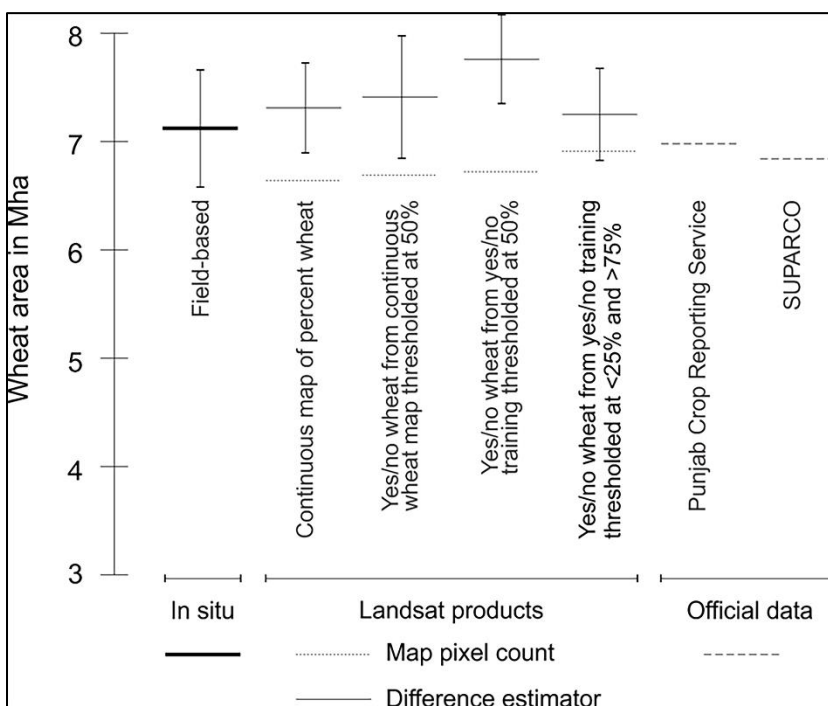
Figure 3.9. Wheat area estimates from field data, the four RapidEye-trained Landsat-derived map products, and official data from CRS and SUPARCO. For the Landsat-derived map products, both the map pixel counts and difference estimator results are shown. Uncertainties of ±1 standard error are shown for the area estimates derived from the probability sample of field (*in situ*) data.

1.9.2. Accuracy of the Wheat Maps

The four wheat maps produced from the RapidEye training data are shown in figure 3.10. The overall accuracies of the four wheat maps were relatively similar ranging from 87% to 90% (Table 3.2). User's accuracies of wheat were generally

higher than producer's accuracies for wheat for the four map products indicating that omission error of wheat was generally more problematic than commission error of wheat.

District-level wheat area from the CRS final wheat report for 2014–2015 was compared to our map products in figure 3.11. The r^2 values for our four map products do not reveal a performance difference, whether using sub-pixel training and per cent wheat mapping (Map 1) or homogeneous wheat/no wheat training for wheat classification (Map 4). Results suggest that commercially acquired high-resolution data as a training input have no advantage over classical methods of training pure pixels into categorical classes. For most districts, the map estimates agreed with the CRS estimates except for the Rahim Yar Khan district, which is a desert zone. The map products showed higher wheat acreage than the CRS estimate for this district.
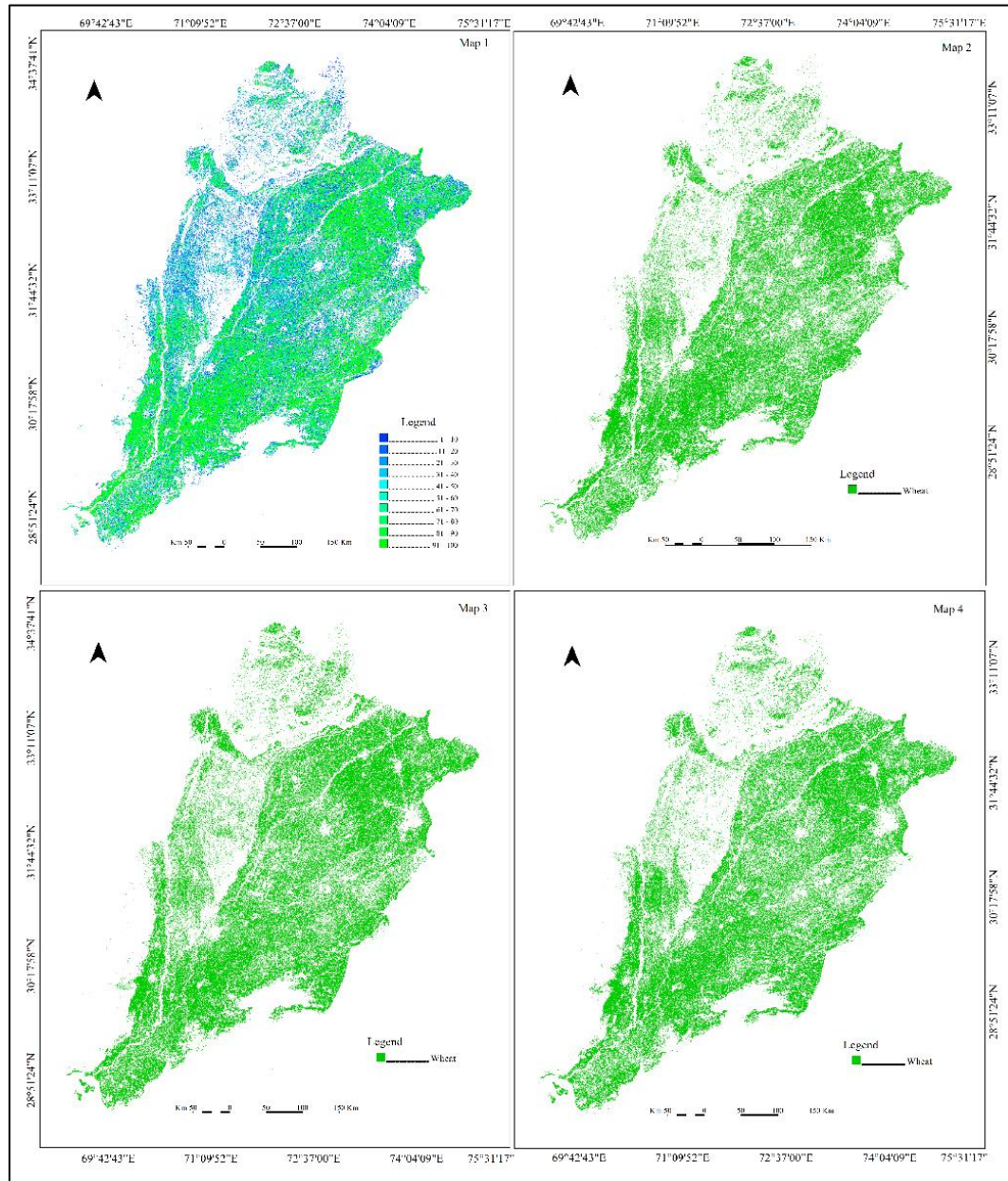
Figure 3.10. Results of the four wheat maps classified from Landsat time-series data and using 30 m training data derived from RapidEye. (Map 1) Per cent wheat map; (Map 2) 50% thresholded per cent wheat map; (Map 3) Binay wheat map derived with RapidEye categorical training; (Map 4) binary wheat map derived with training ≤25% and ≥75%.

Table 3. 2: Comparison of accuracies of four map products, two derived using continuous training data and two derived using wheat/no-wheat training data, along with final area estimates

Map Product	Overall Accuracy (%) (SE)	User Accuracy (%)		Producer Accuracy (%)		Wheat Area (Mha) from Difference Estimator (Standard Error)
		Wheat (SE)	No-Wheat (SE)	Wheat (SE)	No-Wheat (SE)	
Continuous map of per cent wheat derived from RapidEye per cent wheat training (Map 1)	88 (4)	87 (3)	89 (5)	79 (9)	94 (2)	7.31 (0.83)
Binary map of wheat/no wheat derived from continuous wheat map thresholded at 50% (Map 2)	90 (4)	90 (3)	90 (5)	80 (8)	95 (2)	7.41 (1.13)
Binary map of wheat/no wheat derived from wheat/no wheat RapidEye training thresholded at 50% (Map 3)	90 (4)	91 (3)	90 (5)	81 (8)	96 (2)	7.76 (0.82)
Binary map of wheat/no wheat derived from yes/no RapidEye training thresholded at ≤25% and ≥75% (Map 4)	87 (4)	84 (5)	88 (6)	77 (8)	92 (2)	7.25 (0.85)
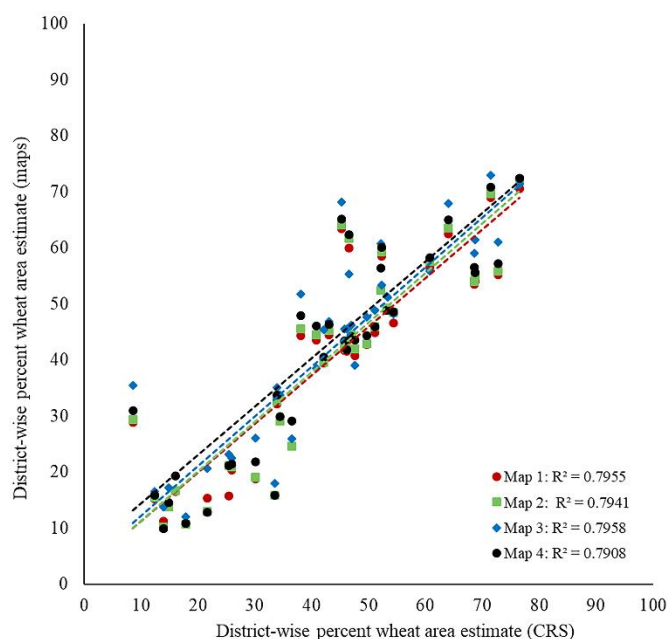
Figure 3.11. District-level wheat area from Landsat-based wheat maps and CRS wheat area estimates for Punjab.

1.10. Discussion

The four wheat maps we produced for Punjab, demonstrated relatively similar overall, user's and producer's accuracies supporting the idea that 30 m wheat/no wheat mapping was a viable approach, and a key advantage of such an approach is

that it can be implemented without the expense or processing of high-resolution

commercial data. We employed the same training data pool in all cases, from per cent

wheat per pixel training data to a subset of only pure yes/no training data ($\leq$25% and

$\geq$75% test). Our other key objective was to determine the benefit of the different

wheat maps when used for the purpose of reducing the standard error of sample-based

wheat area estimate. Specifically, we compared the standard errors when each map

was incorporated in a difference estimator of wheat area. The pure pixel map (i.e.,

Map 4) combined with the difference estimator yielded a standard error of 0.85 Mha,

which was nearly the same as the standard error of 0.82 Mha achieved by the per cent

wheat map used in the difference estimator. For the purpose of reducing the standard

error of the area estimate, the per cent wheat map was not substantially better than the

wheat/no wheat map, so based on this case study, the evidence does not indicate

additional value is gained by producing the per cent wheat map. Moreover,

incorporating the wheat/no wheat map in the difference estimator of wheat area

substantially reduced the standard error relative to the standard error (1.08 Mha) of

the direct estimator (the direct estimator is what would be used if we had no wheat

map). Therefore, we can conclude that an image analyst with experience in

identifying winter wheat cover could create a wheat/no wheat map that would yield a

substantial reduction (nearly 20%) in standard error for the area estimate of wheat

based in the field sample data.

An analysis of specific map errors based on comparison to field data revealed

some of the complexity of the Punjab agricultural landscape. Many of the omission

errors were for wheat under orchards, which is a fundamental limitation, not easily

overcome using satellite data. Other omission errors were in rain-fed wheat production areas of semi-arid environments due to the lack of dense wheat cover and a higher contribution of soil background reflectance. Commission errors were associated with other winter crops, such as clover (Khan et al. 2016). While landscape heterogeneity impacted map accuracies less, factors such as crop type, intercropping, and intensification also reduced overall accuracies. It is these kinds of mapping limitations that require the combined use of the map with field data to achieve precise area estimates.

Figure 3.12 shows the three metrics that contributed most to the decision tree models estimating wheat cover, illustrating the importance of longer wavelengths in characterizing wheat. Figure 3.13 shows full-resolution subsets of RapidEye and Landsat input data and wheat maps. Differences in spatial resolution between RapidEye and Landsat imagery are clearly evident. However, the per cent wheat map products derived from the aggregated 5 m wheat/no wheat training data exhibited a discrete appearance made up of largely 100% wheat and 100% no wheat at 30 m training cells. Results from Landsat (figure 3.13e–h) were visually congruent with the training data and each other. Given that Punjab is characterized by relatively fine-scale land tenure, there is an expectation that mixed pixels would challenge crop characterization using medium spatial resolution data such as Landsat (30 m). For example, SUPARCO, the Space and Upper Atmosphere Research Commission of Pakistan, employs high spatial resolution SPOT 5 m data for mapping crops due to this fact. However, our results show that winter wheat is a fairly homogeneous land cover target. When examining spatial contiguity of 100% wheat pixels from our per

cent wheat map, we found an effective field size of 42 ha. The spatial contiguity of cultivated winter wheat was also evident in the 5 m RapidEye data. Figure 3.14 illustrates the histogram of 5 m wheat/no wheat training data aggregated to 30 m spatial resolution, compared to predicted 30 m per cent wheat. Despite the fine-scale land tenure, winter wheat was such a dominant crop that 30 m data captured it as a largely wheat/no wheat categorical (binary) theme. Crop diversity in the Kharif (summer monsoon) season is much greater and may require sub-pixel or finer-scale categorical characterizations. However, for winter wheat, Landsat was a sufficient input.

The demonstrated approach could easily complement the conventional "Village List Frame" method used by the Crop Reporting Service of Punjab by providing an interim assessment in lieu of the more field-intensive and delayed CRS reporting. Less intensive field sampling, guided by an in-season wheat/no wheat map could provide timely information on wheat production and support key decisions regarding wheat management, transportation and storage. The delayed results from the standard CRS method preclude such timely decision making. Importantly, such a capability can be implemented using freely available Landsat data, making the approach a cost-effective improvement for pre-harvest policy decision making.
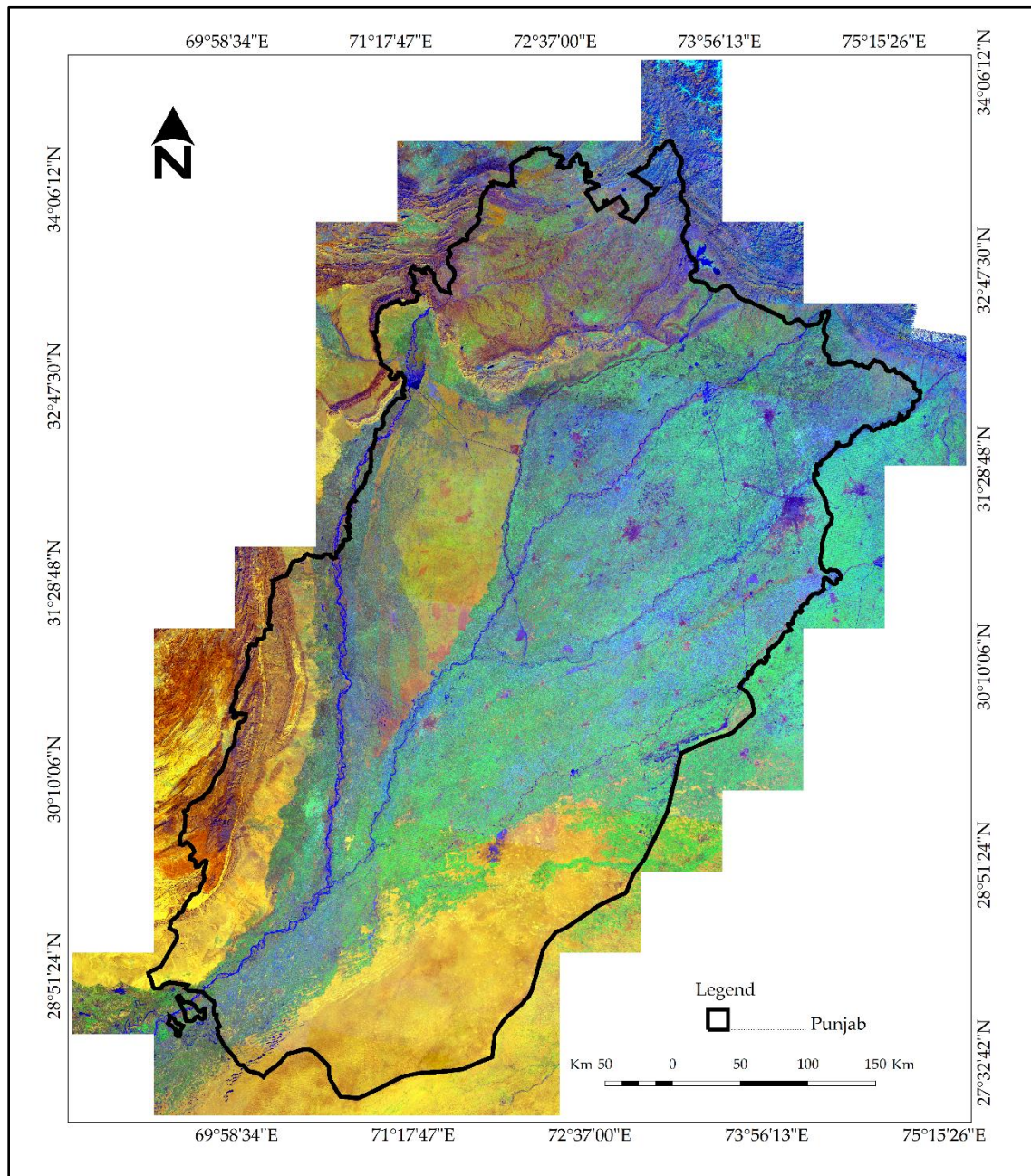
Figure 3.12. Composite of the top three Landsat metrics used to estimate wheat cover: mean of SWIR (1.6 µm) reflectance values between the 10th and 50th percentile ranked by thermal reflectance values (in Red), mean of NIR reflectance values between the 10th and 50th percentile ranked by thermal reflectance values (in Green), and the mean of the last three NDWI reflectance values (in Blue).
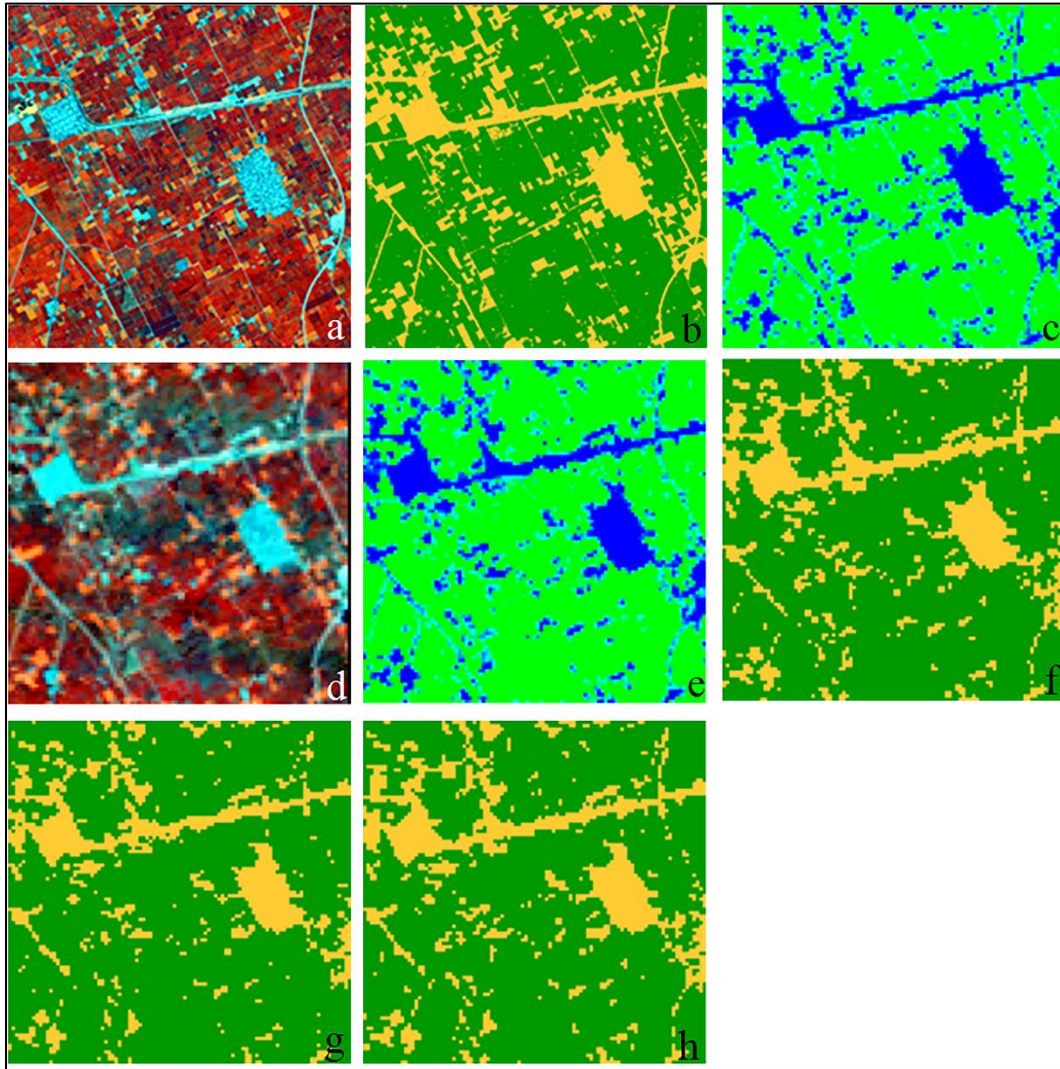
Figure 3.13. Top row: (**a**) RapidEye false color composite of red-NIR-red edge data; (**b**) wheat/no wheat 5 m map (green = wheat, yellow = no wheat); and (**c**) per cent wheat from 5 m map aggregated to 30 m spatial resolution. Middle row: (**d**) Landsat false color composite of red-NIR-SWIR (1.6 µm); (**e**) per cent wheat from Landsat; and (**f**) wheat/no wheat map of per cent wheat thresholded at 50%. Bottom row: (**g**) wheat/no wheat map from yes/no RapidEye training thresholded at 50%; and (**h**) wheat/no wheat map from yes/no RapidEye training thresholded at ≤25% and ≥75%.
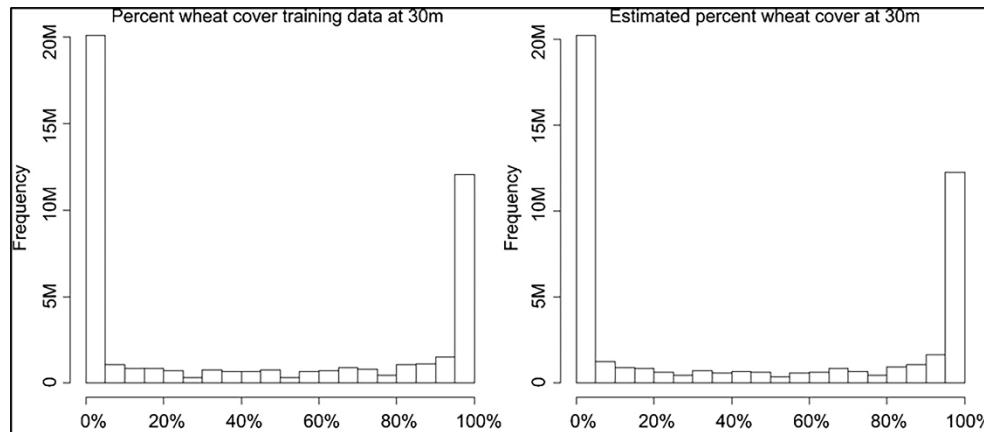
Figure 3.14. Histogram of RapidEye-derived wheat training data aggregated to per cent cover at a 30 m spatial resolution and Landsat-derived per cent wheat cover for the same grid cells used as training data.

1.11. Conclusions

Rabi season or winter wheat maps derived from Landsat data for the 2014–2015 Rabi growing season in the Punjab province of Pakistan correspond closely to official statistics and field validation data. The high accuracies of the wheat maps supports the utility of the maps for depicting the spatial distribution of wheat and potential benefits to the maps for reducing standard error of area estimate when the wheat maps are combined with stratified sampling of field data. For many landscapes characterized by small field sizes and fine-scale land tenure, an evaluation of freely available medium spatial resolution data should be made before presuming that commercial high-resolution data are required. Calibration of mapping algorithms (training data) can likely be manually created with conventional visual interpretation without the need for high-resolution reference imagery. Other landscapes where a single crop dominates, such as soybean in northeast China, or paddy rice in parts of Southeast Asia, may be similarly characterized. The value of our approach is in the comparatively low level of resources needed to implement the method and the ability

to derive pre-harvest crop area estimates. For Pakistan, such results are important for improving wheat crop management, storage and transportation, as well as decisions on exports and imports of wheat grain in addressing food security issues.

Chapter 4: An operation automated mapping algorithm to facilitate efficient in-season estimation of wheat area for Punjab, Pakistan.

1.12. Introduction

Smallholder agricultural systems with intensive management practices and human activities exhibit rapid change in land cover and land use (Wardlow and Egbert 2008). It is difficult in rapidly changing agricultural landscapes to timely and accurately predict vital agricultural statistics for effectively managing postharvest crop conditions to address food insecurity for dependent populations. The smallholder intensive agricultural landscapes are highly sensitive to a number of external pressures including climate impact (Stathers et al. 2013, Zhou et al. 2014, Abbasian and Pound 2013, ADB 2009), market dynamics (David 1986, Kahan 2013, Kaditi 2012) and management inputs (Morton 2007, Doraiswamy et al. 2003, Erickson 1984, Minamiguchi 2005). This sensitivity ultimately adds to food security issues of dependent populations. In such systems, accurate and timely crop forecasts provide inputs (Khan et al. 2016, Giri and Long 2014) for policy and operational level decisions (World Bank 2011). However, conventional crop forecasting statistics are labor intensive, expensive and yet mostly result in outputs months after harvest of a crop (Verma et al. 2011, Akhtar 2012, Atzberger 2013, Dempewolf et al. 2013). Remote sensing provides an alternative to produce quicker and near real time crop area forecasts (Dempewolf et al. 2013). It is desirable to produce estimates prior to

harvest that could be confidently and reliably used in operational decision making (Akhtar 2012, Dempewolf et al. 2013, Bauer 1975).

Remote sensing studies have proliferated with the availability of civilian earth observation satellite sensors (Rogan and Chen 2004), with early applications focused on agriculture (Boatwright and Whitefield 1986, Gallego 2004). The continuous synoptic coverage of the earth's physical resources from space (Woodcock et al. 2008, Wardlow and Egbert 2008, Becker-Reshef et al. 2010) has evolved from low-resolution remote sensing data to free of charge available medium resolution Landsat and Sentinel-2 data, promising more ready inputs for agricultural monitoring. The use of medium resolution data such as Landsat is desirable as compared to heritage high cadence, low spatial resolution data for agricultural monitoring (Loveland et al. 2000, Turner et al. 1995). Improved data volumes from medium spatial resolution Landsat and Sentinel-2 data provide the opportunity for large geographic coverage, and adequate spatial and temporal resolution for crop characterization (Wardlow and Egbert 2008, Khan et al. 2018, Khan et al. 2016, Hansen et al. 2002, Hicke et al. 2004). The processing of large volumes of data has necessitated the development of automated techniques in remote sensing (Adesuyi 2016) and developing methods with minimum manual processing in image analysis (Huth et al. 2012). Automation of high volumes of remote sensing data with reliable and timely results (Cihlar 2000, Defries and Chan 2000, Knorn et al. 2009, Rogan and Chen 2004) can strengthen planning and decision support systems and reduce costs (Carfagna 2001). There is a clear opportunity for improving the delivery of timely and accurate crop maps, which could respond to policy needs and action on the ground in addressing situations

arising from food shortages or surpluses (Akhtar 2012, Verma et al. 2011, Khan et al. 2016, Dempewolf et al. 2014).

Automation is defined differently depending on the methods and techniques used in land cover classification (Asmat and Zamzami 2012, Comber et al. 2004). In this study, we view automation as the application of a turn-key, fixed decision tree algorithm to classify source Landsat multi-spectral time series metrics into wheat / not wheat categories. In this manner, the method is similar to the MODIS Land Science Team (Justice et al. 2002) suite of land cover products that rely on standard annual MODIS time-series inputs and fixed decision tree algorithms to characterize global land cover (Friedl et al. 2002, Hansen, DeFries, Townshend, Sohlberg, et al. 2002). Decision trees are efficient in handling noisy or missing data as well as non-linear relations between features and classes (Giri and Long 2014). For the presented method, training data and imagery from historical years are used to build a model, which is then automatically applied to data from subsequent years.

The overarching objective of this research is to develop an operational process for estimating wheat area prior to harvest for Punjab Province, the bread-basket for Pakistan. The process relies on an automated within growing season wheat mapping model to 1) map prior year wheat extent in order to define strata for allocating the sample pixels to be visited in the field, 2) determine presence of wheat at the sample field locations, and 3) map current growing season wheat to be used as an auxiliary variable in a survey sampling regression estimator (Cochran 1977) to reduce the standard error of the wheat area estimate derived from the sampled field data. The automated within growing season mapping of wheat enables the most up to date

information of wheat extent to be used in the regression estimation procedure. In this article, we evaluate the accuracy of the automated mapping algorithm based on its application to several years of data, and assess the implications of incorporating a within-season map to reduce the standard error of the estimated wheat area based on a case study sample from 2016.

1.13. Study area

Pakistan with its five provinces and one region is eighth in the world by production of wheat. Punjab with 205,344 km^2 has the second largest land area among provinces and provides about 75% of the country's wheat production (Figure 4.1, location of Punjab). The province's 12.4 million hectares (Mha) of cultivated land (SUPARO 2012) plays a significant role in ensuring food security for over 207 million people in the country (GoPakistan 2017, Branca et al. 2011). The province is divided into three major agro-ecological zones: (1) the Potohar plateau in the north with rain-fed agriculture, accounting for 10% of the total agricultural area of the province (2) the arid desert and semi-desert in the south and central region of the province with little agricultural production; and (3) the main irrigated crop growing region of Indus basin (Qasim 2012). The province assists economic development of Pakistan where about 66% of the rural community is associated with agriculture (Dempewolf 2013). The province's importance for agriculture in Pakistan and in the region for wheat production makes it the best candidate for our research.
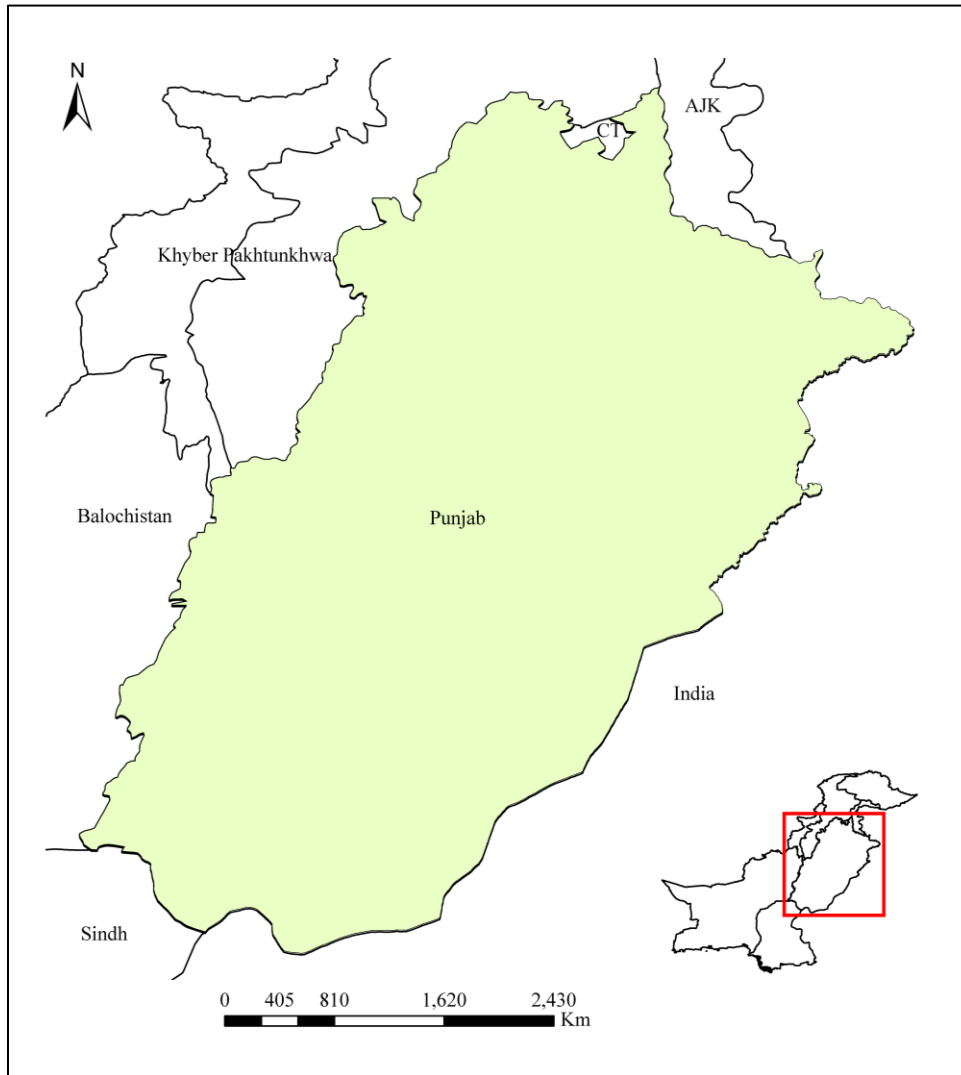
Figure 4.1: The study area, Punjab province in Pakistan.

1.14. Methods

1.14.1. Data sets

The Landsat imagery for the Rabi growing season starting in December and ending in March for years 2012-13, 2013-14, 2014-15, 2015-16 and 2016-17 (here after referred to as 2013, 2014, 2015, 2016, and 2017) were used to create sets of multi-temporal spectral metrics for each year to map wheat in Punjab. A total of 2,103 level 1 terrain corrected (L1T) images from 20 WRS2 Path and Rows were used including 1,003 Landsat 8 OLI and 1,100 Landsat 7 ETM+ scenes (Table 4.1).

Table 4.1: Number of Landsat images used in generating multi-temporal spectral Landsat metrics

Data	Year					Total
	2013	2014	2015	2016	2017	
Landsat 7 ETM+	197	211	208	232	252	1100
Landsat OLI 8	63	228	206	248	258	1003
Total	260	439	414	480	510	2103

We employed six spectral bands from Landsat 7 ETM+: blue (BLUE 0.45 –

0.52 µm), green (GREEN 0.52 – 0.60 µm), red: (RED 0.626–0.693 µm), Near

Infrared (NIR 0.776–0.904 µm), Short-wave Infrared (SWIR1: 1.567–1.784 µm) and

(SWIR2: 2.097–2.349 µm); Six spectral bands of Landsat 8 OLI, including blue

(0.450 – 0.453 µm), green (0.525-0.600 µm), red (0.630–0.680 µm), NIR (0.845–

0.885 µm), SWIR1 (1.560–1.660 µm), and SWIR2 (2.100–2.300 µm) and

corresponding Moderate Resolution Imaging Spectroradiometer (MODIS) bands,

band 1 (0.62 – 0.67µm), band 2 (0.841 – 0.876 µm), band 3 (0.459 -0.479 µm), band

4 (0.545 – 0.565 µm), band 5 (1.23 – 1.25 µm), band 6 (1.628 – 1.652 µm) and

band 31 (10.780 – 11.28 µm) were used. Thermal infrared bands (ETM+ 10.40–

12.50 µm and TIRS 10.60–11.19 µm) were used for multi-temporal spectral metrics

production (see below), but were not included as variables for mapping. Normalized

Difference Vegetation Index (NDVI) (Tucker 1979) and Normalized Difference

Water Index (NDWI) (Gao 1996) values were calculated for all observations as inputs

to generate metrics (Khan et al. 2016), which were created using all cloud-free

Landsat observations within the wheat growing season.

The Landsat multi-spectral data for each year were processed by conversion to

top-of-atmosphere reflectance (Chander et al. 2009), which were then normalized

using MODIS top-of-canopy reflectance data composite as a normalization target

(Potapov et al. 2012). The per-pixel observation quality assessment was performed

following the method described in Potapov et al. (2012) to highlight clear-sky

observations. All clear-sky observations within the defined study period for each of

the years (2013, 2014, 2015, 2016 and 2017) were aggregated and used to derive a set

of spectral-statistical derivations called multi-temporal spectral metrics. Metrics

represent a generic feature space that facilitate large area mapping and have been

used extensively with Advanced Very High-resolution Radiometer (AVHRR) and

MODIS data (Hansen and DeFries 2004, Chang et al. 2007) and more recently with

Landsat data (Khan et al. 2016, Potapov et al. 2012). Landsat-based metrics were

calculated between a start and end date of the Rabi growing season (December,

January and February, allowing us to create a feature space corresponding to major

phenological stages of winter wheat cultivation (e.g., peak of growing season,

warmest time of year, etc.).

To create a set of multi-temporal spectral metrics, we ranked all cloud-free

Landsat observations per pixel corresponding to (i) band reflectance value; (ii) NDVI

value; (iii) NDWI value; (iv) brightness temperature value. For each spectral band

and ranking method, minimum, 10th, 25th, 50th, 75th, and 90th percentiles, and

maximum values were recorded as a set of metrics. In addition, we calculated and

recorded mean reflectance for all values between the minimum and 10th percentile,

minimal and 25th, 10th and 25th, 25th and 50th, 50th and 75th, 25th and 75th, 10th

and 50th, 75th and maximal, 90th percentile and maximal, 10th and 90th percentile,

and minimal and maximal values for each band and ranking. In addition to metrics,

time-sequential monthly composites for December to March were created based on a median value taken from all clear-sky observations within each calendar month to facilitate image interpretation and assignment of training data.

Topographic data were also used as independent variables in the wheat classification algorithms. Topographic data included elevation, slope and aspect. These layers were computed from 30 m spatial resolution void–filled seamless Digital Elevation Model (DEM) derived from the National Aeronautics and Space Administration (NASA) Shuttle Radar Topography Mission (SRTM) (downloaded from CGIAR-CSI: http://srtm.csi.cgiar.org).

1.14.2. Classification algorithm

The landscape of Punjab has variations in geographic, edaphic and climatic factors, crop varieties and management practices (Wardlow et al. 2007, Wardlow 2006; Wardlow and Edgebert 2008,) that contribute to the complexity of satellite data (Sharma 2013) for the province. To characterize wheat in this complex landscape of intensive smallholder agriculture, we used a bagged decision tree algorithm (Breiman 2001, Hansen et al. 1996). The intra-class variability for wheat in Punjab due to climate contained in Landsat multi-spectral time series data (hereafter referred to as Landsat data), can be effectively handled by non-parametric decision trees that operate on thresholds in multi-spectral space (Hansen et al. 2000). Decision trees have advantages over conventional classification techniques and produce higher classification accuracies (Hansen et al. 1996, Friedl and Brodley 1997) while still able to accommodate large datasets (Punia 2011).

Classification trees employ an entropy measure, referred to as deviance, to split multi-dimensional space of dependent variables into successively more homogeneous hyper volumes, called nodes. The best univariate split was sought from all independent variables, and the process was repeated until a perfect tree was fit or pre-set conditions for termination of tree growth were met. We terminated each classification tree when additional splits decreased model deviance by less than 0.001 of the deviance of the total training set population (Bwangoy et al. 2010, Bwangoy et al. 2013). To further avoid over fitting, we used a set of seven bagged tree models each derived from a 20% random sample of training pixels. Each tree produced a per pixel probability of wheat cover class membership; the per-pixel median of the seven model outputs was taken as the result (Potapov et al. 2012). Wheat was categorized if this median value was equal to or greater than 50%.

1.14.3. Training data for developing automated model

We derived our training data from pre-existing wheat maps for 2014 (Khan et al. 2016) and for 2015 ((map 4 in (Khanet al. 2018)). Original training data for these maps were collected on the basis of wheat phenology in Pakistan, following the crop calendar (SUPARCO 2012), previous work (Dempewolf et al. 2014, Khan et al. 2016, Khan et al. 2018) and prior knowledge of the area. For this study, training data were taken directly from the existing 2014 and 2015 maps where both agreed on wheat and no wheat extent. Limited manual training was performed in areas where the two maps exhibited differences in wheat extent. Water bodies were masked out during data preparation and compositing using the water mask from the Global Forest Cover Change product (Hansen and Loveland 2012).

1.14.4. Map products from the automated model

The training data were related to 2014 and 2015 Landsat growing season metrics in order to derive a model that could then be applied to the same metrics from other years. For this study, the automated model derived from the 2014 and 2015 Landsat metrics was applied to 2013, 2016, and 2017 metrics, as well as 2014 and 2015 metrics. For 2013, limited Landsat 8 data were available, while 2016 and 2017 had higher observation frequency than either 2014 or 2015 (Table 1). The area of wheat derived from pixel counts for all years was compared to official data from the Punjab Crop Reporting Service to assess the consistency of the operational automated model with official data. We also assessed the accuracy of the wheat maps produced from this model for each year in which we had obtained *in situ* reference sample data (2014, 2015, and 2016).

1.14.5. Area estimation from reference data

To estimate cultivated wheat area and to assess the accuracy of the classification results, we used field data collected during the year 2016. For field sampling, we adopted a combination of field visit and photo-interpretation as the response design to obtain the reference wheat / not wheat classification (Stehman and Czaplewski 1998). The sampling design was a stratified, two-stage cluster sample. Following the methods described in Khan et al. (2016) and Khan et al. (2018), Punjab was partitioned into 5 km x 5 km spatial blocks (i.e., the "clusters" of the cluster sampling design). We assigned each block to one of three strata based on wheat area as indicated from the 2015 wheat map (map 4) from Khan et al. (2018). Three wheat strata were defined for the 2016 field sample: low (0–45%), medium (45–75%) and

high (>75%) wheat cover. For practical considerations related to travel costs, we constrained the sample to 45 sample blocks. The blocks within each stratum were selected by simple random sampling. In each selected sample block, we randomly selected 20 sample pixels (30 m x 30 m) with a target to visit at least 10 pixels per block. The 20 sample pixels within each block were listed in random order, and the field visits were conducted following that random order. If a pixel could not be visited in the field, it would be replaced by the next pixel in the randomized list. For each sampled pixel, we quantified the per cent wheat area using field interpretation with additional information from Google Earth™ incorporated if non-cropland cover such as trees and built-up area was found within the sample pixel. The percentage of wheat in each of the sampled pixels was recorded using 10% increments (i.e. 0%, 10%, 20%, 30%, etc.). Wheat areas were estimated using 1) a stratified two-stage cluster sample direct expansion estimator (SAS, Version 9.3, Cary, North Carolina, USA), 2) a per stratum regression estimator, and 3) a regression estimator applied to sample data from a simple random sample i.e., no strata. If the simple random sample combined with a regression estimator achieves comparable precision to estimates obtained from a stratified sampling design, the less complex simple random design would be preferable for operational implementation. All methods were evaluated for the 2016 growing season data as the basis of the wheat area estimates.

1.15. Results

1.15.1. Wheat area estimation

Stratification for field data acquisition was based on the 2015 wheat map of Khan et al. (2018). Table 2 shows results of 2016 estimated wheat area from the

reference sample data using the direct expansion stratified estimator and a simple

regression estimator. Per stratum wheat area estimates and standard errors for each

scenario are shown in Table 4.2. Results show the largest contributor to the variance

of the direct estimator to be from the low wheat stratum (76%), with marked

improvement when applying the regression estimator with 2016 automated map and

also 2015 map used in stratification. Of particular interest is the reduction in variance

of stratum 1, 55% by 2015 map vs. 68% by 2016 automated map. However,

automated map for 2016 has performed slightly better than the 2015 map with 24%

variance of the total for stratum 2 against 34% by 2015 map, and 7% in stratum 3

against 11% respectively..

Table 4.2: Per stratum wheat area estimates (Mha) and standard errors (SE)

Stratum	N_h	Direct expansion estimator (SE)	Per cent of total variance	Regression estimator using 2016 automated map (SE)	Per cent of total variance	Regression estimator using 2015 map (SE)	Per cent of total variance
1	4142	1.553 (0.551)	76	1.828 (0.386)	68	1.768 (0.311)	55
2	2301	2.607 (0.255)	16	2.635 (0.227)	24	2.648 (0.243)	34
3	1643	2.604 (0.171)	7	2.402 (0.132)	7	2.751 (0.139)	11
Total	8086	6.764 (0.629)		6.865 (0.467)		7.167 (0.418)	

Further tests employed the automated 2016 map in regression and post-

stratified estimator procedures (Table 3). The stratified sampling design with 15

sample blocks per stratum was beneficial relative to simple random sampling (i.e., no

strata) as the standard error for simple random sampling would have been 0.810 Mha

compared to the standard error of 0.629 for the stratified estimator. For regression

estimator tests, we used the turn-key 2016 and 2015 wheat maps as the auxiliary

variables. The lowest standard errors employ the regression estimator with

comparable results for both stratified and simple random sampling (Table 4.3).

Table 4.3: Standard Error comparison for different options of sampling strategies

Sampling strategy	SE of estimated total area of wheat (Mha)
Stratified random, regression estimator (2015 map)	0.418
Simple random, regression estimator (2015 map)	0.440
Simple random, regression estimator (2016 automated)	0.440
Stratified random, regression estimator (2016 automated)	0.467
Stratified random, direct expansion estimator	0.629
Simple random	0.810

Punjab wheat areas from the automated model pixel counts were compared

with official Crop Reporting Service of Punjab (CRS) and in-situ reference data in

Table 4.4. The wheat areas from 2015 and 2016 were nearly the same as CRS data,

only 0.85% and 1.57% higher, respectively.

Table 4.4: Mapped area comparison (pixel counts) with CRS estimates and sample-based estimate

Year	Map area (Mha)	CRS area (Mha)	Difference (Mha)
2013	6.83	6.51	0.32
2014	6.96	6.90	0.06
2015	7.04	6.98	0.06
2016	7.02	6.91	0.11
2017	7.24	6.75	0.49

1.15.2. Validation of wheat maps

We related our field data for per sample pixel crop type from 2014 (Khan et

al. 2016), 2015 (Khan et al. 2018) and 2016 to the respective annual turn-key wheat

maps (Figure 4.2), calculating accuracy measures. Overall accuracies from automated

mapping range from 79% with a standard error of SE=4% for 2014 to 86% (SE = 3%)

for 2015 (Table 5). Overall results represent map products that exhibit low bias, with wheat commission errors ranging from 15-25% and omission errors 20-30%. The lack of strong bias supports the pixel counts as a relatively accurate indicator of wheat extent. In comparison to the overall accuracy of 76% (SE = 7%) for a 2014 map achieved with manual labelling of training pixels (Khan et al. 2016), the map for the same year generated with our automatic classification algorithm resulted in an overall accuracy of 79% (SE 4%). Similarly for 2015, the overall accuracy of 87% (SE = 4%) achieved with custom training data (map 4 in Khan et al. 2018) is similar to that generated with the automated method of 85% (SE = 2%).
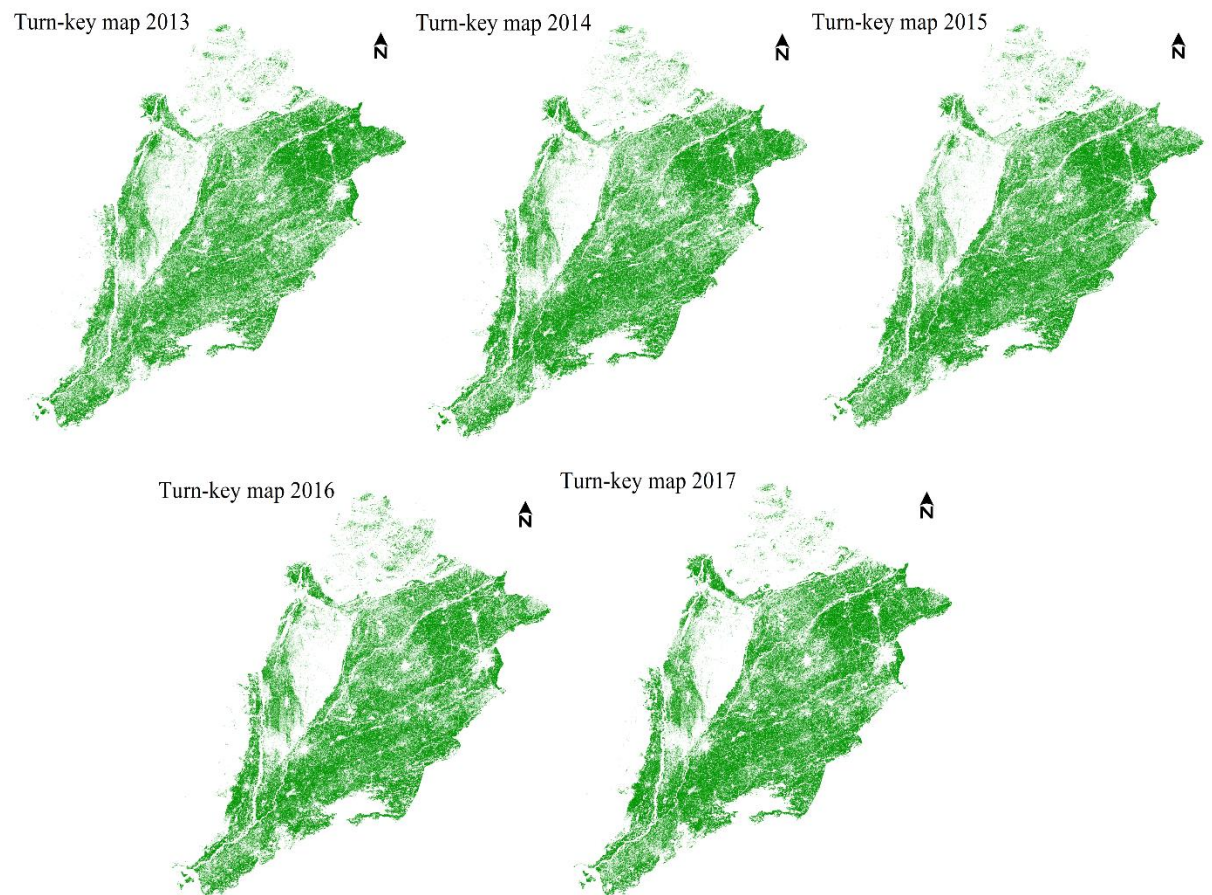
Figure 4.2: Turn-key wheat maps derived for 2013 - 2017

Table 4.5: Mapped area comparison with CRS estimates

Accuracy (Standard Error)	Wheat/not-wheat land cover	Map		Map		
		2014 (Khan et al. 2016)	Turn-key map 2014	2015 (Khan et al. 2018: map 4)	Turn-key map 2015	Turn-key map 2016
User'acc. (SE) %	Wheat	62 (8)	75 (6)	84 (5)	85 (4)	81 (3)
	Not-wheat	84 (7)	81 (5)	88 (6)	87 (3)	88 (2)
Prod. Acc. (SE) %	Wheat	70 (7)	70 (7)	77 (8)	74 (5)	80 (3)
	Not-wheat	78 (8)	84 (4)	92 (2)	93 (2)	88 (2)
Overall acc. (SE) %		**76 (7)**	**79 (4)**	**87 (4)**	**86 (3)**	**85 (2)**

1.16. Discussion

1.16.1.   Automated mapping and area estimation

Our automated classification model addresses several important issues in wheat

monitoring in Pakistan. First, accurate within season maps of winter wheat can be

automated. In comparison to the classification model calibrated using the manually

collected training data Khan et al. (2016) and Khan et al. (2018), the automated

method of classifying Landsat multi-temporal multi-spectral data resulted in

comparable accuracy (Table 4.5). The automated model produces growing season

wheat cultivation maps well before harvesting, with positive benefits for management

and policy decision-making. Second, these maps can be used as an auxiliary variable

in regression estimators to provide precise area estimates, where the area estimates

are based on field-visited determination of wheat presence at the sample location.

Resulting wheat area estimates provide information suitable for decision-making. Of

particular interest concerning ease of implementation is the comparable standard

errors achieved using simple random sampling versus stratified random sampling of

the 5 km x 5 km blocks. From an operational standpoint, simple random sampling

can be more easily implemented, including calculations and communication of the

method. For simple random and stratified random sampling, the use of the regression

estimator decreased the standard error by 46% and 34%, respectively, compared to the direct expansion estimator with stratified sampling. The standard errors of the two regression estimator were similar, with the stratified sampling design yielding 5% lower standard error compared to simple random sampling (0.418 to 0.440Ma). The improvement in standard error of stratified sampling of 5% may not be of sufficient magnitude to justify the additional complexity of this design relative to simple random sampling.

The method could be extended to include crop yield, where in-situ yield data could be collected for the same sample sites as used to estimate crop area. Given that probability sampling is implemented, both area and yield estimates and associated uncertainties can be combined to generate production data with known uncertainty. Auxiliary variables appropriate for use in regression estimator methods in estimating provincial-scale yield are an open question. Research on wheat yield has met with success employing peak phenological greenness measures (Becker-Reshef, Vermote et al. 2010, Dempewolf, Adusei et al. 2014). Such data can be easily extracted from the Landsat time-series data used in mapping wheat area. Overall, methods for creating reliable production data with low latency are feasible and should be pursued in future research.

1.16.2. Land use change in Punjab

Our results show that Punjab exhibits a relatively stable winter wheat area year to year (Table 4). At the 5 km x 5 km scale of the sample blocks, pairwise correlations between wheat area of any two maps exceeded 0.9, and the correlation

between mapped wheat area with wheat area estimated from the reference (field)

exceeded 0.8. These results suggest the prospect of using a fixed sampling frame

over all years, under the assumption that the geographic patterns of wheat production

will not change over time. Such an assumption could become dubious if

environmental circumstances change due to climate change or more immediate land

use changes. Recently, Pakistan has been declared a water scarce country, with a

change in water availability of about 80%, from 5280 m^3 per capita in 1950 to 1040

m^3 per capita in 2010 (Daanish, Majed, and Natalie 2013). Population growth

primarily accounts for this change, which translates to drawing water for other than

agricultural use. Municipal water use increased by 81% from 1.534 km^3/year in 1951

to 183.5 km^3/year in 2008 (UNDP 2016). The surface water available in rabi season

of 2017-18 was 24.2 million acre feet (MAF), 2.8% below 24.9 MAF in Rabi season

of 2008-09 (Ministry of Finance 2018). The rising trends in population growth

coupled with geo-political water conflicts affecting water flows in the major rivers

and climate change will have drastic consequences for wheat production and crop

composition in Punjab. Winter rainfall from January to March is crucial for wheat

production, particularly the dry land farming areas. Winter rainfall (Jan – Mar)

recorded in 2017 was 32.3 millimetre (mm) in comparison to the long-term average

of 74.3 mm. Wheat area in 2017-18 was 8.734 Mha, 5% below in comparison to

9.199 Mha in 2013-14, and 3.4% below to that of 2009-10 (Ministry of Finance

2018). The area under canal irrigation in Pakistan shrunk from 7.89 Mha (1990 – 91)

to 6.86 Mha in 2009-10. Land area irrigated by other sources such as wells, tube

wells, canal tube wells and other increased from 8.86 Mha of 1990-91 to 12.56 Mha in 2009-10 (Jurriens et al. 1996, Takashi 2003, GoPakistan 2014).

Natural population increase, migration from rural to urban areas, the absence of a national land use zoning policy and other factors have led to the largely unorganized expansion of major Punjab cities, including Lahore (7.3 million), Faisalabad (3.1 million) and Islamabad-Rawalpindi (3.8 million) (Qadeer 2014). These cities are expected to grow between 45 and 56 per cent by 2025 (United Nations 2018). Lahore's growth has roughly doubled since 2000; over the same period, Pakistan as a whole and the province of Punjab both have increased in population by 30-45% (Kalim and Bhatty 2004, Shirazi and Kazmi 2014) (Kalim and Bhatty, 2004). Urban hierarchies have also emerged, with thirteen other cities in Punjab now defined as large cities with populations of more than 200,000 inhabitants (Mayo 2012, Aziz et al. 2014). Overall, urbanization rates in Punjab have increased from 17% in 1951 to 36% at present, the highest in South Asia (Kugelman 2013, 2014), with expected rates of 50% by 2025 (Kugelman 2014). The population density for Punjab is nearly 500 persons/km2 and is expected to reach 1000 persons/km2 by 2050. The reduction of the arable land base of Punjab is largely due to these urbanization dynamics (Irshad et al. 2007) and could result dramatic changes in the geographic location and overall extent of wheat cultivation in Punjab, especially given that most land available for expansion is of high agricultural productivity. All such factors will contribute to land cover changes, likely affecting the smallholder heterogeneous agriculture of Punjab.

1.17. Conclusion

Automated wheat area mapping offers promise for efficient within season crop area estimation. The automated model was found to have comparable accuracy to wheat maps produced by manually determined training data, so the capacity of the automated maps to reduce standard errors of wheat area estimates was comparable to that of maps produced by the traditional approach. The low latency monitoring of wheat area employing a fast and scalable turn-key model using free-of-charge medium resolution satellite data will provide data required to make timely assessment of cropping patterns. The model, if adopted by institutions such as CRS Punjab, the agency responsible for generating crop statistics, can save human effort and financial resources while producing actionable within-season information. This will ultimately contribute to making timely policy decisions addressing post-harvest shortage or surplus of grain. The model will also help in timely decisions on storage, transportation, and import/export, benefitting government organizations and farmers.

Chapter 5: Conclusion

1.18. Application of medium resolution data in heterogeneous agricultural systems

In the research we demonstrated that medium resolution Landsat 30 m data has sufficient spatial and within growing season temporal coverage to successfully map Rabi (winter) season wheat under a heterogeneous small holder agriculture system. Using single date imagery of available free medium resolution Landsat data could result in data gaps, thus affecting map accuracy and wheat area estimation. To avoid data gaps, multi-temporal multi-spectral metrics were generated using all available per-pixel Landsat cloud free observations during winter wheat (or rabi) growing season. The use of all available Landsat data to create a feature space appropriate for mapping large area crop type was demonstrated, building upon previous forest extent and change mapping efforts (Potapov et al. 2012, Hansen et al. 2013). For countries without robust geospatial survey data or those seeking more timely data on crop extent, national-scale mapping using Landsat data is a viable option.

1.19. Sample-based unbiased reference wheat area estimate

A two stage stratified random sample was applied for an independent wheat area estimate. The blocks' population was stratified using antecedent wheat maps from previous years and each of the blocks in the population was assigned to one of the three strata, using per-block wheat proportion. To allocate samples to a strata, we used antecedent wheat maps, MODIS based wheat per cent layer for 2013-14 from Dempewolf et al. (2014), and Landsat based wheat map for 2014-15 from Khan et al. (2016) and wheat map for 2015-16 from Khan et al. (2018). Although this sample was small in relation to the large area of the province, yet generated a small standard

error. This supports high accuracy of the model we have used and its applicability in addressing policy-level decisions in addition to concluding that Landsat data has sufficient spatial and temporal coverage for producing a reliable in-season wheat area estimate. The independent wheat area estimate from the field sample depends on capacity of a field investigator in correctly identifying the sample pixel and recording wheat proportion in that. This capability enhances the accuracy of the wheat area estimate with reliable error estimates. Integration of per sample mapped data from our wheat maps with the in-situ sample data, reduced the standard error significantly in comparison to direct estimation of wheat area from the field samples. This demonstrated that medium resolution based maps are effective in generating unbiased wheat area estimates using stratified random sampling. Our sampling design in comparison to the conventional sampling "area list frame" is simple, efficient and cost-effective to implement. Wheat maps derived from Landsat data for the 2014–2015 Rabi growing season in the Punjab province of Pakistan correspond closely to official statistics and field data. The high accuracies of the wheat maps reflect the spatial distribution of wheat and provide potential benefits for reducing standard error of area estimate when the wheat maps are integrated with stratified sampling of field data.

1.20. Operational automated wheat area estimation model

The wheat area estimates, we produced with visual interpretation and manual labelling on Landsat composites of spectral multi-temporal Landsat metrics and automatically derived training to calibrate our classification model were closely related to our independent in-situ wheat area estimates and to the official statistics issued for the respective years and seasons by the CRS Punjab. The automatic model calibration resulted in smaller standard error in comparison to visually interpreted training data. This further strengthens our confidence in operational use of our model

for small field heterogeneous cropping systems. Our operational wheat area estimation model predicted wheat with standard error of around five per cent, which indicates to reliability and robustness of the model. The model provided reliable wheat area estimates with potential of becoming basis for within growing season policy level decisions in comparison to post harvest information generated by the conventional area estimation method. The model has the potential to be:

- Adopted to other crop types such as rice in Pakistan, for which within season multi-spectral multi-temporal metrics can be created based on per pixel observations.

- Adopted for other regions particularly under dry weather conditions;

1.21. Sources of errors

In province level large area mapping, various sources of commission and omission errors resulted in user and producer in-accuracies. In addition to spectral variations due to climate regimes, soil conditions and crop varieties, multi-cropping and irrigation sources also provided inputs for errors in our classification. Though, the standard error was small, yet generated by wheat crop mixed with mango and tangerine orchards, and small fields of clover and garlic that could not be segregated from wheat in a 30 m x 30 m pixel spatial resolution coverage. Wheat growth in dry lands is dependent on rainfall and soil moisture. In dry and drought conditions, failure of wheat results in sparse vegetation cover and almost near bare ground cover. Remote sensing data capture this sparse crop condition as bare ground in general than a crop and therefore result in error production. A threshold for ground covered by wheat of a certain canopy density could be applied as low cover wheat appearing as bare ground is likely not a significant contributor to overall production. For planted area estimates, such a rule would introduce omission errors, but not likely deleteriously affect wheat production estimation.

1.22. Use of High-resolution data vs. medium resolution data

In heterogeneous cropping smallholder agriculture, use of high-resolution data can enhance crop identification and result in higher map accuracies. Our research demonstrates that despite tenured average field size in Punjab of 5 ha, the effective field size is larger than 42 ha, as calculated from our continuous wheat cover map. This effective wheat field size is spatially large enough to be captured and represented spectrally in 30 m spatial resolution data. In our comparison of wheat maps produced with training derived from RapidEye high-resolution data and with conventionally drawn pure wheat and not-wheat pixels, resolved to almost the same accuracy and standard errors. From this, we concluded that for characterizing a crop in small field sizes and fine-scale land tenure landscapes, an evaluation of freely available medium spatial resolution data should be made before presuming that commercial high-resolution data are required. Calibration of mapping algorithms (training data) can likely be delineated directly without the need for high-resolution reference imagery. Therefore, visual interpretation of medium resolution imagery by a skilled image analyst with experience in identifying spectral responses of wheat against other land covers, can produce high quality wheat maps, which can be used as auxiliary variable with field data to reduce standard error and improve accuracy. Availability of 10 m and 20 m Sentinel 2 imagery has improved temporal resolution and aid in crop identification and enhance training capability. Integration of sentinel2 data with Landsat data will have significant advantages, particularly in crop identification and training for model calibration. However, results from our research indicate that using higher resolution data has no significant impact in winter wheat area estimation and reducing standard error.

1.23. Potential for operational use in decision support system

The method presented here has advantages over the currently used "Village List Frame" method of the CRS Punjab, particularly in the possibility of delivering actionable cultivated area data at or near the end of the growing season. Because the method uses freely available data and can be applied before wheat crop harvest, it potentially has high value for decision support system concerning wheat production and trade. Specifically, wheat crop management, storage and transportation arrangements, decisions on exports and imports of wheat grain and food security can be facilitated using the results from the demonstrated method if implemented at or near the end of the Rabi season.

Other landscapes where a single crop dominates, such as soybean in northeast China, or paddy rice in parts of Southeast Asia, may be similarly characterized. The value of our approach is in the comparatively low level of resources needed to implement the method and the ability to derive pre-harvest crop area estimates. For Pakistan, such results are important for improving wheat crop management, storage and transportation, as well as decisions on exports and imports of wheat grain in addressing food security issues. In contrast and against general perception, using high-resolution RapidEye data didn't result in a higher accuracy and therefore has no significant value addition and significance.

The model, if adopted by institutions such as CRS Punjab responsible for generating crop statistics, can save on time, human effort, and financial resources with reliable estimates of wheat area available before harvest, thus strengthens decision support system. This will ultimately contribute to making timely policy decisions addressing post-harvest shortage or surplus of grain. The model will also help in timely decisions on storage, transportation, and import/export. This can benefit government organizations and farmers equally. This research also found that simple random with regression estimator has equivalent results to stratified random

with regression estimator. The simple random with regression estimator is therefore recommended as it has advantages over the stratified random by significantly reducing field effort, saving time in collection of data, and enabling in-season wheat area estimates for policy level decision making ahead of harvesting. Need for timely information on crop statistics likely will increase over time, particularly in countries with severe climate change impacts such as Pakistan (Atzberger 2013). The operational models with relatively easy method, less time to implement and low resource inputs requirement will have precedence and therefore our model of crop area estimation will be suitable for countries like Pakistan. Our method applied to wheat area estimation in Punjab depends on availability of cloud free per pixel observations within growing season. The method will perform in countries where dry conditions persist during wheat growing season, while its application in cloudy regions of the globe, such as tropics, will be limited.

1.24. Way forward

We believe that this method can be easily translated for production estimation of wheat and other crops. The additional data requirements will be crop cuts from the sampled pixels. A rule based crop cuts in conjunction with proportional wheat area estimate per sampled pixel, can be used to estimate yield and when combined with area, overall production. We recommend this task for further research to enhance utility of our automatic crop model, and to benefit policy making and improving food security of millions of people in Pakistan.

References

Abbasian, A., and J. Pound. 2013. Food Outlook - Biannual report on Global Food Markets. In *Food Outlook*. Rome, Italy: Food and Agriculture Organization of United Nations.

ADB. 2009. *Building Climate Resilience in the Agriculture Sector of Asia and the Pacific*. Manila, Phillippines: Asian Development Bank.

Adesuyi, Ayodeji Steve. 2016. "Automating land cover classification using time series NDVI: A case study in the Berg river catchment area." MA Masters Degree thesis, Department of Geography and Environmental Science, Stellenbosch University.

Akhtar, Ibrarul Hassan. 2012. "Pakistan needs a new crop forecasting system." 05/16/2012. Accessed July 22nd, 2014. http://www.scidev.net/global/climate-change/opinion/pakistan-needs-a-new-crop-forecasting-system.html.

Allen, J. Donald. 1990. "A look at the remote sensing applications program of the National Agricultural Statistics Service." *Journal of Official Statistics* 6:393-409.

Arnette, J. T., N. C. Coops, L. D. Daniels, and R. W. Falls. 2015. "Detecting forest damage after a low severity fire using remote sensing at multiple scale." *Interntional Journal of Applied Earth Observation and Geoinformation* 35:239-246.

Arvidson, T., J. Gasch, and S. N. Goward. 2001. "Landsat 7's long-term acquisition plan - an innovative approach to building a global imagery archive." *Remote Sensing of Environment* 78 (1-2):13-26. doi: 10.1016/s0034-4257(01)00263-2.

Asmat, A., and S. Z. Zamzami. 2012. "Automated House Detection and Delineation using Optical Remote Sensing Technology for Informal Human Settlement." *Procedia - Social and Behavioral Sciences* 36:650-658. doi: https://doi.org/10.1016/j.sbspro.2012.03.071.

Atzberger, Clement. 2013. "Advances in Remote Sensing of Agriculture: Context Description, Existing Operational Monitoring Systems and Major Information Needs." *Remote Sensing* 5 (2):949.

Atzberger, Clement, and Felix REmbold. 2013. "Mapping the Spatial Distribution of Winter Crops at Sub-Pixel Level Using AVHRR NDVI Time Series and Neural Nets." *Remote Sensing* 5:1335-1354. doi: 10.3390/rs5031335

Aziz, A., S. M. Mayo, I. Ahmad, M. Hussain, and M. Nafees. 2014. "Determining town based socioeconomic indices to sensitize development in Lahore, Pakistan." *Technical Journal, UET TAxila, Pakistan* 19 (IV):22-29.

Azhar, B. A., Chaudhry M. G. and M. Shafique. 1972. "A model for forecasting wheat production in Punjab." *Pakistan Development Review*, 11 (2): 407 - 415.

Azhar, B. A., Chaudhry M. G. and M. Shafique. 1974. "A forecast of wheat production in the Punjab for 1973-74." *Pakistan Development Review*, 13 (1): 106 - 112.

Bailey, Jeffrey T., and Claire G. Boryan. 2010. Remote Sensing Applications in Agriculture at the USDA National Agricultural Statistics Service. United States Department of Agriculture.

Bairagi, G. D., and Z. Hassan. 2002. "Wheat Crop Production Estimation Using Satellite Data." *Indian Society of Remote Sensing* 30 (4):213-219.

Baruth, B., Royer, A., Klisch, A., Genovese, G. 2008. The use of Remote Sensing within the MARS crop yield monitoring system of the Euorpean Commission. The International Archives of the Photogrammetry, Remote Sensing and Spatial Information Sciences.

Basso, B., D. Cammarano, and E. Carfagna. 2013. Review of Crop Yield Forecasting Methods and Early Warning Systems. Report presented to first meeting (18-19 July) of the Scientific Advisory Committee of th Global Strategy to improve agricultural and rural Statistics.: FAO, Headquarters, Rome, Italy.

Bastiaanssen, W. G. M., and S. Ali. 2003. "A new crop yield forecasting model based on satellite measurements applied across the Indus Basin, Pakistan." *Agriculture, Ecosystems and Environment.* 94:231-240.

Bauer, M. E. 1975. "The role of Remote Sensing in determining the distribution and yield of crops." *Advances in Agronomy* 27 (C):271-304.

Becker-Reshef, I., C. Justice, E. Vermote, C. Tucker, A. Anyamba, J. Small, Ed. Pak, Ed. Masuoka, J. Schmaltz, M. Hansen, K. Pittman, C. Birkett, D. Williams, C. Reynolds, and B. Doorn. 2010. "Monitoring Global Croplands with Coarse Resolution Earth Observations: The Global Agriculture Monitoring (GLAM) Project." *Remote Sensing* 2:1589-1609.

Becker-Reshef, I., E. Vermote, M. Lindeman, and C. Justice. 2010. "A generalized regression-based model for forecasting winter wheat yields in Kansas and Ukraine using MODIS data." *Remote Sensing of Environment.* 114 (6):1312-1323. doi: 10.1016/j.rse.2010.01.010.

Bhatti, A. M. and S. Nasu. 2010. "Domestic water demand forecasting and management under changing socio-economic scenario." Soceity for Social Management Systems.

Boatwright, G. O., and V. S. Whitefield. 1986. "Early warning and crop condition assessment research." *IEEE Transactions on Geosciences and Remote Sensing* GE-24 (1).

Boryan, C., Y. Zhengwei, M. Rick, and C. Mike. 2011. "Monitoring US agriculture: the US Department of Agriculture, National Agricultural Statistics Service, Cropland Data Layer Program." *Geocarto International* 26 (5):341-358.

Branca, G., N. McCarthy, L. Lipper, and M. C. Jolejole. 2011. Climate-smart Agriculture: A Systhesis of Empirical Evidence of Food Security and Mitigation Benefits from Improved Cropland Management. Food and Agriculture Organization of the United Nations (FAO).

Breiman, L. 1996. "Bagging predictors." *Machine Learning* 24 (2):123-140. doi: 10.1023/a:1018054314350.

Breiman, L. 2001. "Using iterated bagging to debias regressions." *Machine Learning* 45 (3):261-277. doi: 10.1023/a:1017934522171.

Breiman, L., J. Friedman, R. Olshen, and C. Stone. 1984. *Classification and Regression Trees*. Monterey, CA: Wadsworth and Brooks/Cole.

Broich, Mark, Matthew C. Hansen, Peter Potapov, Bernard Adusei, Erik Lindquist, and Stephen V. Stehman. 2011. "Time-series analysis of multi-resolution optical imagery for quantifying forest cover loss in Sumatra and Kalimantan, Indonesia." *International Journal of Applied Earth Observation and Geoinformation* 13 (2):277-291. doi: https://doi.org/10.1016/j.jag.2010.11.004.

Bwangoy, J-R B., M. C. Hansen, P. Potapov, S. Turubanova, and R. S. Lumbuenamo. 2013. "Identifying nascent wetland forest conversion in the Democratic Republic of the Congo." *Wetlands Ecology and Management* 21 (1):29-43. doi: 10.1007/s11273-012-9277-z.

Bwangoy, J-R B., M. C. Hansen, D. P. Roy, G. De Grandi, and C. O. Justice. 2010. "Wetland mapping in the Congo Basin using optical and radar remotely sensed data and derived topographical indices." *Remote Sensing of Environment* 114 (1):73-86. doi: 10.1016/j.rse.2009.08.004.

Carfagna, E. 2001. "Cost-effectiveness of remote sensing in agricultural and environmental statistics." Conference on Agricultural and Environmental Statistical Applications, Rome, Italy.

Carfagna, Elisabetta, and F. Javier Gallego. 2005. Using Remote Sensing for Agricultural Statistics. In *International Statistical Review / Revue Internationale de Statistique*, edited by International Statistical Institute (ISI): [Wiley, International Statistical Institute (ISI)].

Chander, G., B. L. Markham, and D. L. Helder. 2009. "Summary of current radiometric calibration coefficients for Landsat MSS, TM, ETM+, and EO-1 ALI sensors." *Remote Sensing of Environment* 113 (5):893-903. doi: 10.1016/j.rse.2009.01.007.

Chang, J., M. C. Hansen, K. Pttman, C. Dimiceli, and M. Carroll. 2007. Corn and soybean mapping in the United States using MODIS time-series data sets. Agronomy Journal: American Society of Agronomy.

Chaudhry, G. M. and A. R. Kemal. 1974. "Wheat production under alternative production functions." Pakistan Development Review, 13(2): 407-415.

Cihlar, J. 2000. "Land cover mapping of large areas from satellites: status and research priorities." *International Journal of Remote Sensing* 21 (6-7):1093-1114. doi: 10.1080/014311600210092.

Comber, A. J., A. N. R. Law, and J. R. Lishman. 2004. "Application of knowledge for automated land cover change monitoring." *International Journal of Remote Sensing* 25 (16):3177-3192. doi: 10.1080/01431160310001657795.

Craig, Michael. 2010. "A History of Cropland Data Layer at NASS." https://www.nass.usda.gov/Research_and_Science/Cropland/CDL_History_MEC.pdf.

Craig, Michael, and Dale Atkinson. 2013. A Literature Review of Crop Area Estimation. Accessed July 2, 2018.

Crnojevic, V., P. Lugonija, B. Brkljac, and B. Brunet. 2014. "Classification of small agricultural fields using combined Landsat-8 and RapidEye imagery: case study of northern Serbia." *Journal of Applied Remote Sesning* 8:18.

CRS, Punjab. 2014. Second estimate of wheat crop in the Punjab for the year 2013-14. Lahore: Govt. of Punjab.

CRS, Punjab. 2015. Rabi crop estimates data book 2014-15. Crop Reporting Service, Punjab.

Daanish, M., A., Majed, and N. Natalie. 2013.Understanding Pakistan's water-security nexus. Washington DC USA, United States Institute of Peace, 36.

David, Orden. 1986. "Money and Agriculture: The dynamics of money-financial market-agricultural trade linkages." *Agricultural Economics Research* 38 (3):14-28.

Defries, R.S., and Jonathan Cheung-Wai Chan. 2000. "Multiple criteria for evaluating machine learning algorithms for land cover classification from satellite data." *Remote Sensing of Environment* 74:503-515.

DeFries, Ruth S., Christopher B. Field, I. Fung, Christopher O. Justice, S. Los, Pamela A. Matson, E. Matthews, Harold A. Mooney, Christopher S. Potter, Prentice K., Piers J. Sellers, John R. G. Townshend, Compoton J. Tucker, Susan L. Ustin, and Peter M. Vitousek. 1995. "Mapping the land surface for global atmospher-biosphere models: Toward continous distributions of vegetation's functional properties." *Journal of Geophysical Research* 100 (D10):20867-20882.

Dempewolf, J. , B. Adusei, I. Becker-Reschef, B. Barker, P. Potapov, M. Hansen, and C. Justice. 2013. "Wheat production forecasting for Pakistan from satellite data." Geoscience and Remote Sensing Symposium (IGARSS), 2013 IEEE International, Melbourne, VIC, 21-26 July 2013.

Dempewolf, J., B. Adusei, I. Becker-Reschef, M. Hansen, P. Potapov, A. Khan, and B. Barker. 2014. "Wheat yield forecasting for Punjab Province from Vegetation Index Time Series and Historic Crop Statistics." *Journal of Remote Sensing* 6(10):9653-9675.

Doraiswamy, P. C., S. Moulin, P. W. Cook, and A. Stern. 2003. "Crop yield assessment from remote sensing." *Photogrammetric Engineering and Remote Sensing* 69 (6):665-674.

Drusch, M., U. Del Bello, S. Carlier, S. Colin, V. Fernandez, F. Gascon, B. Hoersch, C. Isola, P. Laberinti, P. Martimort, A. Meygret, F. Spoto, O. Sy, F. Marchese, and P. Bargellini. 2012. "Sentinel-2: ESA's Optical High-Resolution Mission for GMES Operational Services." *Remote Sensing of Environment* 120:25-36.

Erickson, J. D. 1984. "The LACIE Experiment in Satellite Aided Monitoring of Global Crop Production." In *The Role of Terrestrial Vegetation in the Global Carbon Cycle: Measurement by Remote Sensing*, edited by G. M. Goodwell, 191-217. New York, USA: John Wiley & Sons Ltd.

Everaers, Pieter. 2009. "The present state of agricultural statistics in developed countries: situation and challenges." In *Agricultural Survey Methods*, edited by Roberto Benedetti, Marco Bee, Giuseppe Espa and Federica Piersimoni, 409. United Kingdom: John Willey & Sons Ltd.

FAO. 2012. Baseline Survey - Agriculture Information System: Technical Report. FAO/UN, SUPARCO, Italy. Rome, Italy: Food and Agriculture Organization.

FAO. 2013. Pakistan: Review of the wheat sector and grain storage issues. . Rome, Italy: Food and Agriculture Organization/World Bank Cooperative Program.

Fermont, Anneke, and Todd Benson. 2011. Estimating yield of food crops grown by smallholder farmers: A review in the Uganda context. International Food Policy Research Institute.

Food and Agriculture Organization, United Nations. 2015. FAOSTAT; http://faostat3.fao.org/home/E accessed on April 15, 2015.

Food and Agriculture Organization, United Nations (FAO). 2011. Global strategy to improve agricultural and rural statistics. Rome, Italy: FAO.

Friedl, M. A., D. K. McIver, J. C. F. Hodges, X. Y. Zhang, D. Muchoney, A. H. Strahler, C. E. Woodcock, S. Gopal, A. Schneider, A. Cooper, A. Baccini, F. Gao, and C. Schaaf. 2002. "Global land cover mapping from MODIS: algorithms and early results." *Remote Sensing of Environment.* 83 (1 - 2):287 - 302.

Gallego, F. J. 2004. "Remote sensing and land cover area estimation." *International Journal of Remote Sensing.* 25 (15):3019-3047. doi: 10.1080/01431160310001619607.

Gallego, F. J., M. Craig, J. Michaelsen, B. Bossyns, and S. Fritz. 2009. Best practices for crop area estimation with remote sensing. Luxembourg: Group on Earth Observations (GEO).

Gallego, J., M. Craig, J. Michaelsen, B. Bossyns, and S. Fritz. 2008. Workshop on best practices for crop area estimation with remote sensing data: summary of country inputs. Italy: Group on Earth Observations(GEO), GEOSS Community of Practice Ag Task 0703a, EC JRC, ISPRA.

Gallego, Javier, Elisabetta Carfagna, and Bettina Baruth. 2010. "Accuracy, objectivity and efficiency of remote sensing for agricultural statistics." In *Agricultural Survey Methods*, edited by Roberto Benedetti, Marco Bee, Giuseppe Espa and Federica Piersimoni, 409. United Kingdom: John Wiley & Sons Ltd.

Gallego, Javier, and Jagues Delince. 2010. "The European land use and cover area-frame statistical survey." In *Agricultural Survey Methods*, edited by Roberto Benedetti, Marco Bee, Giuseppe Espa and Federica Piersimoni, 409. United Kingdom: John Willey & Sons Ltd.

Gao, B. 1996. "NDWI - A normalized difference water index for remote sensing of vegetation liquid water from space." *Remote Sensing of Environment.* 58(3):258-266.

Gerald, K. Moore. 1979. "What is a picture worth? A history of remote sensing / Quelle est la valeur d'une image? Un tour d'horizon de teledetection." *Hydrological Sciences Bulletin* 24 (4):477 - 485.

Giri, Chandra, and Jordan Long. 2014. "Land cover characterization and mapping of South America for the year 2010 using Landsat 30 m satellite data." *Remote Sensing.* 6 (9494 - 9510). doi: 9494-9510; doi:10.3390/rs6109494

GonzÁLez-Alonso, F., and J. M. Cuevas. 1993. "Remote sensing and agricultural statistics: crop area estimation through regression estimators and confusion matrices." *International Journal of Remote Sensing* 14 (6):1215-1219. doi: 10.1080/01431169308904405.

GoPakistan. 2010. Agricultural Census 2010 - Pakistan Report. www.pbs.gov.pk accessed on 01 April 2015: Pakistan Bureau of Statistics, Govt. of Pakistan.

GoPakistan. 2011. Agriculture Statistics. www.pbs.gov.pk/content/approved-crop-calendar-0.: Pakistan Bureau of Statistics, Govt of Pakistan.

GoPakistan. 2014. Pakistan Economic Survey 2013-14. edited by Ministry of Finance. Islamabad: Ministry of Finance.

GoPakistan. 2017. Provisional province wise population by sex and rurual/urban. Pakistan Bureau of Statistics at www.pbs.gov.pk accessed on 20 February 2018: Govt. of Pakistan.

Griffiths, W. G. Thomson and T. Coelli. 1999. "Predicting ouput from seemingly unrelated area and yield equations." Working paper series in Agriculture and Resource Economics, Graduate School of Agricultural and Resources Economics, University of New England. 99.

Hansen, C. M., R. DeFries, J. R. G. Townshend, L. Marufu, and R. Sohlberg. 2002. "Development of a MODIS per cent tree cover validation data set for Western Province, Zambia." *Remote Sensing of Environment* 83:320-335.

Hansen, C. M., EA. Egorov, D. P. Roy, P. Potapov, Junchang Ju, S. Turubanova, I. Kommareddy, and T. R. Loveland. 2011. "Continous fields of land cover for the conterminous United States using Landsat data: first results from the Web-Enabled Landsat Data (WELD) project." *Remote Sensing Letters* 2 (4):10. doi: 10.1080/01431161.2010.519002.

Hansen, M. C, R Dubayah, and R. DeFries. 1996. "Classification trees: An alternative to traditional land cover classifiers." *International Journal of Remote Sensing* 17 (5):1075-1081.

Hansen, M. C., R. S. DeFries, J. R. G. Townshend, R. Sohlberg, C. Dimiceli, and M. Carroll. 2002. "Towards an operational MODIS continuous field of per cent tree cover algorithm: examples using AVHRR and MODIS data." *Remote Sensing of Environment.* 83 (1):303-319. doi: https://doi.org/10.1016/S0034-4257(02)00079-2.

Hansen, M. C., and T. R. Loveland. 2012. "A review of large area monitoring of land cover change using Landsat data." *Remote Sensing of Environment* 122:66-74. doi: 10.1016/j.rse.2011.08.024.

Hansen, M.C., and R. DeFries. 2004. "Detecting long-term global forest change using continuous fields of tree cover maps from 8-km Advanced Very High-resolution Radiometer (AVHRR) data for the years 1982 - 1999." *Ecosystems* 7:695-716.

Hansen, M.C., P.V. potapov, R. Moore, M. Hancher, S.A. Turubanova, A. Tyukavina, D. Thau, S. V. Stehman, S. J. Goetz, T. R. Loveland, A. Kommareddy, EA. Egorov, L. Chini, C. O. Justice, and J. R. G. Townshend. 2013. "High-Resolution Global Maps of 21st-Century Forest Cover Change." *Science* 342 (6160):4. doi: 10.116/science.1244693.

Hansen, Matthew C., David P. Roy, Erik Lindquist, Bernard Adusei, Christopher O. Justice, and Alice Altstatt. 2008. "A method for integrating MODIS and Landsat data for systematic monitoring of forest cover and change in the Congo Basin." *Remote Sensing of Environment* 112 (5):2495-2513. doi: 10.1016/j.rse.2007.11.012.

Hanuschak, G. A. 2010. Timely and accurate crop yield forecasting and estimation: History and initial gap analysis. Food and Agriculture Organization of the United Nations.

Hanuschak, G. A., and R. Mueller. 2002. Cost and Benefit Analysis of a Cropland Data Layer. In *NASS Research Reports 234296.*

Hanuschak, G. A., R. Sigman, M. E. Craig, M. Ozga, R. C. Luebbe, P. W. Cook, D. D. Kleweno, and C. E. Miller. 1980. "Crop-Area Estimates from Landsat; Transition from Research And Development to Timely Results." *IEEE Transactions on Geoscience and Remote Sensing* GE-18 (2):160-166. doi: 10.1109/TGRS.1980.350268.

Heremans, Stien, Bert Bossyns, Herman Eerens, and Jos Van Oshoven. 2011. "Efficient collection of training data for sub-pixel land cover classification using neural networks." *International Journal of Applied Earth Observation and Geoinformation* 13 (4):657-667. doi: 10.1016/j.jag.2011.03.008.

Hicke, Jeffrey A., David B. Lobell, and Gregory P. Asner. 2004. "Cropland Area and Net Primary Production Computed from 30 Years of USDA Agricultural Harvest Data." *Earth Interactions* 8 (10):1-20. doi: 10.1175/1087-3562(2004)008<0001:caanpp>2.0.co;2.

Hubback, J. A. 1946. "Sampling for Rice Yield in Bihar and Orissa." *Sankhya: The Indian Journal of Statistics (1933 - 1960)* 7 (3):281-294.

Huddleston, Harold F. 1978. Sampling techniques for measuring and forecasting crop yields. United States: U.S. Department of Agriculture.

Huth, Juliane, Claudia Kuenzer, Thilo Wehrmann, Steffen GEbhardt, Vo Quoc Tuan, and Stefan Dech. 2012. "Land Cover and Land Use classification with TWOPAC: towards automated processing for pixel- and object-based image classification." *Remote Sensing* 4:2530-2553. doi: 10.3390/rs4092530

Irshad, M. , M. Inoue, Faridullah, Hossain K. M. Delower, and A. Tsunekawa. 2007. "Land desertification - An emerging threat to environment and food security of Pakistan." *Journal of Applied Sciences* 7 (8):1199 - 1205.

Jabeen, A., X. S. Huang., and M. Aamir. 2015. "The Challenges of Water Pollution, Threat to Public Health, Flaws of Water Laws and Policies in Pakistan." *Journal of Water Resource and Protection* 7:1516-1526.

Junior, Jurandir Zullo, Priscila Pereira Coltri, Renata Ribeiro do Valle Goncalves, and Luciana Alvim Santos Romani. 2014. "Mult-resolution in remote sensing for agricultural monitoring: A review." *Revista Brasileira de Cartografia* 66 (7):1517-1529.

Jurriens, M., P. P. Mollinga, and P. Wester. 1996. Scarcity by design, Protective Irrigation in India and Pakistan. Netherlands: Wageningen Agricultural University, Department of Irrigation & Soil & Water Conservation,.

Justice, C. O., J. R. G. Townshend, E. F. Vermote, E. Masuoka, R. E. Wolfe, N. Saleous, D. P. Roy, and J. T. Morisette. 2002. "An overview of MODIS Land data processing and product status." *Remote Sensing of Environment* 83:3 - 15.

Kaditi, Eleni A. 2012. "Market dynamics in food supply chains: The impact of globalization and consolidation on firms' market power." *Agribusiness* 29 (4):410-425. doi: DOI: 10.1002/agr.21301.

Kahan, David. 2013. Market-oriented farming: An overview. Rome, Italy: Food and Agriculture Organization of the United Nations (FAO).

Kalim, R., and S. A. Bhatty. 2004. "Quantification of socio-economic deprivation of squatter settlements' inhabitats: A case study of Lahore." 6th Global Conference on Business and Economics, USA.

Khan, A., M.C Hansen, P. Potpova, S.V Stehman, and A.A Chattha. 2016. "Landsat-based wheat mapping in the heterogeneous cropping system of Punjab, Pakistan." *International Journal of Remote Sensing* 37 (6):1391-1410. doi: 10.1080/01431161.2016.1151572.

Khan, A., M. C. Hansen, P. V. Potapov, Adusei, B., A. Pickens, A. Krylov, and S. V. Stehman. 2018. "Evaluating Landsat and RapidEye Data for Winter Wheat Mapping and Area Estimation in Punjab, Pakistan." *Remote Sensing* 10 (4):489.

King, L., B. Adusei, S.V. Stehman, P. V. Potapov, X. Song, A. Krylov, C. D. Bella, T. Loveland, D. M. Johnson, and M. C. Hansen. 2017. *A multi-resolution approach to national-scale cultivated area estimation of soybean*. Vol. 195.

Kleweno, David D., and Charles E. Miller. 1981. 1980 AgRISTARS DC/LC Project Summary: Crop Area Estimates for Kansas and Iowa. U.S. Department of Agriculture, Statistical Research Division.

Knorn, Jan, Andreas Rabe, Volker C. Radeloff, Tobias Kuemmerle, Jacek Kozak, and Patrick Hostert. 2009. "Land cover mapping of large areas using chain classification of neighboring Landsat satellite images." *Remote Sensing of Environment* 113 (5):957-964. doi: https://doi.org/10.1016/j.rse.2009.01.010.

Kugelman, Michael. 2013. Urbanisation in Pakistan: Causes and consequences. Norwegian Peacebuilding Resource Center.

Kugelman, Michael, ed. 2014. *Pakistan's Runaway Urbanization: What Can Be Done?* Washington DC, USA: The Wilson Center.

Latifovic, R., and I. Olthof. 2004. "Accuracy assessment using sub-pixel frctional error matrices of global land cover products derived from satellite data." *Remote Sensing of Environment* 90:153-165.

Lohr, S. L. 2010. *Sampling Design and Analysis*. 2nd ed. Boston, MA: Brooks/Cole.

Loveland, Thomas R., and Jhon L. Dwyer. 2012. "Landsat: Building a strong future." *Remote Sensing* 122:22-29. doi: 10.1016/j.rse.2011.09.022.

Loveland, Thomas R., B. C. Reed, Jesslyn F. Brown, D. O. Ohlen, Z. Zhu, L. Yang, and J. W. Merchant. 2000. "Development of a global land cover characteristics database and IGBP DISCover from 1 km AVHRR data." *International Journal of Remote Sensing* 21 (6-7):1303-1330. doi: 10.1080/014311600210191.

Lydia, D. G., S. Hagemann, and C. Golz. 2000. Observed historical discharge data from major rivers for climate model validation. Hamburg, Germany: Max-Planck-Institute for Meteorology.

Maas, Stephan J. 1998. "Estimating Cotton Canopy Ground Cover from Remotely Sensed Scene Reflectance." *Agronomy Journal* 90:384-388. doi: 10.2134/agronj1998.00021962009000030011x.

Macdonald, R. B. 1984. "A summary of the history of the development of automated remote sensing for agricultural applications." *IEEE Transactions on Geoscience and Remote Sensing* GE-22 (6):473-482. doi: 10.1109/TGRS.1984.6499157.

MacDonald, R. B., F. G. Hall, and R. B. Erb. 1975. "The Use of LANDSAT Data in a Large Area Crop Inventory Experiment (LACIE)." Symposium on Machine Processing of Remotely Sensed Data, Purdue University, West Lafayette, IN, June 3-5, 1975.

MacDonald, R. B., and David Landgrebe. 1967. "Remote Sensing for Agriculture and Natural Resources from Space." National Symposium of American Astronomical Society (1967), Huntsville, AL, June 14, 1967.

MacDonald, R.B, and F. G. Hall. 1980. "Global Crop Forecasting." *Science* 208 (4445):670-679. doi: 10.1126/science.208.4445.670.

Mahalanobis, P. C. 1945. "Report on the Bihar Crop Survey: Rabi Season 1943 - 44." *Sankhya: The Indian Journal of Statistics (1933 - 1960)* 7 (1):29 - 106.

Markham, Brian L., and John L. Barker. 1985. "Spectral characterization of the LANDSAT Thematic Mapper sensors." *International Journal of Remote Sensing* 6 (5):697-716. doi: 10.1080/01431168508948492.

Mayo, S. M. 2012. "Determination of urban settlement pattern for optimal regional development in Punjab." Ph.D, Department of City and Regional Planning, University of Engineering and Technology Lahore - Pakistan.

Minamiguchi, N. . 2005. "The application of Geospatial and Disaster information for food insecurity and agricultural drought monitoring and assessment by the FAO GIEWS and ASia FIVIMS." Workshop on reducing food insecurity associated with natural disasters in Asia and the pacific, Bangkok, Thailand, 27-28 January 2005., 27-28 July 2005.

Ministry of Finance. 2014. Pakistan Economic Survey 2013-14. http://www.finance.gov.pk/survey_1314.html - accessed on July 3rd, 2018: Ministry of Finance, Government of Pakistan.

Ministery of Finance. 2018. Pakistan Economic Survey 2017-18. http://www.finance.gov.pk/survey/chapters_18/Economic_Survey_2017_18.pdf. accessed July 3rd, 2018. Ministry of Finance, Government of Pakistan.

Morton, John F. 2007. "The impact of climate change on smallholder and subsistence agriculture." *Proceedings of the National Academy of Sciences* 104 (50):19680-19685. doi: 10.1073/pnas.0701855104.

Mosiman, B.N. 2003. "Exploring Multi-temporal and Transformation Methods for Improved Cropland Classification Using Landsat Thematic Mapper Imagery." Master's Department of Geography, University of Kansas.

Mueller, R., and R. Seffrin. 2006. "New methods and satellites: A program update on the NASS cropland data layer and acreage program." ISPRS WG VIII/10 Workshop 2006: Remote Sensing Support to Crop Yield Forecast and Area Estimates, Stresa Italy.

Mukhtar M. E. and H. Mukhtar. 1988. "Input use and productivity across farm sizes: A comparison of the two Punjabs." Pakistan Development Review, 42 (1): 1 - 27.

Mulla, David J. 2013. "Twenty five years of remote sensing in precision agriculture: Key advances and remaining knowledge gaps." *Biosystems Engineering* 114 (4):358-371. doi: http://dx.doi.org/10.1016/j.biosystemseng.2012.08.009.

Nellis, M. D., K. P. Price, and D. Rundquist. 2009. "Remote Sensing of cropland agriculture." In *The SAGE handbook of remote sensing*, edited by T. Warner, M. Duane Nellis and G. Foody. 55 City Road, London: SAGE Publications, Inc.

Olofsson, Pontus, Giles M. Foody, Martin Herold, Stephen V. Stehman, Curtis E. Woodcock, and Michael A. Wulder. 2014. "Good practices for estimating area

and assessing accuracy of land change." *Remote Sensing of Environment* 148:42-57. doi: https://doi.org/10.1016/j.rse.2014.02.015.

Ouaidrari, H., and F. E. Vermote. 1999. "Operational Atmospheric Correction of Landsat TM Data." *Remote Sensing of Environment* 70:4-15.

Pittman, K., M. Hansen, I. Becker-Reschef, P. V. Potapov, and C. P. Justice. 2010. "Estimating Global Cropland extent with Multi-year MODIS Data." *Remote Sensing* 2 (7):20. doi: 10.3390rs2071844.

Potapov, P V, J Dempewolf, Y Talero, S V Stehman, C Vargas, E J Rojas, D Castillo, E Mendoza, A Calderon, R Giudice, N Malaga, and B R Zutta. 2014. "National satellite-based humid tropical forest change assessment in Peru in support of REDD+ implementation." *Environ. Res. Lett* 9 (124012). doi: https://doi.org/10.1088/1748-9326/9/12/124012.

Potapov, Peter V., Svetlana A. Turubanova, Matthew C. Hansen, Bernard Adusei, Mark Broich, Alice Altstatt, Landing Mane, and Christopher O. Justice. 2012. "Quantifying forest cover loss in Democratic Republic of the Congo, 2000-2010, with Landsat ETM plus data." *Remote Sensing of Environment* 122:106-116. doi: 10.1016/j.rse.2011.08.027.

Qadeer, M. A. 2014. "Do's and Don'ts of Urban Policies in Pakistan." In *Pakistan's Runaway urbanization*, edited by Michael Kugelman, 144. Washington DC, USA: The Wilson Center.

Qasim, M. . 2012. *Determinants of Farm Income and Agricultural Risk Management Strategies: The case of rain-fed farm households in Pakistan's Punjab*. Edited by Beatrice Knerr. Vol. 3. International Rural Development: kassel university press GmbH, Kassel, Germany.

Qureshi, S. K. 1974. "Rainfall, acreage, and wheat production in West Pakistan: A Statistical Analysis." *Pakistan Development Review*, 13(3): 566 - 593.

Reed, B. C., J. F. Brown, D. VenderZee, T. R. Loveland, J. W. Merchant, and D. O. Ohlen. 1994. "Measuring phenological variability from satellite imagery." *Journal of Vegetation Science* 5:703-714. doi: 10.2307/3235884.

Rembold, F., and F. Maselli. 2006. "Estimating inter-annual crop area variation using multi-resolution satellite sensor images." *International Journal of Remote Sensing* 25 (13):2641-2647. doi: 10.1080/01431160310001657614.

Reynolds, C. 2001. "Input Data Sources, Climate Normals, Crop Models, and Data Extraction Routines Utilized by OGA/IPAD." Third International Conference on Geospatial Information in Agriculture and Forestry, Denver, Colorado, November 5 - 7, 2001.

Ripley, B. D. 1996. *Pattern Recognition and Neural Networks.* New York, USA: Cambridge University Press.

Rogan, John, and DongMei Chen. 2004. "Remote sensing technology for mapping and monitoring land-cover and land-use change." *Progress in planning* 61 (2004):301-325. doi: 10.1016/S0305-9006(03)00066-7.

Roohi, R. 2006. Irrigated areas of Pakistan. Workshop presentation at WRRI, NARC, Islamabad on September 26, 2006.

Saeed, U., Jan, D., Ahmad K., Ashfaq, A. and Syed A.W. 2017. "Forecasting wheat yield from wheather data and MODIS NDVI using Random Forests for Punjab

Province, Pakistan. " *International Journal of Remote Sensing*, 38(17): 4831 - 4854.

Saleem, M. A. 1989. "Farmers' attitude towards risk in dryland wheat production areas in Jordan." *Dirasat-Agricultural Science*, 16(7):28-52.

Sarndal, C.-E., B. Swensson, and J. Wretman. 1992. *Model Assisted Survey Sampling*. New York, NY: springer.

Schuster, C., M. Forster, and B. Kleinschmit. 2012. "Testing the red edge channel for improving land-use classifications based on high-resolution multi-spectral satellite data." *International Journal of Remote Sensing* 33 (17):5583-5599. doi: 10.1080/01431161.2012.666812.

Shirazi, S. Ali, and S. J. H. Kazmi. 2014. "Analysis of population growth and urban development in Lahore - Pakistan using geospatial techniques: Suggesting some future options." *South Asian Studies: a research journal of South Asian Studies* 29 (01):269 - 280.

Singh, R., and R. C. Goyal. 2000. "Use of remote sensing satellite data in crop surveys." PhD, International Journal of Remote Sensing, Indian Agricultural Statistics Research Institute.

Song, Xiao-Peng, P.V. Potapov, A. Krylov, L. King, C. M. D. B., A. Hudson, A. Khan, B. Adusei, S. V. Stehman, and M. C. Hansen. 2017a. "National-scale soybean mapping and area estimation in the United States using medium resolution satellite imagery and field survey." *Remote Sensing of Environment* 190 (Supplement C):383-395. doi: https://doi.org/10.1016/j.rse.2017.01.008.

Stathers, Tanya, Richard Lamboll, and Brighton M. Mvumi. 2013. "Postharvest agriculture in changing climates: its importance to African smallholder farmers." *Food Security* 5 (3):361-392. doi: 10.1007/s12571-013-0262-z.

Stehman, S. V., and R. L. Czaplewski. 1998. "Design and analysis for thematic map accuracy assessment: Fundamental principles." *Remote Sensing of Environment* 64 (3):331-344. doi: 10.1016/s0034-4257(98)00010-8.

Stehman, Stephen V. 2013. "Estimating area from an accuracy assessment error matrix." *Remote Sensing of Environment* 132:202-211. doi: https://doi.org/10.1016/j.rse.2013.01.016.

Stoll, E., H. Konstanski, C. Anderson, K. Douglas, and M. Oxfort. 2012. "The RapidEye constellation and its data products." Aerospace Conference, 2012, IEEE.

SUPARCO. 2012. Punjab CRS. Baseline survey, Agriculture Information System. Building provincial capacity for crop forecasting and estimation. A joint FAO, UN, SUPARCO and Crop Reporting Service, Government of Punjab Publication.: SUPARO and Government of Punjab.

SUPARCO. 2014. Crop Situation: Rabi Crops Situation 2013-14. PAK-SCMS Bulletin: SUPARCO.

SUPARCO. 2015. Rabi Crop 2014-15. Pakistan Space and Upper Atmosphere Research Commission (SUPARCO).

Takashi, Kurosaki. 2003. "Specialization and diversification in agricultural transformation: The case of West Punjab, 1903 - 92." *Amer. J. Agr. Econ.* 85 (2):372 - 386.

Tucker, C. J. 1979. "Photographic Infrared Linear Combinations for Monitoring Vegetation." *Remote Sensing of Environment* 8(2):127-150.

Turner II, B. L., D. Skole, S. Sanderson, G. Fischer, L. Fresco, and R. Leemans. 1995. *Land-use and land-cover change, Science/Research plan*, *IGBP Report : 35/HDP Report NO. 7*. Stockholm, Sweden, and Genva, Switzerland: IGBP Report No. 35/HDP Report NO. 7.

Tyukavina, A., A. Baccini, M. C. Hansen, P. V. Potapov, S. V. Stehman, R. A. Houghton, A. M. Krylov, S. Turubanova, and S. J. Goetz. 2015. "Aboveground carbon loss in natural and managed tropical forests from 2000 to 2012." *Environmental Research Letters* 10 (7):074002.

Unal, E., A. Mermer, O. Urla, N. Ceylan, H. Yildiz, and M. Aydogdu. 2006. "Pilot study on wheat area estimates in Turkey." ISPRS WG VIII/10 Workshop 2006: Remote sensing support to crop yield forecast and area estimates, Stresa, Italy.

United Nations. 2018. United Nations DESA/ Population Division: World Urbanization Prospects 2018. https://population.un.org/wup/.

Ustin, Susan L. 2004. *Remote Sensing application in Agriculture*. Edited by Susan L. Ustin. Third ed, *Manual of Remote Sensing, Remote Sensing for Natural Resource Management and Environmental Monitoring*: American Society of Photogrammetry and Remote Sensing.

Verma, U., D. S. Dabas, R. S. Hooda, M. H. Kalubarme, M. Yadav, M. S. Grewal, M. P. Sharma, and R. Prawasi. 2011. "Remote sensing based wheat acreage and spectral-trend-agrometeorological Yield Forecasting : Factor Analysis Approach." *Statistics and Applications* 9 (1 & 2):1-13.

Vogelmann, J. E., M. H. Stephen, Y. Limin, R. L. Charles, K. W. Bruce, and V. D. Nick. 2001. "Completion of the 1990s National Land Cover Data Set for the Conterminous United States from Landsat Thematic Mapper Data and Ancillary Data Sources." *Photogrammetric Engineering and Remote Sensing*.

Vuolo, Francesco, Nikolaus Neugebauer, Salvatore Bolognesi, Clement Atzberger, #039, and Guido Urso. 2013. "Estimation of Leaf Area Index Using DEIMOS-1 Data: Application and Transferability of a Semi-Empirical Relationship between two Agricultural Areas." *Remote Sensing* 5 (3):1274.

Wardlow, B. D., and S. L. Egbert. 2008. "Large-area crop mapping using time-series MODIS 250 m NDVI data: An assessment for the U.S. Central Great Plains." *Remote Sensing of Environment* 112 (3):1096-1116. doi: 10.1016/j.rse.2007.07.019.

WB, and FAO. 2011. Global strategy to improve agricultural and rural statisitcs. Rome, Italy: The World Bank; Food and Agriculture Organization of the United Nations.

Woodcock, C. E. , R. Allen, M. Anderson, A. Belward, R. Bindschadler, W. B. Cohen, F. Gao, S. N. Goward, D. Helder, E. Helmer, R. Nemani, L. Oreopoulous, J. Schott, P. S. Tenkabalil, E. F. Vermote, J. Vogelmann, M. A. Wulder, and R. Wynne. 2008. "Free access to Landsat imagery." *Science* 320:1011-1012.

WorldBank. 2011. Global strategy to improve agricultural and rural statistics. Washington DC, USA: The World Bank and Food and Agriculture Organization of the United Nations.

Worldbank. 2014. Health Nutrition and Population Statistics; available online http://databank.worldbank.org (accessed on 11 October, 2014).

Wulder, Michael A., Jeffrey G. Masek, Warren B. Cohen, Thomas R. Loveland, and Curtis E. Woodcock. 2012. "Opening the archive: How free data has enabled the science and monitoring promise of Landsat." *Remote Sensing of Environment* 122:2-10. doi: https://doi.org/10.1016/j.rse.2012.01.010.

Yao, Fengmei, Lili Feng, and Jiahua Zhang. 2013. "Corn Area Extraction by the Integration of MODIS-EVI Time Series Data and China's Enviornment Satellite (HJ-1) Data." *J Indian Soc Remote Sens* 42 (4):859-867.

Zheng, Yang, Bingfang Wu, Miao Zhang, and Hongwei Zeng. 2016. "Crop Phenology Detection Using High Spatio-Temporal Resolution Data Fused from SPOT5 and MODIS Products." *Sensors (Basel, Switzerland)* 16 (12):2099. doi: 10.3390/s16122099.

Zhou, W., J. Zhang, Y. Pan, and R. Zhu. 2014. "Remote sensing assisted multi-level crop acreage estimation: An application of small area estimation in Heilongjiang province." 2014 The Third International Conference on Agro-Geoinformatics, 11-14 Aug. 2014.

Zhu, T. 2014. Climate Change and Extreme Events: Impacts on Pakistan's Agriculture. edited by Waqas H. Xie, C., Ringlerc M. Mohsin Iqbal, M. Arif Goheer and T. Sulser. Washington DC: International Food Policy Research Institute (IPFRI).